Experimental evolution of plasmid genomes

Dissertation

zur Erlangung des Doktorgrades

der Mathematisch-Naturwissenschaftlichen Fakultät

der Christian-Albrechts-Universität zu Kiel

vorgelegt von

Judith Ilhan

Kiel, 2019

Erste Gutachterin:	Prof. Dr. Tal Dagan
Zweiter Gutachter:	PD Dr. Charles M.A.P. Franz
Tag der mündlichen Prüfung:	01.02.2019
Zum Druck genehmigt:	01.02.2019

Declaration

I hereby declare that the thesis entitled “Experimental evolution of plasmid genomes“ has been carried out in the Institute of General Microbiology at the Christian-Albrechts University of Kiel, Kiel, Germany, under the guidance of Prof. Dr. Tal Dagan and Prof. Dr. Itzhak Mizrahi. The work is original and has not been submitted in part or full by me for any degree at any other University. I further declare that the material obtained from other sources has been duly acknowledged in the thesis. My work has been produced in compliance to the principles of good scientific practice in accordance with the guidelines of the German science foundation. I hereby assure that I have not been revoked any of my academic degrees.

_____

Judith Ilhan

Table of contents

1 Abstract

The ubiquity of plasmids in all prokaryotic phyla and habitats and their ability to transfer between cells marks them as prominent constituents of prokaryotic genomes. Many plasmids are found in their host cell in multiple copies. The multi-copy state of plasmids leads to an increased mutational supply of plasmid-encoded genes and genetically heterogeneous plasmid genomes. Nonetheless, the segregation of plasmid copies into daughter cells during cell division is considered to occur in the absence of selection on the plasmid alleles. Consequently, I hypothesize that genetic drift of plasmid alleles during cell division has implication for the evolutionary rates of plasmids by lowering the number of accumulating mutations that are expected from the mutational supply. To test this hypothesis, I performed an experimental evolution experiment of low- and high-copy non-mobile plasmids in an *Escherichia coli* host. The results of the experiment revealed that the evolutionary rate of multicopy plasmids does not reflect the increased mutational supply expected according to their copy number. The results further suggest that many plasmid mutations are quickly lost due to genetic drift during cell division. Here I term this special type of allele dynamics in the population as 'segregational drift'. Thus, segregational drift of multicopy plasmids interferes with the retention and fixation of novel plasmid variants. Furthermore, an examination of the experimentally evolved hosts reveals a significant impact of the plasmid type on the host chromosome evolution. In conclusion, depending on the selection pressure on newly emerging variants, plasmid genomes may evolve slower than haploid chromosomes, regardless of their higher mutational supply. Plasmid copy number is thus an important determinant of plasmid evolvability due to the manifestation of segregational drift.

Zusammenfassung

Das ubiquitäre Vorkommen von Plasmiden in allen prokaryotischen Phyla und Lebensräumen sowie ihre Fähigkeit, zwischen Zellen transferiert zu werden, kennzeichnen sie als bedeutende Bestandteile prokaryotischer Genome. Viele Plasmide liegen in ihrer Wirtszelle in mehreren Kopien vor. Der multiple Kopien-Zustand von Plasmiden führt zu einem erhöhten Mutationsangebot von Plasmid-kodierten Genen und zu genetisch heterogenen Plasmidgenomen. Es wird jedoch angenommen, dass die Segregation von Plasmidkopien in Tochterzellen während der Zellteilung in Abwesenheit von Selektion auf Plasmid-Allele verläuft. Daher stelle ich die Hypothese auf, dass der genetische Drift von Plasmid-Allelen während der Zellteilung Auswirkungen auf die Evolutionsraten von Plasmiden hat, indem die Anzahl der kumulierenden Mutationen, die aufgrund des Mutationsangebots zu erwarten wären, verringert wird. Um diese Hypothese zu testen, führte ich ein Evolutionsexperiment mit nicht-mobilen Plasmiden mit niedriger und hoher Kopienzahl in *Escherichia coli* durch. Die Ergebnisse des Experiments zeigen, dass die Evolutionsrate von Plasmiden mit multiplen Kopien nicht das erhöhte Mutationsangebot widerspiegelt, das gemäß ihrer Kopienzahl zu erwarten wäre. Die Ergebnisse legen ferner nahe, dass viele Plasmidmutationen aufgrund des genetischen Drifts während der Zellteilung schnell verloren gehen. Hier bezeichne ich diese besondere Allel-Dynamik in der Population als "Segregationsdrift". Dementsprechend beeinträchtigt der Segregationsdrift die Retention und Fixierung neuer Plasmidvarianten von Mehrfachkopien-Plasmiden. Darüber hinaus zeigt eine Untersuchung der experimentell entwickelten Wirte einen signifikanten Einfluss des Plasmid-Typs auf die Entwicklung des Wirts-Chromosoms. Zusammenfassend kann gesagt werden, dass, je nach Selektionsdruck auf neu aufkommende Varianten, Plasmidgenome ungeachtet ihrer höheren Mutationszufuhr langsamer als haploide Chromosomen evolvieren können. Die Plasmid-Kopienzahl ist aufgrund der Manifestation des Segregationsdrifts eine wichtige Determinante der Evolvierbarkeit von Plasmiden.

2 Introduction

Plasmids are genetic elements that colonize prokaryotic cells where they replicate independently of the chromosome. Plasmids are considered as a major driving force in prokaryotic ecology and evolution as they can be transferred between cells, making them potent agents of lateral gene transfer (Lederberg 1946, Thomas and Nielsen 2005) and microbial warfare (Czárán et al. 2002, Majeed et al. 2010). Plasmids may contribute to the evolution of their host via the acquisition of genes encoding for new functions that are beneficial under specific growth limiting conditions (e.g., antibiotics resistance (Porse et al. 2016) or resistance to heavy metals (Gullberg et al. 2014, Dziewit et al. 2015)), or during adaptation to new habitats (e.g., catabolic functions (Schmidt et al. 2011)). Nonetheless, the importance of plasmids goes beyond microbial evolution as they are widely used as vectors for genetic engineering (Simon et al. 1983, Bevan 1984) as well as for applications in biotechnology (Ullrich et al. 1977) and synthetic biology (Shetty et al. 2008). Therefore, understanding plasmid biology and evolution is of major interest for basic microbiology research and biological applications.

2.1 Plasmid invasion and persistence

Mechanisms of plasmid invasion into a host cell are either active or passive. Conjugation, for example, is an active invasion mechanism since conjugative plasmids encode the proteins involved in the plasmid transfer. Plasmids that just encode the transfer core components, require for their conjugal transfer the presence of a co-residing plasmid encoding the conjugation machinery in the same host cell (reviewed in Shintani et al. 2015). In contrast, self-transmissible plasmids encode both the transfer and conjugative machinery components and can therefore invade a broad range of hosts (e.g., Klümper et al. 2015, Hall et al. 2016).

Non-mobile plasmids can invade hosts via natural transformation and thus, such plasmids can invade niches that are rich in exogenous plasmid-DNA, such as aquatic environments (Xue et al. 2015), biofilms (Williams et al. 1996) and soil microcosms (Lorenz et al. 1991). Plasmid invasion via transformation has been considered to be a rare event. However, recent studies revealed the presence of competence in *Acinetobacter baumannii* (Ramirez et al. 2010, Wilharm et al. 2013) and in addition an uncommon

regulation of competence in *Staphylococcus aureus* (Morikawa et al. 2012, Fagerlund et al. 2014). Such hitherto unknown mechanisms that are characteristic of natural competence, offer an explanation for the presence and variety of non-self conjugative plasmids in these organisms.

Phage-mediated plasmid invasion can occur via generalized transduction (e.g., Hertwig et al. 1999). Similarly, experimental evidence suggests that gene transfer agents (GTAs) can potentially mediate plasmid invasion (Scolnik and Haselkorn 1984). In addition, outer membrane vesicles (OMVs) can also serve as conductors of plasmids entry into a new host as has been shown for both Gram-negative and Gram-positive bacteria (Klieve et al. 2005, Fulsundar et al. 2014). Notably, OMVs have been shown to mediate inter-specific plasmid transfer, e.g., between *A. baylyi* and *Escherichia coli* (Fulsundar et al. 2014). Non-conjugal plasmids can be transferred via nanotubes, e.g., between *Bacillus subtilis* strains, yet the frequency of transfer is about 3 orders of magnitude lower in comparison to plasmid transfer via conjugation (Dubey and Ben-Yehuda 2011).

The entry of plasmids into a naïve host cell may be hindered at different levels. For example, the conjugative transfer of plasmids can be blocked by exclusion systems that maintain plasmid exclusivity within the host (e.g., Sakuma et al. 2013). In addition, defense mechanisms against foreign DNA such as restriction modification systems (Roer et al. 2014), CRISPR-Cas (Marraffini and Sontheimer 2008), or the recently described Wadjet system (Doron et al. 2018) can act on the plasmid upon entry. Another important factor restricting plasmid establishment is plasmid incompatibility. The presence of plasmids that encode related partitioning systems in the same host cell can lead to interference during plasmid partition and the consequent loss of one (or both) of the plasmids (Hyland et al. 2014).

Plasmid long-term persistence is determined by a combination of several factors, including plasmid mobility dynamics, the presence of host-beneficial genes, plasmid stability mechanisms, and the level of co-adaptation between the plasmid and the host. The persistence of plasmids carrying selective traits (i.e., beneficial) strongly depends on the environmental conditions and might thus be transient. Examples are plasmids that carry resistance genes that enable bacteria to grow under selective conditions of antibiotics or heavy metals (e.g., Harrison et al. 2015). In contrast, plasmids that are beneficial for the maintenance of the host lifestyle are expected to be highly persistent over longer time-scales. An example for such a ‘lifestyle plasmid’ is observed the *Burkholderia cepacia* complex whose members depend on plasmid-encoded virulence factors for their pathogenic interaction with the host (Agnoli et al. 2011). Another example for a ‘lifestyle plasmid’ is the plasmid-encoded rhamnose operon in *Roseobacter* that has

been shown to be essential for the host life cycle and its ecological success. The rhamnose operon is essential for biofilm formation and the absence of the plasmid entails a loss of the ability to switch between motile and sessile forms (Michael et al. 2016).

Notably, plasmid persistence can also occur independently of a plasmid-encoded beneficial function. Plasmids that persist in the absence of a beneficial function typically encode a “survival kit” that includes, in addition to mechanisms for stable replication, an active partitioning mechanism, and a multimer resolution system that ensures reliable inheritance of plasmids to daughter cells over generations (reviewed in Baxter and Funnell 2014). Persistent plasmids may also encode specific survival mechanisms, for example addiction systems, that function in post-segregational killing of plasmid-free cells, thus leading to an only-hosts population. Examples are restriction modification or toxin-antitoxin (TA) systems that are often observed in plasmid genomes. For example, all four plasmids in *Synechocystis* sp. PCC 6803 harbor at least three putative TA systems and one plasmid encodes even ten different TA cassettes (Kopfmann et al. 2016).

An important aspect of plasmid persistence is the effect of plasmid maintenance on the host fitness. When an invading plasmid imposes a metabolic burden on the host (i.e., it has a negative effect on the host fitness), non-hosts are expected to take over the population and the plasmid will go extinct. Accordingly, increasing evidence implies that a mechanism for long-term plasmid persistence in naïve bacterial hosts is the reduction of plasmid-associated fitness costs through coevolution (Loftie-Eaton et al. 2016, Porse et al. 2016, Harrison et al. 2015, Yano et al. 2016, San Millan et al. 2014). Plasmid-host coevolution is most likely to occur under positive selection for the plasmid maintenance and it may occur via adaptation of the plasmid backbone to the host replication machinery (Yano et al. 2016, Sota et al. 2010). Additionally, adaptive mutations to the plasmid maintenance may occur in the host chromosome, as was shown in an experimental evolution study of a mercury-resistance megaplasmid in *Pseudomonas fluorescens*. In that experiment, after 450 generations under selective conditions, a mutation at the chromosome-encoded GacS/GacA two-component regulatory system led to an overall down-regulation of translation, which improved host fitness and prevented the plasmid from going extinct (Harrison et al. 2015).

2.2 Plasmid genome evolution

Experimental evolution studies of plasmid-host coevolution opened up opportunities to follow plasmid adaptation and genome evolution in real time. Evolution of the plasmid genome can occur at two levels of magnitude: single-nucleotide mutations or large-scale structural changes (e.g., insertions, deletions, inversions and translocations). On a global

scale, single nucleotide substitutions drive the sequence amelioration of plasmids found in long-term associations with defined host ranges towards the genomic signatures of their hosts (Suzuki et al. 2010). Nucleotide substitutions in the plasmid backbone genes can potentially affect the plasmid replication dynamics and adaptation to the host. Studies of plasmid evolution within naïve hosts under strong selective conditions (e.g., for antibiotics resistance) showed that SNPs in the plasmid backbone can arise rapidly and may lead to the adaptation of a new host range (Fernández-Tresguerres et al. 1995, Maestro et al. 2003, Sota et al. 2010). In addition, the evolution of accessory genes that are encoded on multicopy plasmids (i.e. copy number larger than one) may correspond to gene amplification in prokaryotes (i.e., the presence of multiple paralogs on the chromosome). In other words, the multiple copies of the plasmid-encoded gene are expected to increase the mutation supply rate and enable rapid evolution of the gene. Indeed, a recent experimental evolution study selecting for increased resistance to Ceftazidime demonstrated that adaptive SNPs in bla_{TEM1} encoded on a plasmid with up to 19 copies per cell could emerge within a very short time – only 42 generations of serial transfer (San Millan et al. 2016).

Evolution of large-scale structural variants in plasmids is often observed in the neighborhood of transposons and IS-elements. This suggests that such elements play a prominent role in plasmid genome evolution. Transposition-mediated acquisition of new genes (i.e., insertion) has the potential to have a significant impact on the plasmid fate, for example, via the acquisition of a plasmid addiction system (Loftie-Eaton et al 2016). Additionally, the presence of IS-elements can lead to large-scale deletions via homologous recombination. An example is a large-scale deletion observed in an experimental evolution study of plasmid adaptation in *E. coli* where an IS-element mediated a large-scale deletion that led to a loss of the Type IV secretion system (T4SS) comprising the conjugation machinery (Porse et al. 2016). This deletion rendered the plasmid non-conjugative and consequently it had implications for the maintenance costs of the plasmid and the plasmid host range. The transposition of IS elements between plasmids can furthermore lead to the evolution of plasmid fusions (He et al. 2015).

Gene translocation from the plasmid to the chromosome constitutes an instance of lateral gene transfer and may have implications for the plasmid fate. Thus, the translocation of a beneficial gene from the plasmid to the chromosome may lead to plasmid loss (Stoesser et al. 2016, Harrison et al. 2015). For example, a Tn*5042* transposase-mediated translocation of a 10-genes mercury resistance operon (*mer*) has been observed in *P. fluorescence*. The *mer* translocation led to subsequent loss of the plasmid, yet, most of the population retained the plasmid and the chromosomal *mer* variant rarely reached a high frequency in the population (Harrison et al. 2015). The

results of this experiment suggest that the *mer* translocation was not necessarily beneficial for the host.

Recombination, including homologous recombination (Norberg et al. 2011), among plasmids and other mobile elements appears to be frequent during plasmid evolution, especially between IS-elements and transposons (He et al. 2015, Szabó et al. 2016). The observation of prophages included in plasmid genomes indicates that lysogenic phages can mediate large insertions into plasmids. Thus, transduction constitutes another mechanism for the gain of accessory genes in plasmids. For example, a comparative genomics study of megaplasmids in the *Bacillus cereus* group observed that these plasmids must have resulted from multiple fusion events of smaller plasmids (Zheng et al. 2013), with 29 of 31 megaplasmids containing two or more conserved replicon regions. Thus, plasmid fusions appear to be a frequent phenomenon and may underlie the evolution of plasmids that display modular characteristics through reshuffling of structural modules in the plasmid genome (Zaleski et al. 2015). Notably, the presence of multiple replicons in a plasmid may prevent plasmid incompatibility (Chen et al. 2014) and facilitate interaction with a broad range of hosts (Villa et al. 2010).

2.3 Plasmid copy number and segregational drift

Plasmids differ from the chromosomal genetic component in several key aspects, including a relatively small genome size and a variable ploidy level. Plasmids are often found in multiple copies in the cell where the plasmid copy number (PCN) depends on the replicon type, the host genetics, and the environmental conditions (Nordström 2006, Santos-Lopez et al. 2016). The copy number of natural plasmids ranges between 1-15 for low-copy plasmids (Bazaral and Helinski 1968) and can reach 200 copies for high-copy plasmids (Projan et al. 1987). Plasmids used for biotechnological applications are often modified to have a higher copy number, e.g., 500-700 (Vieira and Messing 1982, Rosano and Ceccarelli 2014), in order to maximize the protein expression level of focal genes. Notably, genes encoded on multicopy plasmids residing within a single host cell may comprise multiple alleles due to independent emergence of mutations in the plasmid copies (Bedhomme et al. 2017, Rodriguez-Beltran et al. 2018). An increased plasmid copy number has the potential to elevate the probability for the emergence of novel mutations in the gene open reading frame. Consequently, the mutational supply of plasmid-encoded genes is increased for multicopy plasmids. Indeed, it has been previously shown that multicopy plasmids have the potential to enable rapid evolution of plasmid-encoded antibiotic resistance genes under strong selective conditions for the antibiotic resistance (San Millan et al. 2016).

The inheritance of multicopy plasmids to daughter cells depends on their segregation mechanism. Some plasmids are equipped with an active partition system. Such systems comprise plasmid-encoded proteins that function in the translocation of plasmid copies toward the cell poles prior to cell division, thereby ensuring stable inheritance (e.g., *parABS* system (Abeles et al. 1985, Baxter and Funnell 2014)). In the absence of a partition system, plasmid segregation into daughter cells depends on the physical distribution of plasmid copies in the cell during cell division (Wang 2017). Notably, plasmid segregation into daughter cells in both routes is considered to occur in the absence of selection on the plasmid allele pool. Consequently, the dynamics of multicopy plasmid alleles in the population has a constant component of random genetic drift. In other words, the distribution of plasmid alleles into daughter cells is independent of the allele impact on the host fitness, also under selective conditions for a plasmid-encoded trait. Here, this phenomenon is termed *segregational drift*. Previous studies suggested that segregational drift plays a role in the evolution of eukaryotic organelles – mitochondria and plastids (Birky 2001). Similar to multicopy plasmids, the mitochondrion organelle is found in multiple copies in the cell (e.g., ~1,700 in mammalian cells (Robin and Wong 1988)), and in addition, each mitochondrion organelle may harbor multiple copies of the mitochondrial genome (e.g., up to 10 copies (Satoh and Kuroiwa 1991)). Thus, the mutational supply on the mitochondrial genome is larger than the mitochondrial genome size by several orders of magnitude. The combination of high mutational supply on the mitochondrion genome and random segregation of the mitochondria during cell division lead to genetic heterogeneity of the mitochondrial genomes within a single cell (termed ‘mitochondrion heteroplasmy’ (Birky 2001)). Notably, many of the mitochondrial alleles are found in very low frequency, thus the mitochondrial genetic heterogeneity is observed only with the application of deep-sequencing approaches (e.g., He et al. 2010). The consequences of segregational drift to the evolution of multicopy plasmids have been so far overlooked.

2.4 Objectives

Here we hypothesize that segregational drift has implication for the evolutionary rates of plasmids by lowering the number of accumulating mutations that are expected from the mutational supply. Population genetics theory postulates that the effect of random genetic drift on allele dynamics is inversely correlated with the effective population size. In a larger population, the impact of genetic drift on the dynamics of allele frequency is reduced (see Lanfear et al. 2013 for review). Thus, the implications of segregational drift to plasmid genome evolution are expected to be dependent on the plasmid population size within the cell, i.e., the plasmid copy number. To test this hypothesis we compare the evolutionary rates of two model plasmids: a low-copy plasmid having ca. 10 copies per cell and a high-copy plasmid having ca. 100 copies per cell. The mutational supply of the high-copy plasmid is thus considered to be ca. 10-fold in comparison to the low-copy plasmid. In the absence of segregational drift, the high copy plasmid is expected to accumulate much more mutations in comparison to the low-copy plasmids. In contrast, if segregational drift has an impact on plasmid genome evolution we would expect that the number of accumulating mutations on the high-copy plasmid would be equal, or smaller, in comparison to the low-copy plasmid.

3 Material and Methods

3.1 Bacterial strains and growth conditions

Escherichia coli K-12 substr. MG1655 (DSM no. 18039, DSMZ) and a mismatch-repair deficient *E. coli* MG1655 derivative strain (Δ*mutS*) were used in the evolution experiment. *Escherichia coli* DH5α (Hanahan 1983) was used during construction of plasmids. All strains were routinely grown at 37°C in LB medium with aeration. When required, growth medium was supplemented with 100 µg ml^{-1} ampicillin, 15 µg ml^{-1} kanamycin or 3 µg ml^{-1} tetracycline. The evolution experiment was performed in M9 medium ($M9/amp_{100}$) prepared as described (Sambrook and Russell 2012), supplemented with 0.4% (w/v) glucose, 0.1% (w/v) casamino acids, 20 mg L^{-1} uracil, 0.5 mg L^{-1} thiamine, 0.005% (v/v) Antifoam 204 (Sigma-Aldrich), and 100 mg L^{-1} ampicillin.

3.2 General DNA techniques

Phusion polymerase (Thermo Fisher Scientific) was used for amplification of DNA-fragments for cloning. DNA fragments obtained from restriction analysis were purified using the Wizard SV Gel and PCR Clean-Up System (Promega). PCR products that were judged as specific by gel-analysis, were used for ligations directly from PCR reaction mixtures. Plasmids were isolated using the GeneJET Plasmid Miniprep Kit (Thermo Fisher Scientific). Plasmid constructs were verified by restriction analysis and confirmed by sequencing. To this end, DNA fragments obtained from restriction analysis or PCR were ligated with pJET1.2/blunt cloning vector using CloneJET PCR Cloning Kit (Thermo Fisher Scientific) and delivered into chemo-competent *E. coli* DH5α cells. Inserts were sequenced using the pJET1.2 sequencing primer pair (CloneJET PCR Cloning Kit; Thermo Fisher Scientific). Linear DNA fragments and plasmids were introduced into *E. coli* MG1655 by electroporation using a Bio-Rad Gene Pulser device and parameters reported previously (Dower et al. 1988). PCR-primers are listed in Supplementary Table 2.

3.3 Construction of the host strains (wild-type and Δ*mutS*)

A marker-free *E. coli* MG1655 Δ*mutS* deletion strain was constructed using the λ Red/ET Quick & Easy *E. coli* Gene Deletion Kit (GeneBridges). Briefly, the *mutS* gene was replaced with a PCR generated DNA fragment (primer pair mutS_KO_F/R) containing a

kanamycin resistance marker gene flanked by FRT sites. The replacement of *mutS* with the marker-containing cassette was verified by PCR (primer pair PGK_F/mutS_test_R). One kanamycin resistant clone was chosen for the removal of the kanamycin resistance marker through expression of the site specific FLP recombinase carried on plasmid 707-FLPe (GeneBridges). One resulting kanamycin-sensitive clone that had lost 707-FLPe was chosen and the deletion of the marker-containing cassette was verified by PCR using primer pair mutS_test_F/R.

In order to potentially compare mutations occurring within non-coding segments of DNA, both plasmids and host strains were equipped with segments of randomly composed, non-coding DNA. A 600 bp-stretch of non-coding DNA (art3) was commercially synthesized (GeneArt Strings Service, Thermo Fisher Scientific) and inserted into the Tn*7*-specific *attTn7* site of the wild-type and Δ*mutS* strain following the method described previously (McKenzie and Craig 2006). Briefly, the art3 DNA-fragment was amplified by using primers art3_F and art3_R and cloned into the *Not*I restriction site present in the mini-Tn*7*-transposon carried on the transposition vector pGRG25 (GenBank acc. no. DQ460223). The resulting plasmid was delivered into *E. coli* wild-type and the Δ*mutS* strain and a clone carrying the chromosomal *att*Tn7*::*miniTn7*(art3)* insertion was verified by PCR targeting the Tn*7*-insertion site using the primer pair attTn7_F/R.

3.4 Construction of plasmids pLC and pHC

Plasmid pBBR1MCS-5 (GenBank acc. no. U25061) was used to construct plasmid pLC. The gentamicin resistance cassette was replaced by an ampicillin resistance marker (*bla*). Therefore, a 1,944-bp fragment of plasmid pBBR1MCS-5 comprising the gentamicin resistance gene and the *lacZ*α gene fragment was excised with *BstB*I and *Bsa*I. The resulting plasmid backbone fragment (2,824 bp) comprised the origin of replication, the *rep* gene and a fragment of the *mob* gene. This backbone fragment was blunted and ligated to a blunted *Kpn*I-*Sac*I fragment containing *bla* with its promoter, giving plasmid pBBR1-bla. The *bla* resistance cassette was obtained from pBluescript SK(+) into which the *bla* fragment had been inserted into the *Eco*RV site as a blunted *Cla*I-*Not*I fragment from plasmid pKD4 (GenBank acc. no. AY048743). Next, 600 bp long stretches of random DNA (designated as art1 and art2) were inserted into the *Eco*RI site (art1) and into the *Xho*I site (art2) of pBBR1-bla, giving plasmid pLC (GenBank acc. no. MH238456).

The high copy plasmid pHC (GenBank acc. no. MH238457) was constructed as plasmid pLC, but the *oriV* and the *repA* gene were then replaced by a pUC origin of replication. This was achieved by amplifying the plasmid except for the region comprising the *oriV* and the *repA* gene (using primer pair inv_pLC_F/R)**.** The resulting fragment

(2,735 bp) was treated with T4-Polynucleotide Kinase (New England Biolabs) and ligated to a PCR fragment (916 bp) comprising the pUC-origin of replication amplified from plasmid pCR4-TOPO (Thermo Fisher Scientific) with primer pair pUC-ori_F/R.

3.5 Quantitative Real-Time PCR

Quantitative Real-Time PCR (qPCR) was used to determine plasmid copy numbers (PCN), to test for cross-contamination between culturing vessels in the evolution experiment and to determine transcript levels. Reactions were carried out in a total volume of 10 µl containing 1x iTaq Universal SYBR Green Supermix (Bio-Rad Laboratories), 100 nM of each primer (final concentration) and 1 µl sample. All qPCR reactions including positive and non-template controls were performed in technical replicates on a CFX Connect Real-Time PCR Detection System (Bio-Rad Laboratories) using the following cycling conditions for all reactions: 95°C for 3 min, 40 cycles of 10 s at 95°C and 1 min at 59°C. For melt curve analysis, a dissociation step was added at the end by stepwise increase of temperature ranging from 55°C to 95°C and monitoring changes in fluorescent signal every 0.5°C. Primers for qPCR were designed using SnapGene software v.2.4 (GLS Biotech) and specificity and efficiency were tested using qPCR-generated standard curves and melt-curve analysis of qPCR products. Primer efficiency was calculated using the slope of a standard curve ($R^2 > 0.99$) generated from a 10-fold series dilution of purified DNA (i.e., plasmid or chromosomal DNA) or using DNA from whole cell extracts (see description below). Amplification efficiencies were greater than 1.93 for each primer pair used in this study. Melt curve analysis of each reaction indicated that the primer pairs were specific. In addition, qPCR amplicons were Sanger sequenced. The amplicons shared a 100% nucleotide sequence identity with the corresponding plasmid or chromosomal sequences. Cycle threshold (Ct) values were determined after adjusting the fluorescence signal threshold using CFX Maestro software (Bio-Rad Laboratories). Ct values varied ≤ 2% between technical replicates. All quantifications were made using mean Ct values of technical replicates and considering different amplification efficiencies of primer pairs. As control DNA, chromosomal DNA extracted from *E. coli* MG1655 and plasmid DNA (i.e., pLC and pHC) were used.

Plasmid copy numbers were determined as described by (Skulj et al. 2008), but with primers complementary to the *idnT* gene in the *E. coli* MG1655 background (q_idnT_F/R) and complementary to the *bla* gene (q_bla_F/R) on plasmid pLC and pHC. PCN is defined as the number of plasmids per chromosome. Thus, PCN is calculated as the ratio of the number of plasmid specific amplicons and the number of chromosome specific amplicons. To keep the quantity and quality of nucleic acids unchanged until

qPCR, PCN was determined from whole cell lysates without DNA purification (Skulj et al. 2008). Therefore, aliquots of overnight cultures or chemostat cultures were collected, heated at 98°C for 10 min to disrupt cells, followed by immediate freezing at -20°C for at least 20 min. After thawing, the samples were serially diluted 10-fold and qPCR reactions were carried out using at least two different dilutions of a sample. Samples were always kept on ice while processing. For the determination of single colony PCNs, colonies were picked, streaked on M9 and M9/amp$_{100}$ backup plates and diluted in 20 µl $_{dd}H_20$ and cells were processed as described above. Unless otherwise stated, PCNs were determined as the mean PCN of two sample dilutions and considering primer efficiencies.

Transcript levels of the chromosomal stress-response gene *groEL* and the chromosomal reference gene *idnT* (Zhou et al. 2011) were assessed from chemostat cultures using qPCR. The consistency of transcript levels between replicative cultures was used in addition to optical density measurements at 600nm (OD_{600}) and cell counts as an indicator for the reproducibility of steady state growth. Total RNA was isolated from chemostat cell cultures using a hot SDS/hot phenol method. To this end, cells of 500 µl steady-state chemostat cultures were instantly lysed by adding 250 µl of SDS solution (2% SDS, 16 mM EDTA) preheated to 100°C. After 5 min incubation at 100°C RNA was isolated by two extractions with one volume acid phenol/chloroform solution (Thermo Fisher Scientific) preheated to 65°C and one extraction with one volume of chlorophorm:isoamyl alcohol (24:1). The RNA was isopropanol-precipitated, washed with ice-cold 70% ethanol, dried and dissolved in Diethyl pyrocarbonate-treated water. Quality and quantity of RNA was assessed using gel electrophoresis and and micro-spectrophotometry (Nano Drop Technologies). To remove any genomic DNA contamination, RNA was treated with RNase-free Ambion DNase I (Thermo Fisher Scientific). Removal of DNA was confirmed by performing qPCR on 50 ng of RNA using the *idnT* primer set. RNA samples found to yield Ct-values larger than 32 were judged to be sufficiently free of DNA. First-strand cDNA synthesis of 500 ng total RNA was performed using iScript cDNA synthesis kit (Bio-Rad Laboratories).

In addition to PCR, qPCR was used to test for cross-contamination between chemostat cultures of different genotypes. Therefore, combinations of plasmid specific primers and host genotype specific primers were used. Each sample was tested for the presence of the *mutS* gene and for the presence of both plasmids using the following primer pairs: q_pBB_rep_F/R complementary to the *rep* gene of plasmid pLC, q_pUC_ori_F/R complementary to the *ori* of plasmid pHC, and primer pair q_mutS_F/R complementary to the *mutS* gene in the *E. coli* MG1655 background.

3.6 Chemostat characteristics

Chemostats were assembled from off-the-shelf materials similar in design previously suggested for the cultivation of yeast (Miller et al. 2013). The entire chemostat culturing system consists of four different modules; the culture vessels, the media supply, the air supply and the efflux part. Modifications to the suggested chemostat design were introduced to enable long-term cultivation of bacteria. An air break was placed between the culture vessels and the medium supply tubing to prevent bacterial growth into the medium supply module (Figure 1). An air break is composed of an autoclavable syringe (20 ml), a plug with a needle for the tubing and a syringe filter (PES, 0.2 µm) as an additional barrier.

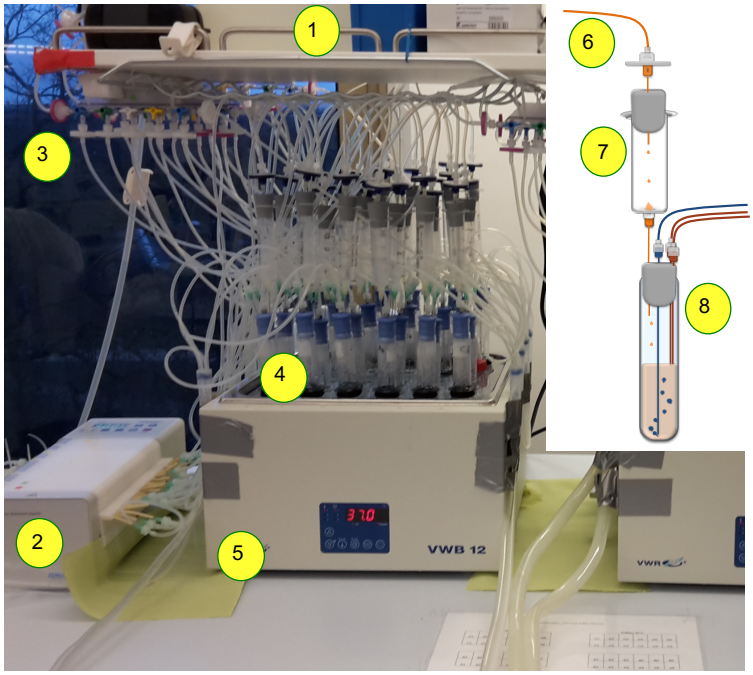

Figure 1. A side view of the chemostat system as it was used in the evolution experiment. Additional details on the establishment are shown in Figure 3. Briefly, the system is composed of 1) Media carboy, 2) Peristaltic pump, 3) Air supply, 4) Culturing units and 5) Water bath. A culturing unit includes 6) Media inflow channel, 7) Air break, 8) Culturing vessel including an air supply channel (blue) and two culture effluent channels (red). Effluent reservoirs are shown in Supplementary Figure 4.

The culture vessels were equipped with a second effluent needle to ensure constant efflux in case of clogging due to biofilm-formation. Furthermore, a gas washing bottle ($_{dd}H_20$ supplemented with a biocide agent) was used instead of gas filters at the outlet of the effluent reservoirs, because of frequent clogging of the filters (i.e., wetting). Similarly, a gas washing bottle meant for air hydration within the air supply module was not included, because of frequent malfunction of downstream gas filters (i.e. wetting of filters). Additionally, no impact of evaporation on the culture was was observed at the dilution rate used in this study. Effluent tubings were kept as short as possible to reduce flow

resistance and thus ensure stable efflux flow. Ultra-smooth Tygon tubing that reduces the risk of particle entrapment was used to prevent biofilm formation at the inner surface of the hoses. A complete list of all material is given in Supplementary Table 3. Samples for measurement of OD, PCN and cell counts were collected from the effluent of the chemostat populations. These samples were equivalent to samples taken directly from the culture vessels (see Section 4.1). Each chemostat was operated at a dilution rate D of 0.27 h^{-1} corresponding to a flow rate of 90 µl min^{-1} and a turnover time of 3.7 h. The uniformity of flow rates provided by the two multiplexed peristaltic tubing pumps was assessed by measuring the volume of M9 medium pumped through all 24 channels of each pump. This test was conducted after calibration of the pumps according to manufacturer instructions. In addition, the uniformity of flow rates was tested each time the tubing was replaced (every 2-3 weeks). There were no significant differences in the media pumped through between the 24 channels of pump 1 and between the 24 channels of pump 2 in any of the tests conducted throughout the course of the experiment. Furthermore, there were no significant differences in volume pumped through between the two peristaltic pumps.

3.7 Experimental evolution

To study the combined effects of mutation supply (i.e., mutation rate of the host), plasmid copy number and growth condition (i.e., temperature), the evolution experiment was conducted using a full factorial 2×2×2 design (Table 1). Therefore, plasmid pLC and pHC, respectively, were transferred into the wild-type and the Δ*mutS* strain, giving for each host genotype two plasmid-carrying subtypes (i.e., wt-pLC, wt-pHC, Δ*mutS*-pLC, and Δ*mutS*-pHC). Six biological replicates of each of these subtypes were then evolved at 37°C and 42°C (Table 1).

Table 1. Experimental design. Factors, levels and number of biological replicates used in the evolution experiment.

Factor		**Levels**			
Host genotype		Wild-type		Hypermutator	
Plasmid type		pLC	pHC	pLC	pHC
Temperature	37°C	6	6	6	6
	42°C	6	6	6	6

Prior to the experiment, a single colony of each subtype was used to found a population that was serially passaged (1:1000) daily for about 100 generations in 5 ml M9/amp$_{100}$ media at 37°C to acclimate the populations to the media conditions. At the onset of the evolution experiment, 50 µl overnight culture of each population was used to inoculate six replicate chemostat cultures with a working volume of 20 ml. The 48 chemostat cultures were grown to stationary densities overnight (i.e., without addition of media) at 37°C or 42°C and then continuously incubated at a dilution rate of 0.27 h^{-1}. Samples were collected as described in Section 4.1 at the time that steady-state growth was achieved (generation 1). Steady state growth was routinely achieved after 26 h (see Section 4.1). Every three weeks (approximately 200 generations), the chemostat cultures were frozen and stored at -80°C in 25% (v/v) glycerol. From these frozen stocks, the chemostat cultures were restarted as follows: 10 ml of the frozen stock culture were pelleted by low-speed centrifugation (5,000 x *g*) for removal of glycerol and the cells were harvested in the final culturing volume of 20 ml and transferred into chemostat vessels. The remaining frozen cultures served as backups for the re-establishment of experimental cultures in case of contamination or loss of culture due to malfunction of the chemostat system. Prior to cryo-preservation of the chemostat cultures, all cultures were reciprocally tested for cross-contamination using qPCR. Additional contamination control was done on a regular basis by plating dilutions of the chemostat cultures on M9 and LB agar plates. Each population was evolved for 90 days at steady-state resulting in approximately 800 generations.

Prior to the evolution experiment, the critical dilution rate was determined for each strain (i.e., pLC-wt, pLC-hypermutator, pHC-wt, pHC-hypermutator) using the method of washout (e.g., Pirt and Callow 1960)). To this end, for each strain three culturing vessels were inoculated and grown to steady-state at 37°C and 42°C as described above. Culture densities were then estimated by colony count after plating a sample on M9 agar. Next, the dilution rate was increased and after reaching stead-state, culture densities were estimated. This procedure was followed for each of the following dilution rates: 0.09 h^{-1}, 0.18 h^{-1}, 0.24 h^{-1}, 0.38 h^{-1}, 0.5 h^{-1}. Because mutations affecting growth parameters of the *E. coli* strains may occur during culturing, the replicates were re-established from the same ancestor after two changes in dilution rate.

Growth rates of the ancestral plasmid carrying strains and the plasmid-free hypermutator and wild-type *E. coli* strains were determined as follows. Cultures were grown overnight in M9 medium to stationary phase, were diluted 100-fold in 10 ml fresh M9 medium and 300 µl were then used to measure the optical density at 600nm in a 96-well microtiter plate, which was incubated at 37°C or 42°C with agitation for at least 14 hours (6 replicates per culture) in a Multiskan GO Microplate Spectrophotometer (Thermo

Fisher Scientific). The OD_{600} was recorded every 10 min and the growth rate was determined by nonlinear fitting of a logistic growth model using R package `Growthcurver` (Sprouffske 2016).

3.8 Proportion of plasmid-hosts and plasmid loss frequency

The fractions of plasmid-bearing cells in ancestral and evolved populations were determined by plating appropriate dilutions of archived cultures on M9 agar with and without ampicillin (termed here differential plating). Colony forming units (CFU) were counted after overnight incubation and the proportion of hosts was estimated as the ratio of mean CFU/ml on selective and mean CFU/ml on non-selective medium. An additional method (streak method) was used to determine the proportion of hosts by streaking single colonies (grown on M9 medium) on M9/amp_{100} and M9 agar to obtain single colonies. After overnight growth at 37°C or 42°C, the proportion of hosts was calculated as the ratio of the number of test colonies grown selective medium and non-selective medium.

Cell population densities were estimated from the chemostat cultures approximately every 100 generations by colony counting to determine the number of viable cells (CFU/ml) or by measurement of optical density (OD_{600}). Cell densities were determined from biomass concentration (OD_{600}) using a fitted standard curve (R^2 = 0.9968) with the linear relationship CFU/ml= 8.23 10^8 × OD - 1.58 × 10^7.

To determine the segregational loss of plasmid pLC and pHC, five single colonies of each strain (i.e., wt-pLC, wt-pHC) were picked from M9/amp_{100} agar plates and grown overnight in 2 ml M9/amp_{100} with constant shaking at 37°C for approximately 4.4 ± 0.42 (*SD*) generations. Appropriate dilutions of stationary cell cultures were plated on M9 agar, incubated overnight at 37°C, and 100 colonies per replicate were streaked onto M9/amp_{200}, M9/amp_{100}, and M9 plates. The number of plasmid-free segregants was determined from the comparison of colonies grown on selective and non-selective plates.

3.9 Whole genome sequencing

The ancestral populations of the wild-type and the Δ*mutS* strain carrying the designated plasmids (wt-pHC, wt-pLC, Δ*mutS*-pHC, and Δ*mutS*-pLC) and the 48 populations evolved for 800 generations were sequenced using Illumina sequencing technology. Population sequencing was used to enable the detection of rare variants and to asses the frequency of alleles within and across populations. Total DNA (genomic DNA plus plasmid DNA) was isolated from archived samples stored at -80°C using the Wizard Genomic DNA Purification kit (Promega). The preparation of DNA for sequencing of the evolved

populations differed between the two plasmids due to the difference in their stability within the host. For pLC-populations, 1 ml of cell suspension from thawed samples was used for DNA extraction. The frequent loss of pHC led to the presence of plasmid-free segregants in the evolved populations. Therefore, in addition to the sequencing of DNA extracted from total pHC-populations, DNA was sequenced from pooled colonies of plasmid-carrying cells. The deep sequencing of plasmid-carrying hosts allows the detection of rare variants from a population of cells with a potentially heterogeneous plasmid allele pool. DNA from total pHC populations was isolated from archived samples as described for pLC-populations. The preparation of DNA from plasmid-carrying cells included a preliminary stage of selection for plasmid-hosts. Thus, frozen chemostat culture samples were first plated on LB plates supplemented with ampicillin (100 μg ml^{-1}) and grown overnight at 37°C or 42°C, to select plasmid-carrying cells. Then, 100 colonies per pHC-population were pooled for extraction of total DNA (i.e., 4x600 colonies in total). Sample libraries for Illumina sequencing were prepared using either the Nextera or Nextera XT library preparation kit. All samples were quantified on a Qubit fluorometer (Invitrogen by Life Technologies) and DNA fragment length distribution was assessed on a TapeStation (Agilent Technologies). Libraries were sequenced on either a HiSeq 2500 platform with 2x125 bp reads or a NextSeq 500 platform with 2x150 bp reads (see Supplementary Table 4 for details). Due to low initial coverage, some libraries of the wt-pLC and wt-pHC populations were re-sequenced on a HiSeq 2500 platform. Sequence reads of evolved and ancestral populations are found in SRA (SRA acc. SRP141152). Plasmid sequences are found in GenBank (pLC: MH238456, pHC: MH238457).

3.10 Variant detection

Sequencing reads were trimmed to remove both Illumina specific adaptors and low quality bases using the program Trimmomatic v.0.35 (Bolger et al. 2014) with these parameters `ILLUMINACLIP:NexteraPE-PE.fa:2:30:10` `CROP:150/125` (NextSeq/HiSeq) `HEADCROP:5 LEADING:20 TRAILING:20 SLIDINGWINDOW:4:20 MINLEN:36`. Quality of sequencing reads was inspected before and after trimming using FastQC v.0.11.5 (Andrews 2016). Plasmid genomes of all ancestor samples were assembled by plasmidSPAdes (SPAdes v.3.9.0; Bankevich et al. 2012, Nurk et al. 2013) using trimmed paired end sequencing reads. To improve assembly speed and accuracy of the high copy plasmid pHC of ancestor samples BBNorm (BBMap tool suite v.35.82; https://sourceforge.net/projects/bbmap/) was used to normalize paired end read data to an average coverage of 200x. This resulted in contigs with overhangs at each end which enabled the mapping of otherwise non-alignable reads. There was no variation between plasmid assemblies of the same type. Therefore, only one assembly of plasmids pLC and pHC was used as a reference for variant detection. Plasmid genome assemblies were verified and annotated using SnapGene software v.2.4 (GLS Biotech). Host chromosomes were assembled by SPAdes (SPAdes v.3.9.0; Bankevich et al. 2012). The contig containing the artificial sequence was extracted using BLAST (Altschul et al. 1990) and it was used to replace the corresponding sequence in the *E. coli* K-12 MG1655 reference genome file (NCBI accession no. NC_000913.3) using SnapGene software.

As illustrated in Figure 2, reads were then mapped to this reference genome and to the assembled plasmid genomes using BWA-MEM v.0.7.5a-r405 (Li and Durbin 2009). Corresponding mapping files of libraries that were sequenced twice were merged using PICARD tools v.2.7.1 (http://broadinstitute.github.io/picard/). Mapping statistics were retrieved using BAMStats v.1.25 (https://sourceforge.net/projects/bamstats/files/). Then, indexing, local realignment of sequencing reads, removal of ambiguous aligned reads and read duplicates were performed using PICARD tools, SAMtools v.0.1.19 (Li et al. 2009) and GATK v.3.6 (McKenna et al. 2010) retaining only paired mapped reads with a minimum mapping quality of 20.

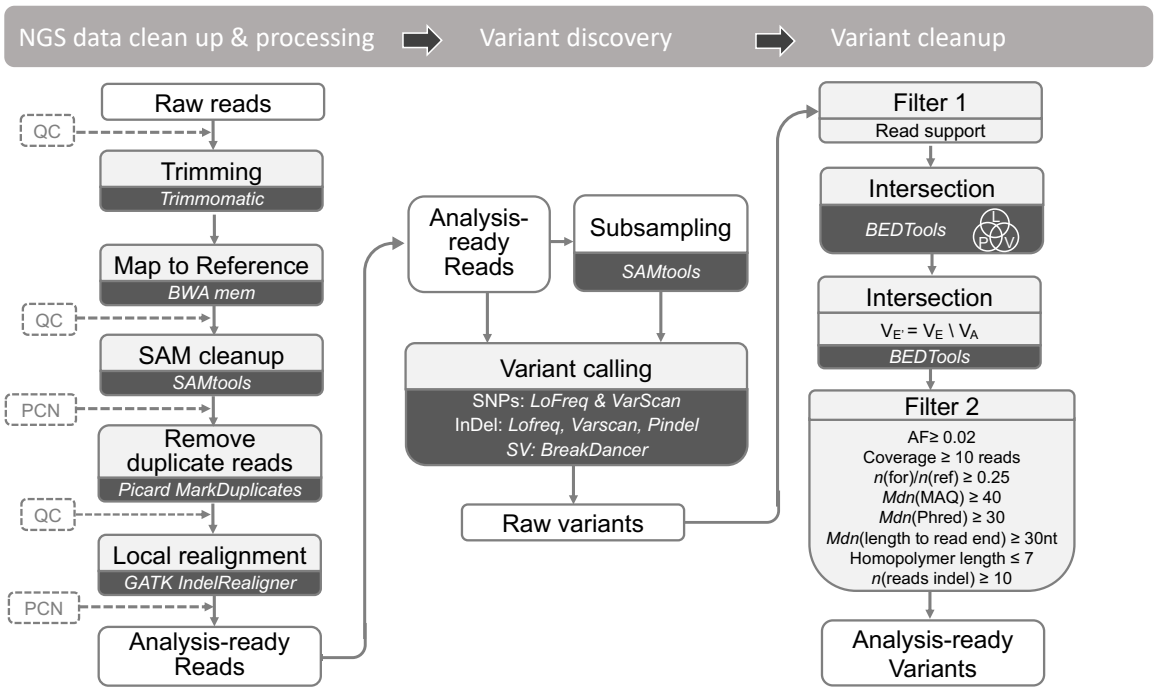

Figure 2. Illustration of bioinformatic pipeline used for variant detection.

To enable a between-sample and between-replicon comparison of measures deduced from the sequencing reads (e.g., number of mutations) that is not biased by differences in sequencing coverage, subsampling of reads was performed. To this end, mapping files were first split by contig (i.e., plasmid and chromosome) using BamTools v.2.4.2 (Barnett et al. 2011) and then subsampled to a mean minimum coverage of 104x using SAMtools (seed 1). Subsampled and non-subsampled (total coverage) BAM-files were then used to call variants. Short indels and SNPs were called using LoFreq v.2.1.2 (Wilm et al. 2012) and VarScan v.2.4.3 (Koboldt et al. 2009). Pindel v.0.2.5b9 (Ye et al. 2009) was used with options `-v 30 -M 2` to detect indels.

The maximum number of reads used to call variants with LoFreq and to call variants with VarScan by using SAMtools mpileup was set to 15,000,000 for non-subsampled datasets. Variants that were supported by alternative reads in one direction only were removed. Furthermore, only variants that were concordantly identified by two or more of the variant calling tools were retained using BEDTools' intersect utility v.2.17.0 (Quinlan and Hall 2010) with parameters `-f 1.0 -r -u`. BEDTools' intersect utility was then used with parameters `-f 1.0 -r -v` to exclude variants present in the corresponding ancestral samples. A custom python script using pysam (https://github.com/pysam-developers/pysam) and R version 3.4.3 (R Core Team 2017) were then used to retain only variants that met the following criteria: allele frequency ≥ 0.02, depth of coverage ≥ 10, ratio of the numbers of forward and reverse reads supporting the variant ≥ 0.25, a minimum medium mapping quality of 40, a minimum medium base quality of 30 and a minimum median length of 30 nt to the end of the reads

supporting the variant, a homopolymer length ≤ 7 and at least 10 reads supporting an indel. Variants that were found in proximity of 20 nt to each other within the same sample were excluded. Variants whose read support at the corresponding position in ancestor samples was not sufficient to detect a variant (<10x) were excluded (an overview on filter steps is shown in Figure 2).

Variant genomic location and the type of mutation, i.e., intergenic, synonymous, non-synonymous, or nonsense, were annotated using an in-house Perl script. Plasmid copy numbers were inferred from the de-duplicated (and non-de-duplicated), non-subsampled BAM files as the ratio of plasmid to chromosomal mean coverage.

3.11 Statistical methods

Statistical data analysis and visualization were carried out in the R environment (R Core Team 2017) using version 3.4.3 and packages reported in Supplementary Table 5.

4 Results

4.1 Optimization of chemostat culturing system

The chemostat system used in this study is based on a modular system suggested by (Miller et al. 2013) for the cultivation of yeast. This culturing system is composed of a media supply module, an air supply that also serves for the stirring of the culture, culturing units, and an effluent module (see Methods for a detailed description). Because the growth of bacteria differs in several components from that of yeast, various culturing tests were conducted to evaluate the growth conditions for bacteria in that chemostat system. In each test, four to six independent chemostat cultures of *E. coli* MG1655 harboring plasmid pLC were grown at steady state for 7-21 days and 37°C. Unless otherwise stated, a dilution rate of 0.18 h^{-1} and a working volume of 20 mL were used. In addition, to test for contamination from external sources and to test for cross-contamination, three chemostat vessels were not inoculated with bacteria. During each test, continuity of stirring and media supply, culture volume, culture density or turbidity, and technical malfunctions were monitored at least two times per day. Based on these tests, several modifications were introduced to enable stable and continuous steady-state growth of bacteria for at least 21 days. During the first culturing test, bacterial biofilm formation within the media supply hoses was observed after approximately five days of steady-state culturing. This was most likely caused by aerosolized bacteria droplets, because the cultures were not in direct contact with the media inlet needle (see Figure 3B) and no shaking was applied during cultivation. The growth of bacteria into the media supply ports had the potential to result in cross-contamination between culturing units as 24 units are connected through one main media supply port (see Supplementary Figure 4A). Therefore, an air break made from off-the-shelf materials was placed between a culturing unit and the media port (see Figure 3B). Further test cultivation including the air break revealed sporadic biofilm formation inside the media supply tubing after seven days of steady state growth. Therefore, to prevent bacterial growth into the media supply hoses, syringe filters were placed between the media supply hoses and the air breaks (Figure 3B) and the filters were exchanged every third day. In addition, the air break units were exchanged at least every six days, because growth of bacteria inside two out of six air break units was observed after twelve days of culturing.

Furthermore, although special care was taken in the choice of hoses, biofilm formation was observed within the effluent tubing leading to blockage of effluent ports. Because the chemostat system was under constant positive pressure built up by tubing pumps, the blockage resulted in the movement of bacterial culture into the air supply. The hydrophobic gas filters downstream the manifold prevented the liquid to further move into the manifold, which could have caused cross-contamination between culture vessels connected through it (details shown in Supplementary Figure 4A). Therefore, to ensure the continuity of the steady-state, a second effluent needle was placed into the culture vessels. Although the second effluent port ensured steady-state culturing for at least ten days, extensive biofilm formation especially in re-used hoses required the exchange of effluent ports every eight to twelve days. Furthermore, owing to the small diameter of the effluent hoses (2 mm), the risk of fast blockage of hoses due to biofilm-formation was higher in comparison to hoses with larger diameters. Moreover, the small inner tube diameter frequently caused disturbance of the steady state as the positive pressure exerted by the pumps was not high enough to push the effluent through the tubing (40 cm length). According to the Hagen-Poiseuille law, the flow resistance within a tube is inversely proportional to the fourth power of the tube radius. Therefore, shortly after the effluent needle port (approximately 15 cm), the hoses were transferred into a tubing with a five-fold larger diameter. As a result, the flow resistance decreased and an improved continuity of the outflow was observed. In this setup, the overflow of six cultures was collected in a communal waste container that was emptied every third day (Figure 3A).

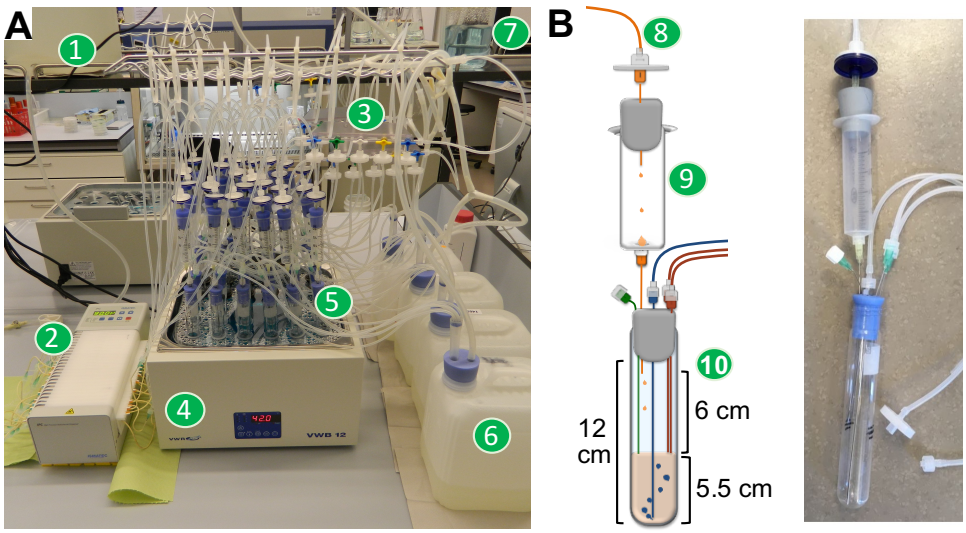

Figure 3. Establishment of a multiplexed miniature chemostat system for culturing of bacteria. (A) Chemostat system as it was used during establishment of the chemostat system: 1) media carboy, 2) peristaltic pump, 3) air supply, 4) water bath, 5) culturing units, 6) effluent reservoir, 7) air hydration bottle. **(B)** A culturing unit includes 8) a media inflow channel, 9) an air break and 10) a culturing vessel that includes an air supply channel (blue), two culture effluent channels (red), a media inlet needle (orange) and a sampling port (green). Note, that the distance from the tip of the media inlet needle to the surface of the liquid culture was approximately 6 cm.

To test for the possibility of contamination and cross-contamination between culturing units by way of the effluent module, six chemostat units that were not inoculated with bacteria were alternately arranged with six inoculated culturing vessels (example shown in Supplementary Figure 4F). For the non-inoculated cultures, effluent lines and culture vessels were monitored for bacterial growth by visual control and by plating appropriate dilutions from the effluent every day for 10 days of steady-state growth. After two days, bacterial contamination was found in two samples taken from the effluent of non-inoculated culturing units (M = 37.5 CFU ml^{-1}, SD = 17.08 CFU ml^{-1}, n = 4). Using PCR and genotype specific primers, it was verified that these were cross-contaminants. To test whether the contaminants grew into the culture vessels or contamination was local at the tips of the effluent tubings, a third sterile effluent needle along with a sterile effluent hose was introduced into the concerned culturing vessels. Samples were then taken from this port after pulling up the other two effluent needles (approximately 0.5 cm) such that the overflow was released through this sampling port. No bacterial contamination was found in any of the samples collected hourly from the two non-inoculated culture vessels within a six hour time frame. This indicated that the bacterial contamination was locally at the tip of the effluent tubing. Furthermore, following this sampling procedure, no contamination was found in any of the non-inoculated culturing vessels at any other sampling time point. This, and the visual inspection of the effluent tubing, further revealed that contamination at the outlet of the effluent tubing did not grow into the culture vessels. Therefore, to prevent cross-contamination during sampling, samples were thereafter collected using the sampling port.

Furthermore, to prevent loss of culture volume due to evaporation and to prevent the cultures from being contaminated with airborne bacteria, Miller et al. (2013) suggested to aerate the cultures with hydrated air and to use gas filters (PTFE membrane filters) downstream the hydration flask. During the culturing tests, frequent clogging of the air filters as a consequence of wetting (condensation) was observed. This resulted in a lack of positive pressure otherwise created by the air supply. As a consequence, liquid culture moved into the air supply hose and steady-state growth ultimately collapsed. However, the hydrophobic gas filters served as a barrier for bacterial culture to be pushed further into the air supply. Hence, in order to keep this barrier, it was not an option to place the gas filter upstream of the air hydration module (e.g., at the outlet of the air pumps). Thus, a culturing test without the hydration module was conducted for seven days of steady state growth. This trial experiment was carried out at 42°C, because evaporation of liquid media is expected to increase with temperature and the evolution experiment was planned to be conducted at 37°C and 42°C temperatures. As an indicator for the amount of evaporated media, the culture volume was monitored and effluent was collected two

times a day. The effluent volume per unit time served as an indirect indicator for loss of culture volume as the insertion depth of the effluent needles within the culture vessels was fixed (shown in Figure 3B) and thus, in case of extensive culture volume loss due to evaporation, the amount of effluent was expected to decrease over time. The culturing test revealed no significant differences between the effluent volumes collected from the chemostats operated with the air-hydration module and without the air-hydration module (P = 0.933, using t-test; details in Supplementary Table 6). Therefore, the air hydration module was excluded from the final chemostat setup, but gas filters were used downstream the manifolds (as shown in Supplementary Figure 4). Similarly, gas filters at the outlet of the collection vessels, meant to prevent the environment from being contaminated with aerosolized bacteria droplets, were not used because of frequent clogging of filters. Instead, a gas washing bottle was used (see Supplementary Figure 4A).

The stability of the modified chemostat system was tested by assessing the density of cultures over 21 days. To this end, six cultures of *E. coli* MG1655 harboring plasmid pLC were grown each at 37°C and 42°C using a dilution rate of 0.24 h^{-1}. To test again for contamination and cross-contamination between culturing vessels, non-inoculated chemostat units were alternately arranged with inoculated culturing vessels (scheme shown in Supplementary Figure 4F). Twice a day, culture volume level, continuity of stirring and media supply were monitored and no malfunctions of equipment or obvious changes in culture volume were observed. As the uniformity of aeration and dilution rate are important aspects for the reproducibility of growth conditions in the different culturing vessels, the dilution rate was determined after approximately 20 generations (3 days) and 170 generations (21 days) of steady state growth. With a target dilution rate of 0.24 h^{-1}, an average dilution rate of 0.24067 h^{-1} (SD = 0.00196 h^{-1}, n = 12) and 0.23927 h^{-1} (SD = 0.00155 h^{-1}, n = 12) were measured after 20 and 170 generations, respectively. Furthermore, culture densities were determined from colony counts every second day. As for the dilution rate, average culture density slightly decreased over time and variability increased (Figure 4). Nonetheless, culture densities were neither significantly different between culturing units (P = 0.098, using Kruskal-Wallis test) nor were culture densities significantly different between sampling time points (P = 0.295, using Kruskal-Wallis test). Although the dilution rates obtained after 20 and 170 generations are not significantly different (P = 0.093; using Wilcoxon signed rank test), I suspected that the slightly lower average dilution rate determined after 170 generations was due to wear of chemostat equipment. A test comparing the flow rates obtained using the pump tubing and using new pumping tubing confirmed that the observed differences in dilution rates were at least partially due to wear of the peristaltic pump tubing.

Therefore, in the evolution experiment, the pump tubing was replaced at least every three weeks.

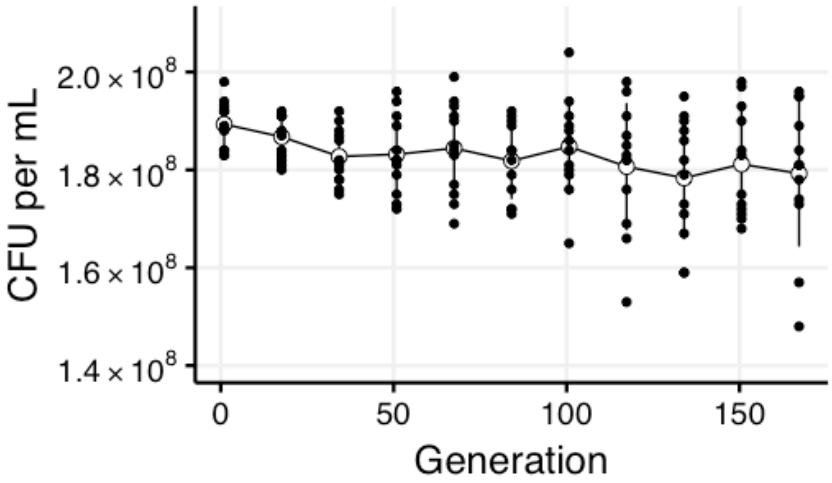

Figure 4. Cell densities obtained during test cultivation using the chemostat system established in this study. Over a culturing period of 21 days (approx. 170 generations), cell densities were assessed from twelve chemostat cultures by colony-count method. Empty circles show the mean CFUs, which are connected by a solid line to show the trend. Raw data is reported in Supplementary Table 7.

Furthermore, as an indicator for the reproducibility of steady state growth between the culturing units, transcription levels of the chromosomal genes *groEL* and *idnT* were determined. The chaperonin-encoding gene *groEL* is essential for protein folding at 37°C and at 42°C (e.g., Georgopoulos and Eisen 1974, Wada and Itikawa 1984) and was used here to test for the reproducibility of bacterial growth in the established chemostat system. The gene *idnT* was used for the normalization of *groEL* transcription levels as it was previously shown to be a reliable reference across different growth conditions (Zhou et al. 2011). GroEL expression is known to be elevated in high temperature growth conditions (e.g., Herendeen et al. 1979, Yamamori and Yura 1980). The overall normalized *groEL* transcript levels are significantly different between the growth temperatures ($P < 0.001$, using *t*-test), but not significantly different across the different sampling time points, neither at 37°C ($P = 0.113$, using Kruskal-Wallis test), nor at 42°C ($P = 0.516$, using Kruskal-Wallis test). This further indicates that the growth conditions and steady-state physiology were consistent between culturing units.

To summarize, the modifications introduced into the chemostat system suggested by Miller et al. (2013) for the cultivation of yeast were here demonstrated to enable stable steady-state culturing of bacteria over at least 21 days. Thus, the modified chemostat system was used in the evolution experiment.

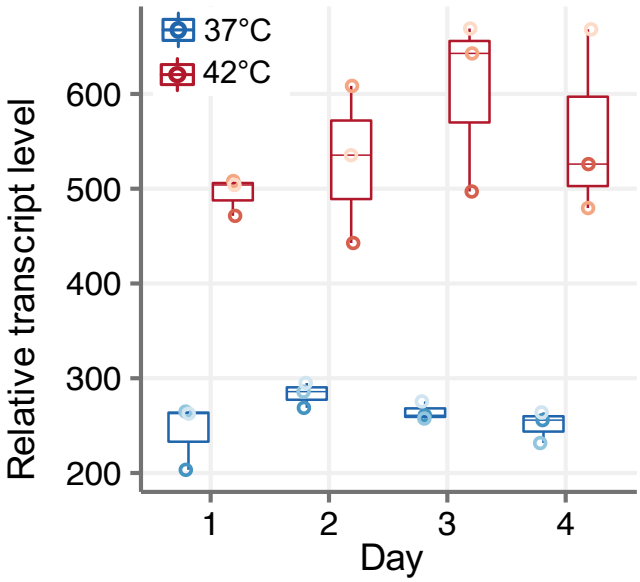

Figure 5. Transcription levels of the chaperonin gene *groEL* in *E. coli* MG1655, pLC. Transcription level of *groEL* gene were determined for a total of six independent chemostat cultures (indicated by different colors) grown at 37°C or 42°C. Samples were collected at four consecutive days after 144 hours of steady-state growth in the established chemostat system. Transcription levels are normalized to that of the reference gene *idnT*. Individual Ct-values are listed in Supplementary Table 8.

4.2 Experimental evolution of low- and high-copy plasmids

To compare the rate of evolution between low-copy and high-copy plasmid replicons an experimental evolution approach was used. In the experiment, two model plasmids having low- or high-copy number were evolved in an *E. coli* host under conditions selecting for the plasmid presence. The low-copy model plasmid (pLC, 5.2 kb; Figure 6) is derived from plasmid pBBR1 (Antoine and Locht 1992) that is known to stably replicate in a broad host range despite lacking an active partitioning mechanism. The plasmid encodes an ampicillin-resistance gene (*bla*; β-lactamase) and is non-mobile (i.e., it is not transmissible via conjugation). The average pLC copy number in the wild-type *E. coli* host was 8.5 ± 0.56 (*SD*, *n* = 6; Figure 6), which is within the range calculated previously for pBBR1 (Jahn et al. 2016). The accessory part of the high copy number model plasmid (pHC, 4.8 kb; Figure 6) is identical to that of plasmid pLC, but the backbone comprises a pUC origin of replication (Vieira and Messing 1982), that is a derivative of the *ori* of plasmid ColE1 (Hershfield et al. 1974). The copy number of plasmid pHC in the wild-type *E. coli* host was approximately 80-fold higher than that of plasmid pLC (705.51 ± 17.78 *SD*, *n* = 6; using qPCR; Figure 6). This is within the typical copy number range of the pUC plasmid backbone (Rosano and Ceccarelli 2014). Notably, in the hypermutator *E. coli* MG1655

background, plasmid copy numbers were, on average, 1.15-fold (pLC) and 1.36-fold (pHC) higher than in the wild-type background.

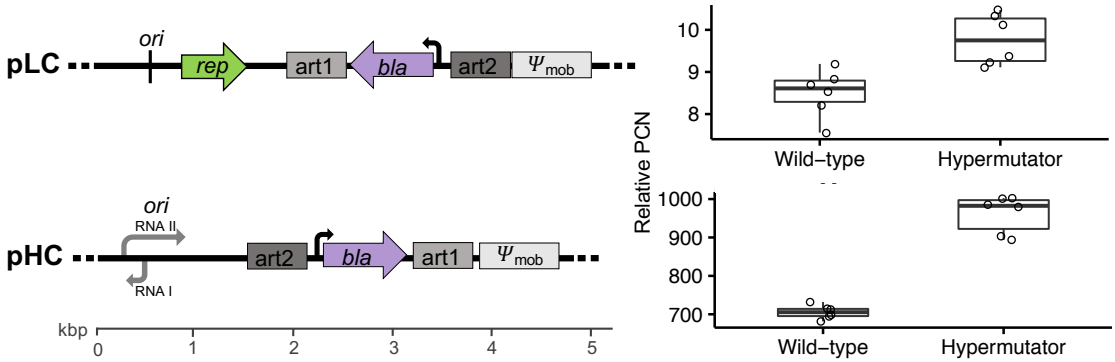

Figure 6. Genetic maps and copy numbers of plasmid pLC and pHC. The plasmids are of comparable genome size and differ in the origin of replication. Both plasmids are equipped with an ampicillin resistance gene (*bla*; β-lactamase) and 600 bp long stretches of randomly composed, non-coding DNA (denoted as art1 and art2). The *mob* gene originally found in pBBR1 was non-functionalized by truncation during plasmid construction (denoted as Ψ_{mob}). Relative plasmid copy numbers were determined at the onset of the experiment (using qPCR; n = 48). Note that PCNs of pLC wild-type are significantly lower than that of pLC-hypermutator (n = 12, P < 0.001; using one-tailed t-test) and that PCNs of pHC wild-type are significantly lower than that of pHC-hypermutator (n = 12, P < 0.001; using one-tailed t-test).

In addition to PCN, the experimental evolution setup accounts for two known determinants of evolutionary dynamics: mutation rate and selection pressure. To vary the mutation rate, the plasmids were evolved in two host genotypes, *E. coli* K-12 substrain MG1655 (wild-type, wt) and a hypermutator derivative of the wild-type strain (Δ*mutS*) in which mutations are expected to arise faster in comparison to the wild-type (e.g., 33-fold (Arjan et al. 1999)). The populations were evolved under two different environmental regimes: at 37°C and at 42°C. Growth of *E. coli* at 42°C is expected to entail an acclimation to the elevated temperature (Guyot et al. 2014), and it has been shown to involve genomic adaptation (Deatherage et al. 2017). The experiment was conducted with six replicates for each combination of the three experimental evolution factors – plasmid replicon type, host genotype and growth temperature. The populations were evolved for 800 generations in continuous culture under selective conditions for ampicillin-resistance. At the end of the experiment, samples of ancestral and evolved populations were sequenced using a population sequencing approach.

Notably, the two model plasmids differ in their stability within the host. While the pLC replicon remained unaltered compared to its pBBR1 ancestor, the high copy number of plasmid pHC comes at the cost of lower plasmid stability due to deletions of stability factors during construction of the pUC replicon (e.g., lack of the multimer resolution site *cer* originally present in plasmid ColE1). The stability of both plasmids in the *E. coli* wild-

type host was assessed using the same selective constraints for the plasmid presence as in the evolution experiment. No plasmid-free segregants of pLC-wt were observed after overnight growth (n = 5), whereas the proportion of pHC-free segregants ranged between 1% and 39% (n = 5; see Section 3.8). Plasmid loss during the evolution experiment has the potential to result in a proportion of plasmid-free cells in the total population. Such plasmid-free cells have a collective resistance to ampicillin thanks to the presence of β-lactamase secreted from plasmid carrying hosts in the environment (e.g., Vega and Gore 2014). Therefore, the proportion of plasmid-hosts in the evolved populations was quantified using replica plating of single colonies. This showed that pLC-hosts accounted for 89% to 100% of the populations in all conditions and replicates (detailed description in Section 4.6). The proportion of pHC-hosts in the evolved wild-type populations ranged between 1% and 78%, while the range of plasmid carrying hosts in the evolved hypermutator populations was between 35% and 98% (Section 4.6). In order to increase the resolution on the existing plasmid allele pool, the genomes of each pHC population was sequenced using two different sampling strategies. In addition to the sequencing of total populations (i.e., plasmid host cells and plasmid-free segregants), the genome of each pHC population was sequenced from pooled samples of 100 colonies of plasmid carrying hosts (see Section 3.9). In the following, the resulting genetic variants reported for pHC populations are based on the pooled colonies data unless stated otherwise.

4.3 Fine tuning of the chemostat dilution rate

In batch culture, significant differences in growth rates are observed between the plasmid-free wild-type strain and plasmid-carrying strains (Figure 7 and Supplementary Table 9). In a chemostat, growth rates are controlled by the dilution rate and the influent substrate concentration (Novick and Szilard 1950). As one of the main objectives of this work was to compare mutation rates between different genotypes, both parameters, the dilution rate and the concentration of the growth limiting substrates were kept constant.

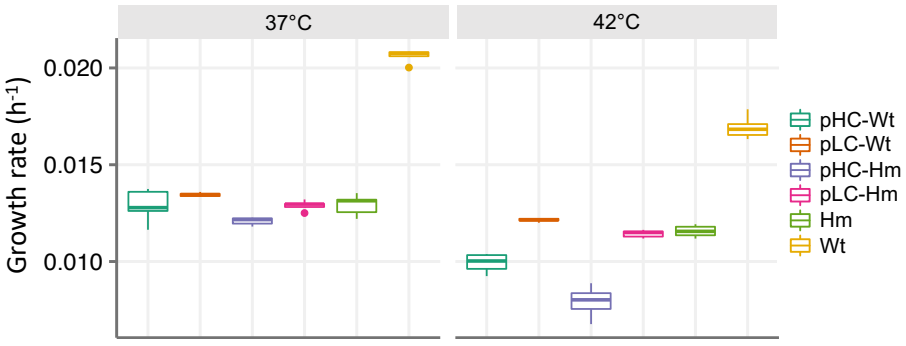

Figure 7. Growth rates of plasmid-carrying and plasmid-free ancestors. Growth rates were determined in batch culture as described in Section 3.7.

Steady-state growth of bacteria can usually be maintained at a specified range of dilution rates D, but these must be below a critical dilution rate D_{crit}. A dilution rate above D_{crit} leads to a washout of the culture as bacteria are not able to grow as fast as biomass is lost through the overflow. Therefore, prior to the evolution experiment, cell densities were estimated for a range of dilution rates and the critical wash-out rate was determined for each combination of host genotype, plasmid type, and temperature. To this end, three biological replicates of each of the four different strains were grown at 37°C and 42°C in the chemostat system established in this work and proven to reliably enable reproduceable steady-state growth (see Section 4.1). After reaching steady-state using a specified dilution rate, culture densities were estimated hourly for 6-8 hours by OD_{600} measurement. As can be seen in Figure 8, the range of dilution rates at which culture densities remained relatively constant ranged between 0.24 h^{-1} and 0.38 h^{-1}. Furthermore, dilution rates in this range gave similar culture densities between genotypes and growth temperatures. Therefore, a dilution rate of 0.27 h^{-1} was chosen as the dilution rate to be used in the evolution experiment.

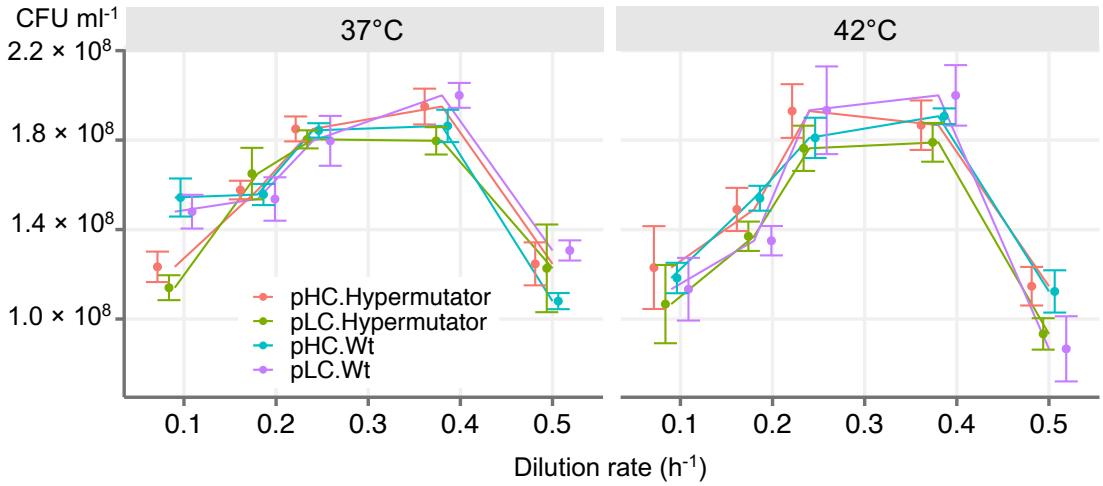

Figure 8. Cell densities of chemostat cultures at different dilution rates. Cell densities were estimated by colony count as described in Section 3.7. Error bars and dots represent means and *SD* of three replicative populations, respectively.

4.4 Population dynamics during experimental evolution

Evolutionary parameters such as mutation supply and genetic drift are known to be greatly influenced by the size of a population (Lanfear et al. 2013). In this study, population sizes were therefore aimed to remain constant during the cultivation in the chemostats. Hence, population sizes of all steady-state chemostat cultures were estimated on a regular basis by monitoring culture volume twice a day and measuring optical densities or population densities from colony counts at least every 100 generations. As can be seen in Figure 9,

population densities of steady-state cultures remained remarkably constant throughout the experiment. Cell densities varied less than 10% between biological replicates sampled at a time (Supplementary Table 10 and Supplementary Table 11), although slight variation in cell densities was observed for colony count based approach. Furthermore, population densities varied by just 6% (CV) between all cultures throughout the experiment ($1.92 \times 10^8 \pm 1.1 \times 10^7$, $M \pm SD$, $n = 432$) and no significant differences between populations of any factor combination was found ($P = 0.55$, using Kruskal-Wallis test). Therefore, it can be assumed that, on average, $3.85 \times 10^9 \pm 2.23 \times 10^8$ ($M \pm SD$) cells grew at steady-state in each of the 48 chemostat cultures and that none of the experimental factors had an effect on population densities over time.

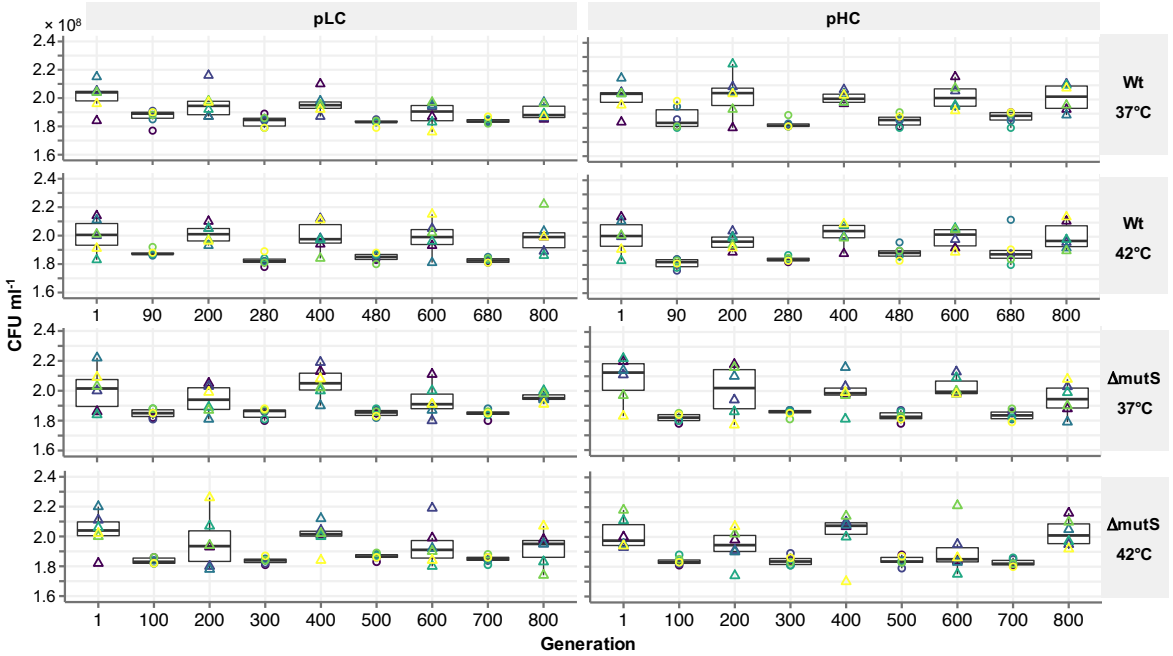

Figure 9. Population densities of the 48 chemostat cultures during the evolution experiment. Cell densities were assessed from cultures at steady-state by plate counting (indicated by triangles) or OD measurements (indicated by circles) (Supplementary Table 10 and Supplementary Table 11). Colors indicate corresponding biological replicates within one experimental factor group.

Although population densities remained constant throughout steady state culturing in the chemostats, small bottlenecks were introduced every 200 generation. Apart from the need to replace chemostat equipment due to wear (e.g., pump tubings), culturing vessels and tubings were replaced every 200 generations. As mentioned in the previous section, special care was taken in the choice of equipment to prevent biofilm formation. Nevertheless, biofilms were observed in some cases at the bottom of the culturing vessels during the experiment. Such biofilms can form subpopulations that evade the dilution process and may constantly supply minority genotypes to the population. long-term formation of such subpopulations was practically prevented, because chemostats were

monitored at least two times a day and possible biofilms were dissolved manually by slewing the air inlet needle.

Furthermore, bacterial droplets can be aerosolized within the culturing vessel and consequently bacteria can grow at parts that are not in direct contact with the liquid culture. The formation of biofilms on the cork of the culturing vessel was the consequence. This caused in some cases the growth of bacteria into the airbreak. Therefore, the whole airbreak-assembly was exchanged every second day to prevent possible growth into the upstream media supply and to prevent the risk of cross-contamination. Nevertheless, the cork itself could not be exchanged that easily because it required the opening of the system and thus contamination of the bacterial culture. Therefore, for maintenance and cleaning purposes, chemostats were disassembled every 200 generations (i.e., every three weeks) and total populations were stored at -80°C (see Section 3.7). Half of each archived population was then used to re-establish the 48 chemostat cultures. This reduction in cell population size corresponds to a minor bottleneck in comparison to typical serial transfer experiments (e.g., Lenski et al. 1991, Vogwill et al. 2016). Although the impact of this bottleneck size was not tested experimentally, it can be assumed that the reduction of roughly 200 million cells to 100 million cells had only a minor impact on the total diversity maintained in the populations.

4.5 Plasmid copy number dynamics

A factor that might affect the mutation supply rate of a plasmid is it's copy number within a population of cells. As outlined in Section 4.2, pLC and pHC plasmid copy numbers were significantly higher in the hypermutator strain in comparison to the wild-type genetic background. After acclimatization of the four genotypes to the media conditions used in the evolution experiment (Section 3.7), plasmid copy numbers remained significantly different between both host genotypes (Figure 10). This indicates, that the host genotype has an impact on plasmid copy number that is independent of media conditions and that these PCN differences were not transient. Furthermore, although each of the pLC populations had undergone just one separated overnight cultivation after they were split from the same ancestral population, pLC plasmid copy numbers varied among the twelve populations used to found the chemostat (CV listed in Figure 10). Nevertheless, the coefficient of variation was less than 10% and the copy number was within the range of plasmid copy numbers reported previously for pBBR1-based plasmids (e.g., Troeschel et al. 2012, Jahn et al. 2016).

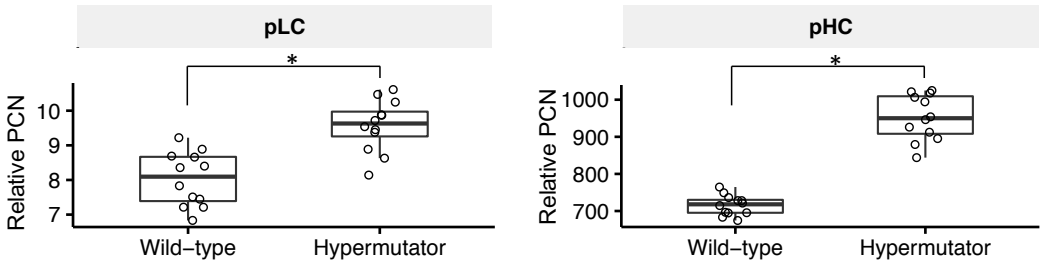

	Wild−type	Hypermutator
M	8.02	9.6
SD	0.78	0.74
CV %	9.7	7.72

	Wild−type	Hypermutator
M	715.56	951.84
SD	27.39	61.56
CV %	3.83	6.47

Figure 10. Plasmid copy numbers within the ancestral populations. Plasmid copy numbers of the four genotypes used in this study (i.e., pLC-wt, pLC-hypermutator, pHC-wt, pHC-hypermutator) were determined after acclimatization to $M9_{amp100}$ medium using qPCR (see Section 3.7). Note, that copy numbers of plasmid pLC and pHC, respectively, are significantly different between between host genotypes (pLC: $P < 0.001$; pHC: $P < 0.001$; using *t*-test).

To investigate plasmid copy number dynamics in the evolving populations, PCNs of chemostat populations were determined every 200 generations. To ensure that the estimated PCNs are representative for the populations, samples were always collected from the effluent of steady-state growing cultures before the chemostats were disassembled. The average plasmid copy number of pLC populations ranged between 5.35 and 25.37 (M = 11.80; SD = 4.48; n = 120). As evident from Figure 11, the largest variation in PCN was observed for pLC populations evolved at 37°C where the PCN of wild-type populations ranged from 6.03 to 25.37 (M = 14.85; SD = 6.28; n = 30) and that of hypermutator populations ranged from 5.53 to 22.04 (M = 11.04; SD = 3.53; n = 30). The variability of PCN within these experimental factor groups was due to an initial increase of PCN reaching a maximum at generation 400 followed by a decrease of PCN towards the end of the experiment. As all pLC-populations showed a slight increase in PCN at generation 400, PCNs were determined twice using archived samples stored at -80°C. No significant differences were observed between PCNs determined from both sample sets collected at generation 400 (P = 0.801; using paired *t*-test). This indicates that the increase in PCN was not due to any technical error during handling of samples or determination of PCNs. Although no disturbances of steady-state growth or malfunctions of chemostat equipment was detected at generation 400, a technical cause for the observed average increase in PCN in all pLC-experimental factor groups cannot be excluded. The highest increase in PCN was observed for pLC-wt populations cultivated at 37°C, where, on average, a 3-fold increase in PCN was detected after 400 generations (individual PCNs are listed in Supplementary Table 14). Nonetheless, PCNs of both pLC experimental factor groups cultivated at 37°C (i.e., wt and hypermutator populations) decreased at generation 600 and no significant differences in PCNs were detected between populations of generation 1 and generation 800 (Table 2).

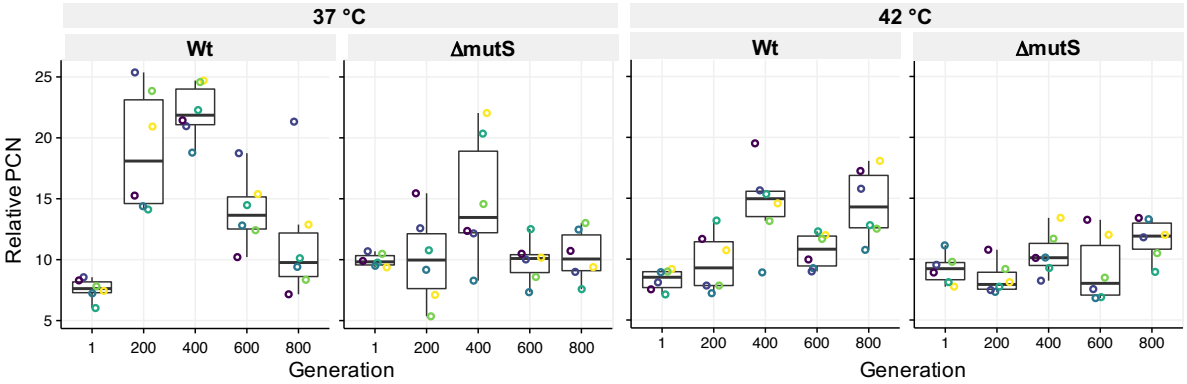

Figure 11. pLC plasmid copy number dynamics in evolving chemostat populations. Plasmid copy numbers were determined for each chemostat population using qPCR at a 200 generation interval. Circles present the mean PCN of two sample dilutions (Supplementary Table 14).

Although pLC populations cultivated at 42°C showed overall smaller variation in PCNs than pLC-populations cultivated at 37°C (Figure 11), a slight increase in PCNs over time was observed. At generation 800, an average PCN increase of about 27% for hypermutator pLC populations evolved at 42°C and an 75% increase in PCN for wt-pLC populations evolved at 42°C were observed (in comparison to average PCN at generation 1). Although the differences in PCN for these populations are significant (Table 2), plasmid copy numbers are within the range previously reported for pBBR1-derivatives in *E. coli* strains (e.g., Troeschel et al. 2012, Jahn et al. 2016).

Table 2. Comparison of pLC plasmid copy numbers between populations of generation 1 and generation 800. Paired t-tests reveal significant differences in PCN between pLC-populations of generation 1 and 800 evolved at 42°C. FDR-corrected *P*-values are reported along with test statistics.

Host genotype	T (°C)	Gener-ation	*M*	*SD*	*M* of the difference	95% CI of the difference		*t*	*df*	*P*
						Lower	Upper			
Wild-type	37	1	7.56	0.9	-3.98	-9.14	1.18	-1.98	5	0.1389
		800	11.54	5.17						
	42	1	8.3	0.87	-6.22	-9.48	-2.96	-4.9	5	0.0178
		800	14.52	2.93						
Hypermutator	37	1	9.95	0.53	-0.41	-2.64	1.81	-0.48	5	0.6533
		800	10.36	2.1						
	42	1	9.2	1.23	-2.45	-4.15	-0.75	-3.704	5	0.0278
		800	11.65	1.7						

While pLC copy numbers remained within a relative narrow range during the course of the evolution experiment, plasmid copy numbers of most pHC populations decreased substantially within the first 200 generations of steady-state growth. As outlined in Section 4.2, plasmid pHC comprises a pUC origin of replication and lacks the *rop*-gene which negatively regulates the copy number. It is well known that pBR322-derivatives are gradually lost in non-selective conditions due to segregational loss, lack of *cer* site and multimerization (e.g., Summers and Sherratt 1988, Chiang and Bremer 1988). The average pHC plasmid copy number decreased by roughly 90% at the end of the

experiment in all experimental factor groups. The decrease in average pHC plasmid copy number is therefore likely due to the segregational loss of plasmids and the formation of a large proportion of plasmid-free cells. Nonetheless, no complete plasmid loss was observed in any of the populations.

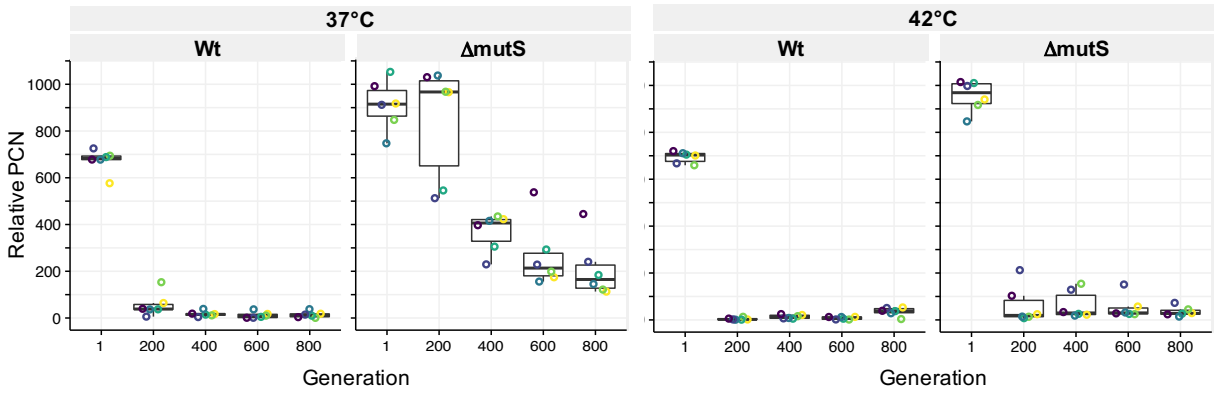

Figure 12. pHC plasmid copy number dynamics in evolving chemostat populations. Plasmid copy numbers were determined for each chemostat population using qPCR at a 200 generation interval. Circles present the mean PCN of two sample dilutions (details in Supplementary Table 15).

The average plasmid copy number summarizes copy number characteristics across all cells in the population. Therefore, this characteristic can obscure the real situation. For example, in a population comprising two subpopulations, plasmid hosts and plasmid-free cells, the average copy number might not represent this condition accurately. To examine the extent of PCN heterogeneity and to further investigate the reason for the plasmid copy number decline, the underlying distributions of pLC and pHC plasmid copy numbers within populations were determined. For this purpose, one pLC-wt and one pHC-wt population from generation 1 in the evolution experiment were diluted, spread on M9 agar plates (without selection, i.e. ampicillin) and incubated at 37°C overnight to grow visible colonies. Single colonies were then picked and prepared for qPCR as described in Section 3.5. Non-selective condition was chosen to allow for the growth of all cells present in the population. As can be seen in Table 3, pLC plasmid copy numbers of single colonies are in the same range of PCNs observed for the total populations sampled from the chemostat cultures.

Furthermore, descriptive statistics (skewness = 0.03, kurtosis = 2.63, Table 3), the QQ plot (Figure 13) and a test for normality indicated that pLC plasmid copy numbers follow a normal distribution (P = 0.942, using Shapiro-Wilk test). Therefore, copy numbers determined for plasmid pLC using total populations can be assumed to represent the plasmid copy number distribution within the population. Furthermore, based on the distribution of pLC plasmid copy numbers determined using single colonies, it can be assumed, that plasmid pLC is relatively stable in the *E. coli* host.

Table 3. Descriptive statistics for pLC-wt and pHC-wt plasmid copy numbers determined from single colonies and total populations. Plasmid copy numbers were determined using single colonies or total populations (i.e., chemostat populations).

		n	Min.	Q1	*Mdn*	*M*	Q3	Max.
pLC-wt	single colonies	35	6.52	11.26	14.41	14.10	16.36	23.16
	total population*	30	6.03	8.77	14.26	14.85	20.95	25.37
pHC-wt	single colonies	91	0.00	104.70	399.80	1214.60	2209.20	7609.80
	total population*	30	0.70	10.21	18.57	154.65	57.99	725.68

*statistics derived from all populations cultivated at 37°C

Plasmid copy numbers of the pHC-wt single colonies ranged from 0 to 7600 plasmids per chromosome. As shown in Figure 13, the majority of colonies showed a relative PCN below 500 copies per chromosome (*n* = 52, *Mdn* = 399.8) and the underlying distribution cannot by approximated by a normal distribution (kurtosis = 5.41; $P < 0.001$, using Shapiro-Wilk test) and is skewed right (skewness = 1.51). This indicates that pHC plasmids are partitioned unequally between daughter cells. Moreover, six colonies had a relative plasmid copy number lower than 1. Differential re-streaking of these colonies on selective and non-selective media as well as colony PCR confirmed that the plasmid was present in five of the six colonies. Nevertheless, copy numbers below 1 suggested that cells within these colonies were heterogenous with respect to plasmid copy number.

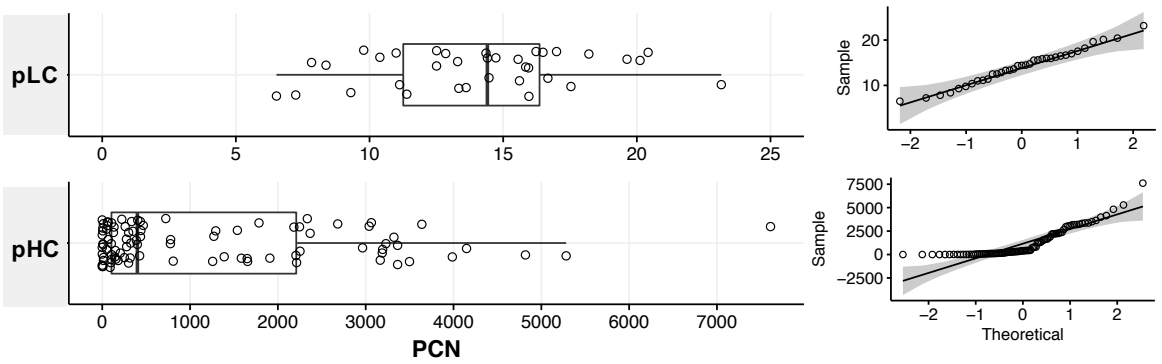

Figure 13. Distribution of plasmid copy numbers of single colonies. PCNs were determined from single colonies by plating appropriate dilutions of one Wt-pLC and one Wt-pHC population on M9 agar each. After ON growth at 37°C, PCNs were determined as described in the methods section. pLC: *n*=35; pHC: *n*=91. Note, that quantile plots are shown on the right.

Therefore, to investigate the copy number heterogeneity within single colonies, three pHC-wt colonies were randomly chosen, streaked on non-selective media and grown overnight to obtain single colonies. Then, twelve single colonies of each of the three test colonies were randomly chosen for the determination of PCNs. The variability (CV) in PCNs of single colonies ranged from 42% to 46% (see Supplementary Figure 5A). Although this analysis is not a direct verification of PCN heterogeneity within single colonies, it indicates the extent of PCN variability of plasmid pHC. In contrast, single

colonies of pLC-wt revealed a maximum variability of 15% (Supplementary Figure 5B). After regrowth on selective medium, PCNs of pHC-wt colonies were significantly higher (0.49-fold to 1.18-fold, on average) in comparison to colonies grown on non-selective media ($P < 0.001$, $n = 36$; using one-tailed *t*-test). In contrast, the comparison of PCNs of pLC-wt colonies revealed that PCNs of colonies grown on selective medium are, on average, 0.04-fold to 0.08-fold higher in comparison to PCNs of colonies grown on non-selective medium ($P = 0.166$, $n = 36$; using one-tailed *t*-test). This demonstrates that the copy number property of plasmid pHC is variable and depends on the selective regime.

To summarize, the copy number of plasmid pLC ranged between 6 to 25 copies per chromosome. As indicated by the PCN distribution of single colonies, pLC copy numbers are distributed normally within a population, which indicates that plasmid pLC is stable under the tested conditions. Plasmid pHC, a derivative of plasmid pBR322 that lacks the multimer resolution site, has a rather heterogenous distribution within the population and is most likely gradually lost from a populations of cells (as indicated distribution of single colony PCNs). Therefore, the decrease in population-wide average plasmid copy number observed during the evolution experiment can be explained by pHC plasmid loss from the population. To further investigate the cause for the pHC plasmid copy number decline, the proportion of plasmid carrying cells was estimated.

4.6 Proportion of hosts

Segregation of plasmids leads to loss of plasmid DNA due to the unequal distribution of plasmid copies between daughter cells during cell division. This phenomenon is well known for high copy number plasmids like pHC that lack an active portioning mechanism and a multimer resolution site. In a population of cells cultivated in a bioreactor, the formation of plasmid-free segregants can overgrow plasmid-carrying cells, which results in a heterogenous population of cells. To investigate the amount of plasmid free cells under the conditions in the evolution experiment the proportion of hosts (i.e., plasmid carrying cells) was estimated from populations sampled at generation 1 and generation 800.

The proportion of hosts was determined using the ampicillin resistance gene encoded on both plasmids as a marker to distinguish plasmid carrying cells from plasmid-free segregants. To this end, two methods, termed here differential plating and streak test, were evaluated with respect to precision, accuracy and limitations. The differential plating method is based on a sample of a population of cells that is spread on selective and non-selective media. The proportion of hosts is then calculated as the ratio of colonies grown on selective media and the number of colonies grown on non-selective media (e.g., Yano et al. 2013). The streak method is based on single colonies that are streaked on selective and non-selective media. The proportion of hosts is calculated as the ratio of colonies

grown on selective media to the total number of tested colonies. The main difference between both methods is the number of random errors (e.g., dilution or counting error) and the sampling units on which all statistical measures are based on. The sample unit of the differential plating method is the total number of colonies counted on a plate, and that of the streak method is a single colony. Both methods were evaluated using six test samples containing pLC-wt cells mixed with plasmid-free wild-type cells to achieve proportions of hosts ranging from 5% to 100%.

Both methods revealed similar estimated proportions and confidence intervals that overlap for proportions larger than 0.05 (see Table 4 and Supplementary Figure 6). Nevertheless, although, the precision reached with the differential plating method was slightly higher for the differential plating method, a higher accuracy (relative error) for the estimated proportion of host can be achieved using the streak method. Therefore, a combination of both methods was used for the determination of the proportion of hosts. Furthermore, to assess the sensitivity (true positive rate) and specificity of the streak method, 100 colonies were randomly selected and were tested for the presence of the plasmid using PCR. This test was done for both plasmids. While the specificity was 100% for both plasmids, the sensitivity of the test method was estimated to be 93% for plasmid pHC and 100% for plasmid pLC. Although the identification of true positive colonies required to test some of the colonies twice, the false identification of true negatives was presumably due to low cell fitness of the tested colonies such that they did not grow as fast as other colonies. Nevertheless, since the streak method is a direct test method and single colonies could be tested for the presence of the plasmid using PCR, the streak method was mainly used to estimate the proportion of hosts.

Table 4. Confidence intervals for two methods used to determine proportions of hosts. The differential plating method and the streak test method were evaluated in a trial experiment using artificially constructed samples with host proportions p_{exp} ranging from 0.05 to 1. For the differential plating method, the estimated host proportion was calculated as the mean proportion *M*(p*obs*) of 15 independent samples and the confidence intervals were calculated for the mean. For the streak method, individual colonies were tested for ampicillin resistance and adjusted proportions p_{obs} and confidence intervals were calculated using the adjusted Wald method (Agresti and Coull 1998). Detailed statistics are given in Supplementary Table 16.

	differential plating				streak test			
p_{exp}	*n*	$M(p_{obs})$	95% CI	relative Error	*n*	p_{obs}	95% CI	relative Error
0.05	15	0.08	0.04 – 0.11	13.38	300	0.03	0.01 – 0.05	0.00
0.1	15	0.11	0.09 – 0.14	9.15	301	0.11	0.08 – 0.15	0.13
0.25	15	0.25	0.22 – 0.28	7.75	300	0.28	0.23 – 0.33	4.67
0.5	15	0.51	0.48 – 0.54	17.50	300	0.52	0.47 – 0.58	9.33
0.75	15	0.73	0.68 – 0.77	36.35	300	0.75	0.70 – 0.80	9.63
1	15	1.00	0.97 – 1.00	97.29	298	0.99	0.99 – 1.00	53.33

In addition, to estimate the bias on the proportion of hosts possibly introduced during freezing and storage of samples, archived cultures and fresh samples were tested. To examine the effect of freezing and reviving on the estimation of the proportion of host, three test samples of each genotype used in the evolution experiment were constructed by mixing the plasmid-free free ancestors with plasmid carrying counterparts in the following ratios: 15%, 75%. Then, the proportion of hosts were estimated before and after freezing, storage at -80°C for six weeks and reviving cultures. Cells were revived on agar plates as the re-growth in liquid medium can shift the proportion of hosts in an unpredictable manner due to differences in growth rates of plasmid-free and plasmid-bearing cells and plasmid loss was known to occur in one overnight growth in liquid culture. Although plasmid loss can occur within the growth span of a single colony as well, it was shown that a true positive can be identified. Although a slightly larger variability in proportion of hosts was observed after freezing in three of the four test groups (see Supplementary Figure 7), there were no significant differences in the estimated proportion of hosts before and after freezing (test results reported in Supplementary Table 17). Thus it can be assumed, that the proportion of hosts can be reliably estimated using the archived cultures.

As can be seen in Figure 14, the proportion of hosts in pLC wild-type and hypermutator populations was 100% at generation 1. After 800 generations, the proportion of hosts was still 100% in all populations cultivated at 37°C (independent of the host genotype), whereas more than half of the populations cultivated at 42°C displayed up to 10% of plasmid-free segregants (see Supplementary Table 18). Although the differences are only marginal, the comparison of proportion of hosts at generation 800 between the two culture temperatures revealed significant differences ($P = 0.039$; using *t*-

test). This may suggest that the formation of pLC plasmid-free segregants at 42°C occurred at a higher rate in comparison to populations cultivated at 37°C. Assuming that plasmid-free segregants are constantly (even at a low rate) generated in a population, the result indicates that plasmid-free segregants had at least a comparable or higher fitness in comparison to plasmid-carrying cells in populations cultivated at 42°C.

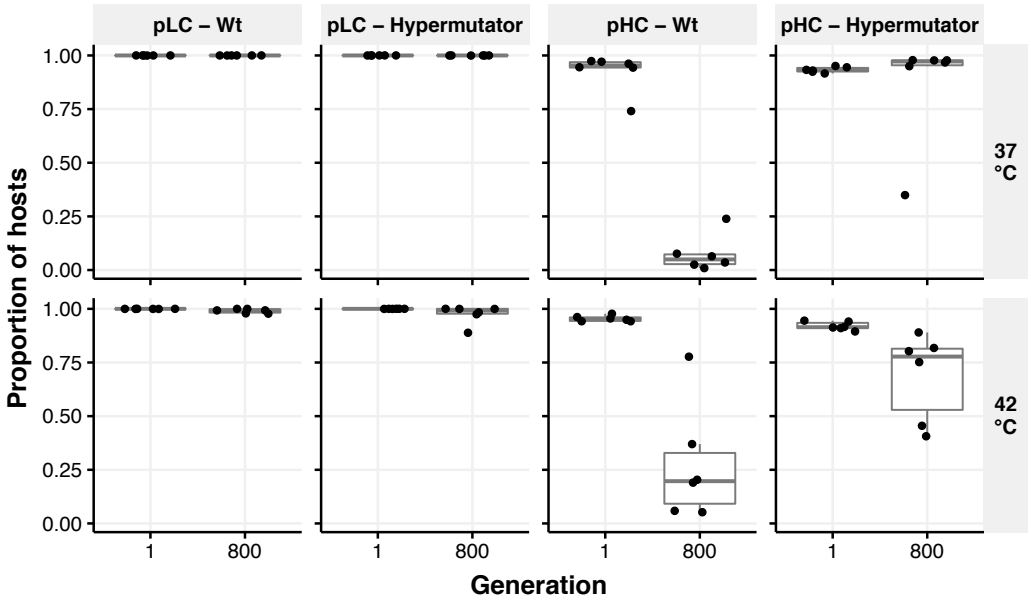

Figure 14. Proportion of hosts at generation 1 and 800 in the evolution experiment. Proportion of hosts were estimated for each of the 48 chemostat populations using the streak method (Section 3.8). Confidence intervals are reported in Supplementary Table 18. Note that the minimum detection limit was 1%.

As described in Section 4.2, a decline in the number of plasmid-carrying cells was observed for pHC-populations at the end of the experiment. Nonetheless, the magnitude of decline differed between genotypes and culture temperatures (Figure 14). While the average proportion of hosts was 0.07 ± 0.07 (*SD; Mdn* = 0.05) for wild-type populations cultivated at 37°C, a higher average proportion of hosts was observed for wild-type populations cultivated at 42°C (0.28 ± 0.25; *Mdn* = 0.2). In contrast to pHC-wt populations cultivated at 37°C, the proportion of hosts in pHC-hypermutator populations cultivated at 37°C was remarkebly high (0.87 ± 0.23, *M* ± *SD*; *Mdn* = 0.97). Similarly, the average host proportion of pHC-hypermutator populations cultivated at 42°C was higher (0.69 ± 0.19, *M* ± *SD*; *Mdn* = 0.78) in comparison to pHC-wt populations cultivated at 42°C.

As it is indicated by the growth rate differences between the ancestral plasmid-carrying and plasmid-free strains (Section 4.3), both plasmid types imposed a fitness burden on their hosts. Therefore, it can be suggested that competitive fitness differences between plasmid carrying cells and plasmid-free segregants had an impact on the establishment and propagation of plasmid-free cells in the chemostat populations. Nevertheless, such fitness differences can decrease due to the emergence of

compensatory mutations (e.g., Harrison et al. 2015; Loftie-Eaton et al. 2017). Thus, in comparison to the fitness differences of the ancestral strains, it might be the case for pHC-wild-type populations cultivated at 42°C that these differences decreased in comparison to populations cultivated at 37°C. On the other hand, for pHC-hypermutator populations, only marginal growth rate differences between the plasmid-free and the ancestral plasmid-carrying strains cultivated at 37°C were observed. Furthermore, there were no significant differences in proportion of hosts between generation 1 and 800 for these populations (P = 0.312, using Wilcoxon signed rank test; Supplementary Table 18). Thus it can be assumed that plasmid carriage had no strong impact for the competitive fitness of plasmid-free and plasmid-cyarrying strains in these populations.

Nonetheless, it needs to be kept in mind that periodic selection occurs in chemostats cultures and this can have profound effect on the frequency of mutants during cultivation (e.g., Dykhuizen and Hartl 1983). Therefore, a mutation that gives a fitness advantage to a plasmid-free cell can lead to an increase in frequency of plasmid-free cells, but a selectively favored mutation arising at a later time will rise in frequency again. Hence, it has to be noted that the frequency of plasmid-carrying cells in the population might have varied in all populations during the course of the experiment.

4.7 Plasmid genome evolution

For the identification of emerging mutations, sequencing reads of the ancestral and evolved populations were trimmed and mapped to the reference *E. coli* MG1655 genome and to the two assembled plasmid sequences. Sequencing coverage varied among the populations and the replicons: the chromosomal coverage ranged between 109x and 327x, while the average coverage on the two plasmids was between 442x and 272,010x (Supplementary Table 19). The ratio of the average coverage on the plasmids to that of the chromosomes reflects the relative copy number of the plasmids within the sequenced samples as the number of fragments in a sequencing library increases with the number of a genetic elements present in a sample (e.g., Becker et al. 2016). As can be seen in Figure 15A, the ratio of mean plasmid to chromosome coverage is within the range of plasmid copy numbers determined for the ancestral populations and for single colonies using qPCR (see Figure 10 and Figure 13). Nevertheless, the library preparation method included PCR amplification of DNA fragments. Thus, beside optical duplicates produced during the sequencing, sequencing reads contained PCR duplicates. The amount of PCR and optical duplicates can be estimated using PICARD tools, but it is technically not possible to distinguish PCR-generated duplicates from natural occurring duplicates as it would be the case for multicopy-plasmids. Read duplicates have the potential to lead to

false representation of allele frequencies by increasing the proportion of an allele present in the duplicates compared to an alternative allele. Additionally, population sequencing (pool-seq) was used to enable the identification of rare, low frequency variants, but the pooled cells or colonies were not individually barcoded such that a distinction of reads belonging to a specific genotype was not possible. Therefore, a de-duplication step was included prior to variant detection.

The deduplication of reads reduced the average coverage on the chromosome by 6.3% ± 1.0%, whereas the average coverage on the plasmids was reduced by 25% ± 11% for plasmid pLC and by 63% ± 13% for plasmid pHC. Similar to the percentage change in number of plasmid reads, relative PCNs were, on average, reduced by 61% ± 14% for plasmid pHC and by 18% ± 11% for plasmid pLC (details shown in Figure 15A). As evident from Figure 15B, there was a strong correlation between the initial number of plasmid reads and the amount of plasmid reads removed during the deduplication procedure (see also Supplementary Table 19 for details). Nonetheless, no such correlation was found for chromosomal reads (Figure 15B) suggesting that the amount of plasmid reads identified as optical and PCR duplicates is related to the number of naturally occurring duplicates. Although such duplicates cannot be distinguished from optical and PCR duplicates using the library preparation method used in this study (e.g., Mansukhani et al. 2018), it can be assumed that the amount of PCR-duplicates coincides with the number of natural duplicates (i.e., plasmid copy number). Indeed, for RNA-seq data, which normally comprises high rates of read duplicates, it has been shown, that read duplication rates due to sampling strongly correlate with the total number of reads, but not with that of PCR duplicates. Therefore, read duplicates were removed to identify variants on chromosomes and plasmids, but were kept for the calculation of relative plasmid copy numbers (similar to quantitative RNA-seq methods; e.g., Parekh et al. 2016, Bansal 2017).

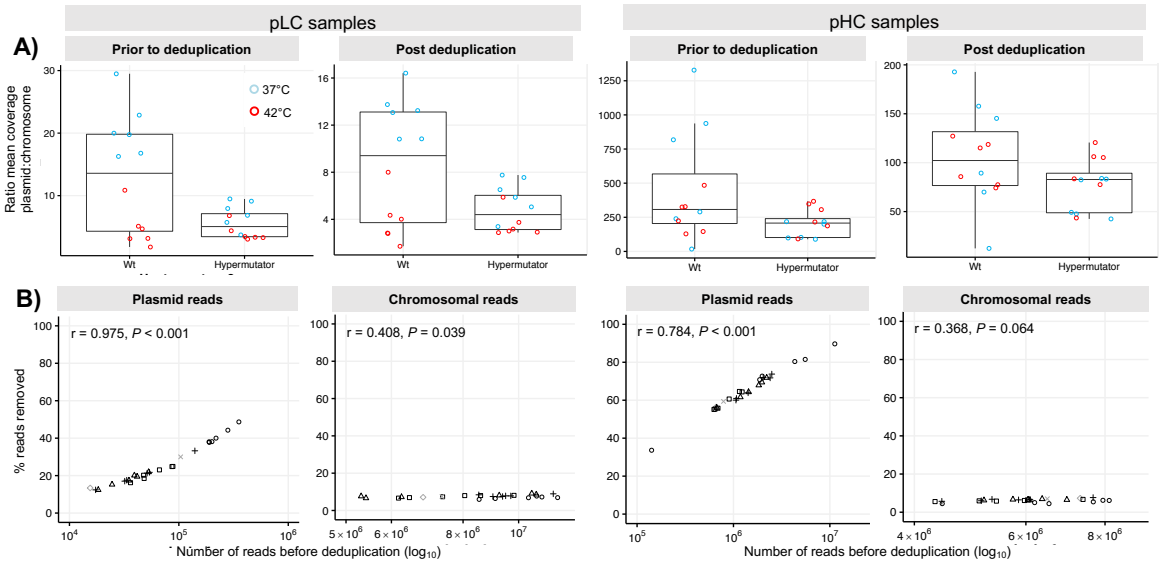

Figure 15. Effect of deduplication on number of reads and relative PCNs. A) Relative PCNs before and after deduplication. **B)** Mean read coverage is shown for the 48 evolved populations for sequencing samples of type 'total' for pLC-bearing populations and of type 'pooled hosts' for pHC-bearing populations. Pearson product-moment correlation coefficient (r) and *P*-values are reported for the test on correlation using non-transformed data (*n* = 24 each).

After deduplication and further filtering of low-quality reads (see Section 3.10), the average coverage on the chromosome ranged between 104x and 300x, while the average coverage on the plasmids was between 325x and 28,054x (Supplementary Table 19). All reference sequence positions were covered at least 40x and an initial inspection of the coverage distribution shown in Figure 16 indicated that no apparent large deletions or sequence duplications occurred in any of the plasmids as no abrupt change in sequencing coverage was observed.

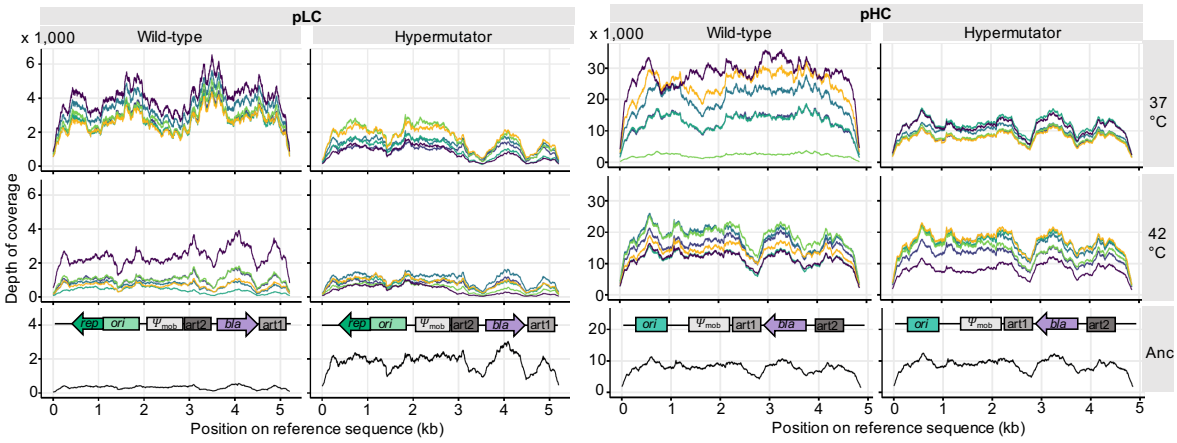

Figure 16. Read coverage on plasmid genomes after deduplication. Read coverage for each position on the two plasmid reference sequences is shown for host samples sequenced after 800 generations of evolution at 37°C and 42°C and for the ancestral samples (Anc). Read coverage was calculated using the deduplicated mapping files. Different colors of line plots indicate biological replicates of an experimental factor group. Annotated reference sequences used for mapping of reads are shown below the evolved samples. Note that local variation in sequencing coverage are likely due to differences in sequence composition (Ekblom et al. 2014).

One aim of this study was to determine the frequency of plasmid mutations in bacterial populations and to compare these frequencies to that of chromosomes. The aforementioned theoretical prediction for mutations on plasmids showed, that those might be of low allele frequency. The high coverage on the plasmid genomes increases the detection sensitivity for rare and low-frequency variants. Nonetheless, in order to compare the number of mutations across replicons and populations, the sequencing reads of each replicon (i.e., chromosome and plasmids) were subsampled to match the lowest-coverage dataset (104x) unless stated otherwise. Furthermore, variants occurring in both ancestral and evolved populations were excluded as well as variants supported by reads in one direction only. A major challenge in detecting rare variants in pooled samples is to distinguish experimental noise such as alignment artefacts or sequencing errors from true polymorphisms with low frequencies. Therefore, to eliminate possible false positive calls, several variant filtering steps were implemented in the analysis pipeline (illustrated in). For example, owing to the previously reported low concordance between different variant calling algorithms (e.g., Li 2014, O'Rawe et al. 2013), three variant callers were used in this study. Furthermore, only variants detected concordantly by at least two of the variant callers were retained. This resulted in a set of 50 plasmid variants identified in the 48 samples. In the following, 23 variants were removed as their allele frequency was below the threshold of 2% and additional five variants were removed because of low alternative base quality. This resulted in 22 variants of which two were single nucleotide substitutions (hereafter termed point mutations) and the remaining 20 were insertion and deletions. Owing to the known difficulties to reliably identify indels (e.g., Spencer et al. 2014), a minimum threshold of 10 alternative reads was required to retain an indel variant resulting in the elimination of 18 indels that did not pass this criteria.

The two point mutations identified using the conservative comparative genomic analysis pipeline are located on plasmid pLC and were observed in two independent populations (Table 5). Both mutations are located in an intergenic region and their allele frequency is lower than 0.10 (see Figure 17). Two single nucleotide insertion mutations observed on plasmid pHC were identified in two independent hypermutator populations cultivated at 37°C. One insertion is located in an intergenic region and one is located within the origin of replication (Figure 17). The insertion mutation located in the pUC-origin of replication on plasmid pHC has the potential to change the secondary structure of RNAI, the antisense repressor of the replication of pBR322-type plasmids (Tomizawa and Itoh 1981). The insertion is located within a bubble of the RNAI secondary structure which serves as a cleavage site of RNase E. DNA replication of ColE1-type plasmids has been shown to be dependent on the rate of endonucleolytic cleavage of RNAI mediated by RNase E (Lin-Chao and Cohen 1991). A comparison of the positional entropy (Huynen et

al. 1997) at this site reveals that the insertion mutation increases the positional entropy in comparison to the reference like RNAI secondary structure (see Supplementary Figure 8). Low values of positional entropy, which is related to positional base pairing probability, indicate a strong agreement among low energy structures in a Boltzmann ensemble (Garcia-Martin and Clote 2015). Therefore, there is the possibility that the formation of the RNA secondary structure is altered at this specific position of the RNA and that the change in the primary structure impacts the site for RNase E cleavage. Furthermore, this mutation also changes the primary structure of RNAII which functions as the preprimer for the DNA polymerase I to start initiation of plasmid replication. The insertion mutation is located at the 5'-end of RNAII, but not within any of the known functional secondary structures (e.g., the three stem loop structures known to interact with RNAI (Tomizawa and Itoh 1981)). Nonetheless, it has to be noted that the plasmids evolved here are in multicopy state where the RNA elements of the plasmid replication initiation are also functional in trans (for example ColE1 plasmid (Muesing et al. 1981)).

Although allele frequencies of both insertion mutations are above 0.3, both insertions are located in homopolymer stretches of seven identical nucleotides. Homopolymer stretches have previously been shown to be one major source for false indel calls (Fang et al. 2014). Furthermore, indel mutations differ from point mutations (i.e., base substitutions) in the way they originate and the way they are repaired (e.g., Lee et al. 2012, Kunkel 2010). Therefore, for the comparison of mutation frequencies only point mutations were considered. Furthermore, only mutations occurring in intergenic regions and non-RNA coding regions were considered for the comparison.

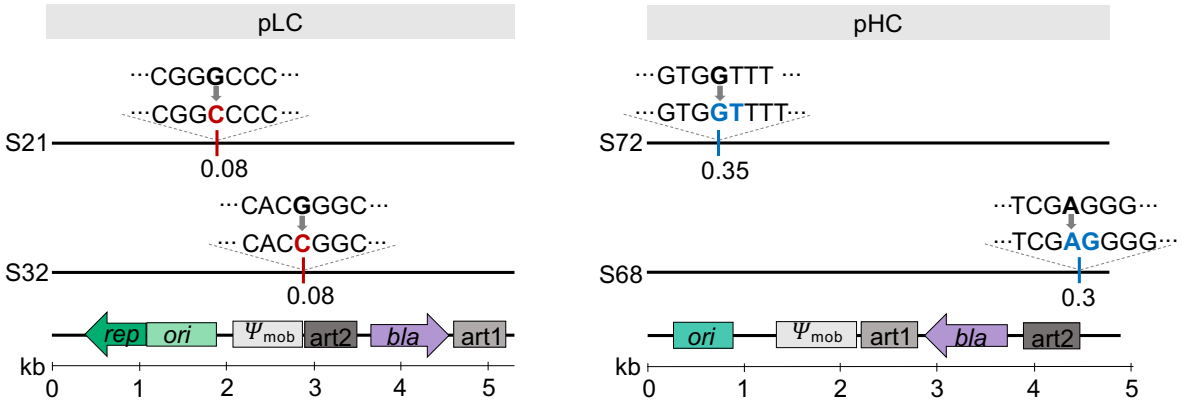

Figure 17. Genomic location of variants identified on plasmid pLC and pHC. Location of point mutations (red) and insertions (blue) are shown along with the change in nucleotide sequence (5'→3') and the respective allele frequency below. Annotated reference sequences used for mapping of reads are shown at the bottom. Two point mutations were identified in pLC-hypermutator populations cultivated at 37°C (S32) and 42°C (S21). Single nucleotide insertions were identified in pHC-hypermutator populations cultivated at 37°C (S72, S68).

Assuming an equal mutation rate between chromosome and plasmid, the paucity of plasmid variants should be evaluated against the background of variants on the host chromosome, where a total of 1,394 point mutations was observed. The expected frequency of point mutations on the two plasmids was therefore calculated using the chromosomal substitution frequency, the plasmid genome size and the plasmid copy number. This shows that mutations are unlikely to occur on either of the plasmid types evolved in the wild-type host due to the combination of low substitution rate and the plasmid small genome size (Table 5). In contrast, the combination of high genetic polymorphism in the hypermutator host with the high copy number of plasmid pHC are likely to result in observable genetic variants on the pHC plasmid within the time span of the experiment (Table 5 and Supplementary Table 21). Nonetheless, the subsampled sequencing data for pHC did not reveal any point mutations occurring on that plasmid.

In order to increase the resolution for the detection of low-frequency point mutations, the same variant calling pipeline was applied to the sequencing read datasets without subsampling (i.e., full sequencing coverage). This analysis revealed one point mutation on plasmid pHC at an intergenic position with a sequencing depth of ~9,600 and a low allele frequency of AF = 0.03 (Table 6). In contrast, considering the full sequencing depth for plasmid pLC, which is on average ~10x lower than that of plasmid pHC, two additional intergenic point mutations were observed (Table 6). Thus, despite the high sequencing depth, the observed number of point mutations on plasmid pHC does not reach the expected frequency of point mutations (Table 5), even when the full sequence coverage is included in the analysis.

The number of point mutations on the pHC plasmid was further validated by the analysis of the total pHC population sequencing data (i.e., samples were prepared without selection for plasmid hosts). Considering the full sequencing coverage, one additional point mutation on the plasmid was detected. The intergenic point mutation was observed with a low allele frequency of AF = 0.04 (Table 6) in one of the pHC populations having the hypermutator host genotype. In addition, the number of point mutations observed on the chromosome in the pooled pHC host populations was compared to that of the total population sequencing data (Supplementary Table 21). The comparison shows that the wild-type populations include, on average, two additional point mutations per population in comparison to the corresponding data of pooled plasmid host colonies. The comparison of hypermutator populations shows that the total population sequencing data includes, on average, 14 point mutations per population less than the pooled colonies sequencing data.

Overall, the above comparison between the two sequencing approaches demonstrates that the number of point mutations observed in the pooled host colonies data is representative both for the number of variants on the pHC plasmid and the chromosome.

Table 5: Number of intergenic and synonymous point mutations detected in the evolved populations. A detailed information used for the calculation of the mean and standard deviation for each of the eight experimental factor groups is shown in Supplementary Table 20. Additional low frequency point mutations were detected on the pLC plasmid considering the full sequencing coverage (see variant details in Table 6). A detailed list of all observed variants on the chromosome is given in Supplementary Table 23. Note that plasmid copy number estimates from the relative sequencing coverage of small plasmids may differ from the estimated PCN using qPCR due to the DNA extraction method as well as the sequencing approach (Becker et al. 2016). The large-scale estimates of PCN from sequencing results are lower than those obtained with qPCR, hence, estimates of the plasmid mutational supply is conservative. The ancestral PCN estimated from the sequencing results are as following: pLC-wt: 2, pLC-hypermutator: 13, pHC-wt: 86, pHC-hypermutator: 116. A comparison of the PCN distribution in the evolved populations reveals that the PCN is significantly different from that of the ancestor plasmid in several of the experimental evolution settings. However, the direction of change (i.e., PCN increase or decrease) is heterogeneous (see Supplementary Table 22 for details).

			Chromosome		Plasmid		
Plasmid type	Host genotype	T (°C)	Observed number of point mutations	Substitution per site per generation[1] $\times 10^{-9}$ (*Mean* ± *SD*)	PCN[2] (*Mean* ± *SD*)	Expected number of point mutations[3] (*Mean* ± *SD*)	Observed number of point mutations
pLC	Wild-type	37	17	2.5 ± 0.7	20.9 ± 4.9	$16.3 \times 10^{-2} \pm 5.0 \times 10^{-2}$	0
		42	16	2.4 ± 1.8	4.8 ± 3.2	$4.5 \times 10^{-2} \pm 4.8 \times 10^{-2}$	0
	Hypermutator	37	148	22.4 ± 5.2	7.1 ± 2.2	$5.0 \times 10^{-1} \pm 1.7 \times 10^{-1}$	1
		42	87	13.2 ± 3.3	4.1 ± 1.4	$1.8 \times 10^{-1} \pm 1.1 \times 10^{-1}$	1
pHC	Wild-type	37	6	0.87 ± 0.6	605.0 ± 501.3	2.0 ± 2.0	0
		42	6	0.87 ± 0.8	294.0 ± 105.8	$7.9 \times 10^{-1} \pm 7.2 \times 10^{-1}$	0
	Hypermutator	37	98	14.3 ± 3.8	154.5 ± 63.4	8.0 ± 5.0	0
		42	147	21.4 ± 11.5	252.6 ± 106.3	19.1 ± 16.2	0

[1] The chromosomal substitution rate is calculated as $R_{Chr} = N_{obs} \times (N_{sites} \times N_{gen})^{-1}$, where N_{obs} is the number of observed point mutations, N_{sites} is the number of intergenic and synonymous sites on the chromosome having a coverage ≥10 and N_{gen} is the number of generations in our experiment.
[2] Plasmid copy number (PCN) was estimated from the sequencing results of evolved populations as the relative coverage of plasmid and chromosome replicons (detailed list in Supplementary Table 19).
[3] The expected number of point mutations on the plasmid is calculated as $N_{exp} = R_{Chr} \times N_{sites} \times$ PCN $\times N_{gen}$, where N_{sites} is the number of intergenic and synonymous sites on the plasmid having a coverage ≥10.

This discrepancy between the observed and expected frequency of point mutations on the pHC plasmid can be explained under the segregational drift hypothesis as due to the rapid loss of most plasmid mutations. The analysis further reveals that the allele frequency of plasmid variants is considerably lower in comparison to that of chromosomal variants. Of the total chromosomal point mutations, 30% reached fixation within the population (AF ≥ 0.9), whereas point mutations on plasmids remain at a low

frequency (AF ≤ 0.09; Figure 18). The stark difference in the allele frequency distribution between the plasmid and chromosomal alleles indicates that the increase in plasmids allele frequency is considerably slower in comparison to chromosomal alleles. This observation is in agreement with the hypothesis according to which mutations that emerge on multicopy plasmid genomes are repeatedly 'diluted' in the population due to segregational drift.

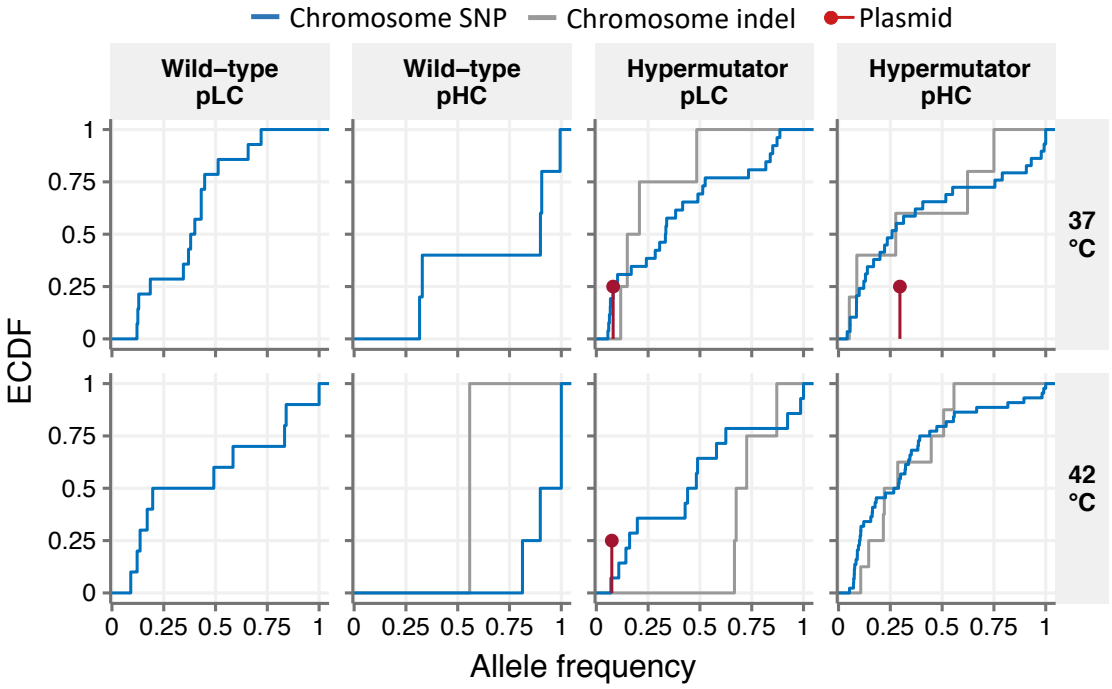

Figure 18. Joint allele frequency plots of variants detected in intergenic regions (excluding RNA-coding genes). Variants (i.e., point mutations and indels) detected in subsampled read datasets (mean coverage 104x) are pooled for all replicate populations evolved under the same factor combination. Allele frequencies of plasmid variants are presented as stem-and-loop due to the data discreteness. A detailed list of allele frequencies, location and annotation is given in Table 6 (for plasmids) and in Supplementary Table 23 (for chromosomes).

Notably, the analysis of the full sequencing data revealed one point mutation in the Rep protein coding region of plasmid pLC. The same point mutation was found in four different populations having the hypermutator and wild-type genotype. Similarity, a search for the Rep protein sequence revealed that the variant is not located within any known hypothetical secondary structure of that protein. Moreover, no indel mutations were identified on plasmid pLC, while seven of the eight variants identified on plasmid pHC using the full sequencing coverage were indel mutations. The discrepancy in the number of point and indel mutations found on plasmid pLC and pHC (Table 5B) might be associated with the sequencing coverage of both plasmids as a high sequencing depth has been previously shown to increase the sensitivity for indel calls (Fang et al. 2014). Nevertheless, it has also noted that an increase in coverage does not impair homopolymer-associated false positive calls (Wiberg et al. 2017). Furthermore, one indel

mutation located in intergenic regions was observed in four different populations (Table 6B). The identification of the same intergenic indel variant in independent samples is likely an indicator for false positives arising from alignment artefacts or indicate a mutational hotspot.

Table 6. Variants detected on plasmids in different samples sequenced after 800 generations of evolution in the chemostats. (A) Variants detected in plasmid host samples (i.e., total populations for pLC and pooled hosts for pHC) using subsampled read datasets (sub). **(B)** Variants detected in plasmid host samples using all sequencing reads (full). **(C)** Variants detected in evolved pHC-populations of sample type 'total population' (TP) using all sequencing reads. Note that variants detected in corresponding samples of 'pooled hosts' are reported in (B). Corresponding pHC-populations are indicated by the combination of plasmid type, host genotype, temperature, and replicate number. Note that also variants with an allele frequency <0.02 are reported. These were included to demonstrate that the sequencing of 'pooled host' samples can increase the resolution for variant detection. Notably, the two variants listed at the end of the table were also found in the corresponding samples of 'pooled hosts', but with an AF < 0.02 (using full coverage dataset). Wt: wild-type; Hm: Hypermutator; TP: total population; PH: pooled hosts. A description of all table fields is given in Supplementary Table 23. Note that the variant position refers to plasmid genome sequences published in GenBank database.

	Sample ID	Dataset	Plasmid type	Host genotype	T (°C)	Replicate	Sample type	Pos	Variant type	REF	ALT	Depth	AF	Variant ID	Variant location and effect	Location annotation
(A)	S32	sub	pLC	Hm	37	2	TP	4	SNP	G	C	111	0.081	i G4C	intergenic (–/-752)	–/beta-lactamase
	S21	sub	pLC	Hm	42	3	TP	4155	SNP	G	C	174	0.075	i G4155C	intergenic (-798/–)	replication protein/–
	S68	sub	pHC	Hm	37	2	PH	2308	INDEL	A	AG	81	0.296	i 2308 +G	intergenic (-744/–)	beta-lactamase/–
	S72	sub	pHC	Hm	37	5	PH	3493	INDEL	G	GT	121	0.347	i 3493 +T	intergenic (-1929/–)*	beta-lactamase/–*
(B)	S07	full	pLC	Wt	42	1	TP	2886	SNP	T	G	1082	0.042	*rep* T158P	T158P (ACC→CCC)	replication protein
	S32	full	pLC	Hm	37	2	TP	4	SNP	G	C	1338	0.028	i G4C	intergenic (–/-752)	–/beta-lactamase
	S33	full	pLC	Hm	37	3	TP	2886	SNP	T	G	1619	0.038	*rep* T158P	T158P (ACC→CCC)	replication protein
	S35	full	pLC	Hm	37	5	TP	2886	SNP	T	G	2271	0.034	*rep* T158P	T158P (ACC→CCC)	replication protein
	S35	full	pLC	Hm	37	5	TP	5142	SNP	A	C	1874	0.043	i A5142C	intergenic (-1785/–)	replication protein/–
	S36	full	pLC	Hm	37	6	TP	4772	SNP	G	A	1229	0.024	i G4772A	intergenic (-1415/–)	replication protein/–
	S19	full	pLC	Hm	42	1	TP	2886	SNP	T	G	948	0.040	*rep* T158P	T158P (ACC→CCC)	replication protein
	S21	full	pLC	Hm	42	3	TP	4155	SNP	G	C	1238	0.071	i G4155C	intergenic (-798/–)	replication protein/–
	S67	full	pHC	Hm	37	1	PH	2308	INDEL	A	AG	8901	0.056	i 2308 +G	intergenic (-744/–)	beta-lactamase/–
	S67	full	pHC	Hm	37	1	PH	2524	INDEL	TA	T	6737	0.021	i 2524 Δ1 bp	intergenic (-960/–)	beta-lactamase/–
	S68	full	pHC	Hm	37	2	PH	2308	INDEL	A	AG	9554	0.339	i 2308 +G	intergenic (-744/–)	beta-lactamase/–
	S69	full	pHC	Hm	37	3	PH	2308	INDEL	A	AG	13498	0.044	i 2308 +G	intergenic (-744/–)	beta-lactamase/–
	S70	full	pHC	Hm	37	4	PH	2159	SNP	C	T	9657	0.026	i C2159T	intergenic (-595/–)	beta-lactamase/–
	S72	full	pHC	Hm	37	6	PH	3493	INDEL	G	GT	12700	0.337	i 3493 +T	intergenic (-1929/–)*	beta-lactamase/–*
	S61	full	pHC	Hm	42	1	PH	821	INDEL	GC	G	12535	0.036	*bla* 744 Δ1 bp	coding (744/861 nt)	beta-lactamase
	S63	full	pHC	Hm	42	3	PH	2308	INDEL	A	AG	16905	0.049	i 2308 +G	intergenic (-744/–)	beta-lactamase/–
(C)	S25	full	pHC	Hm	37	1	TP	2308	INDEL	A	AG	10201	0.055	i 2308 +G	intergenic (-744/–)	beta-lactamase/–
	S25	full	pHC	Hm	37	1	TP	2524	INDEL	TA	T	8070	0.017	i 2524 Δ1 bp	intergenic (-960/–)	beta-lactamase/–
	S26	full	pHC	Hm	37	2	TP	2308	INDEL	A	AG	17461	0.200	i 2308 +G	intergenic (-744/–)	beta-lactamase/–
	S27	full	pHC	Hm	37	3	TP	2308	INDEL	A	AG	18629	0.042	i 2308 +G	intergenic (-744/–)	beta-lactamase/–
	S28	full	pHC	Hm	37	4	TP	2159	SNP	C	T	16467	0.022	i C2159T	intergenic (-595/–)	beta-lactamase/–
	S30	full	pHC	Hm	37	6	TP	3493	INDEL	G	GT	8840	0.370	i 3493 +T	intergenic (-1929/–)*	beta-lactamase/–*
	S13	full	pHC	Hm	42	1	TP	821	INDEL	GC	G	3421	0.006	*bla* 744 Δ1 bp	coding (744/861 nt)	beta-lactamase
	S15	full	pHC	Hm	42	3	TP	2308	INDEL	A	AG	2341	0.016	i 2308 +G	intergenic (-744/–)	beta-lactamase/–
	S15	full	pHC	Hm	42	3	TP	3493	INDEL*	G	GT	3377	0.060	i 3493 +T	intergenic (-1929/–)*	beta-lactamase/–*
	S30	full	pHC	Hm	37	6	TP	2316	SNP*	C	G	7528	0.042	i C2316G	intergenic (-752/–)	beta-lactamase/–

* Note that this mutation is located within the origin of replication

**Note that these variants were also detected in the corresponding sequencing sample of PH (S63 for S15; S72 for S30), but the allele frequency was below the AF threshold of 0.02

4.8 Host chromosome evolution

The comparison between the evolved and ancestral populations revealed that most of the evolved genetic variants are found on the chromosome (*n* = 1,394; see Supplementary Table 23). The majority of the chromosomal variants (90%) are observed in the hypermutator populations where the substitution rate is, on average, 10-fold higher in comparison to the wild-type populations (Table 5). Genetic variants are observed in 638 protein coding genes and ncRNA genes, of which 173 (27%) genes accumulated genetic variants in more than one population. The distribution of common mutated genes reveals a strong signal of parallel evolution among populations evolved under similar settings (Figure 19).

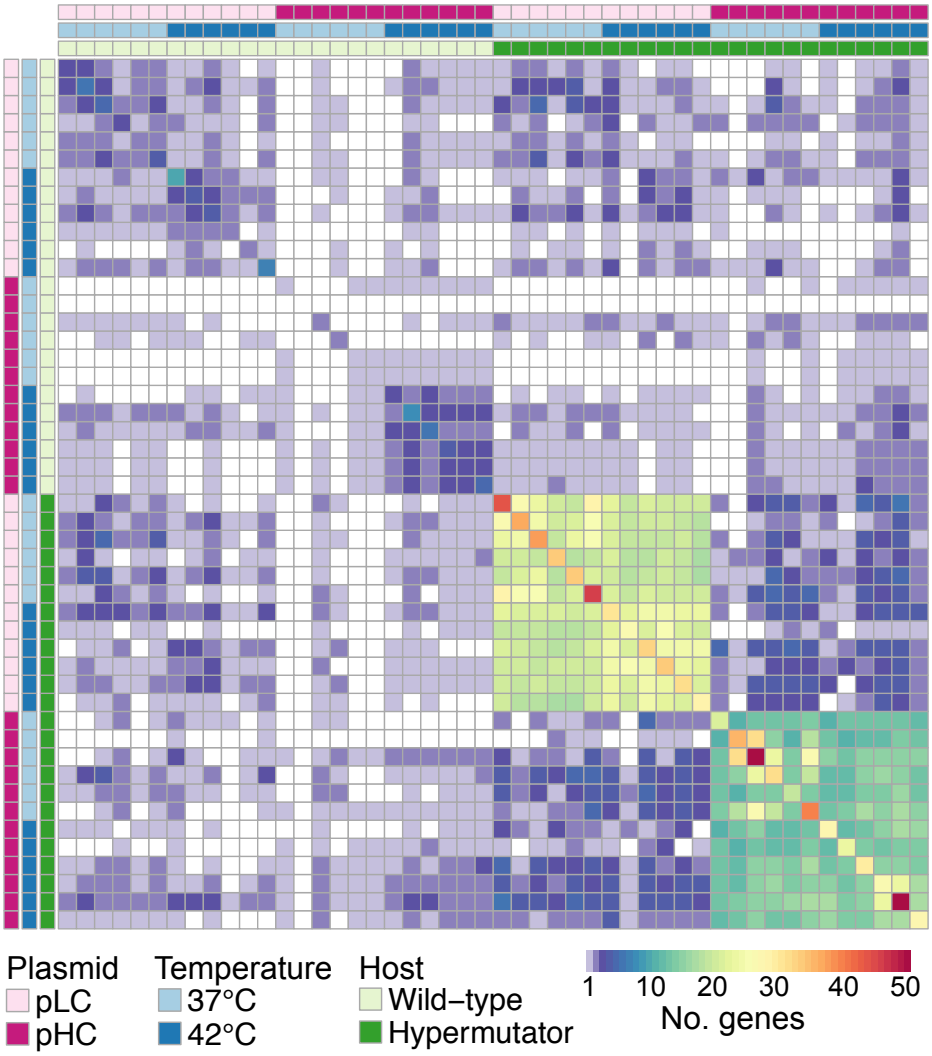

Figure 19. Parallel evolution of the chromosome. A heatmap representing the number of shared mutated genes among the 48 evolved populations. The number of genes mutated in population pair *x*, *y* is calculated as the number of genes in which genetic variants (single base substitutions or indels) are observed in both populations. Cells along the diagonal present the number of genes where a mutation was detected in the corresponding population and at least one additional population. Annotation bars at the top and left represent the experimental factors.

Of the parallel mutated genes, 60 genes (35%) are specific to populations belonging to one of the eight experimental factor combinations, indicating that the combination of host genotype, plasmid replicon type and temperature had an impact on the evolution of these genes. Furthermore, a total of 50 mutated genes (29%) are shared among hypermutator populations having the same plasmid type, regardless of the growth temperature (Figure 19). Hypermutator-pLC populations share, on average, 19.62 ± 2.09 (*SD*) mutated genes, whereas hypermutator-pHC populations show a lower level of parallelism with 14.45 ± 3.30 shared genes on average (*SD*). Furthermore, two small clusters of parallel mutated genes are observed in the wild-type hosts, the first cluster comprises the pLC populations and the second cluster includes the pHC populations evolved at 42°C.

At the resolution of specific mutations, 144 (15%) variants were detected in more than one of the 48 evolved populations (see Supplementary Figure 9 for a detailed representation of frequencies of parallel and population specific variants). The allele frequency of parallel variants is significantly higher than the allele frequency of population specific variants ($P < 0.001$, using two-sample Kolmogorov-Smirnov test, $n_{parallel} = 720$, $n_{specific} = 841$; see Supplementary Figure 10). To quantify the contribution of the three experimental evolution factors to parallel evolution of the host chromosome, the allele frequencies of parallel genetic variants among all populations were compared. This revealed a significant effect of plasmid type ($P = 1.1 \times 10^{-69}$) and temperature ($P = 3.9 \times 10^{-46}$) on the allele frequency variation (using ANOVA on aligned rank transformed allele frequencies (Wobbrock et al. 2011; detailed statistics in Supplementary Table 24). In the wild-type populations, there is a strong interaction between plasmid type and temperature, whereas in the hypermutator populations, the same interaction is observed along with a main effect of the plasmid type (Figure 20). These results thus reveal that the effect plasmid replicon type on the chromosomal allele dynamics is equal or larger in comparison to the growth temperature. Elevated growth temperature has an impact on *E. coli* physiology and consequences to its evolution (Deatherage et al. 2017). A recent study showed that plasmid acquisition may have a physiological effect on its *Pseudomonas aeruginosa* host (Millan et al. 2018). These results suggest that the effect of plasmids on the host metabolism and evolution can be equal or larger than that of the environmental temperatures.

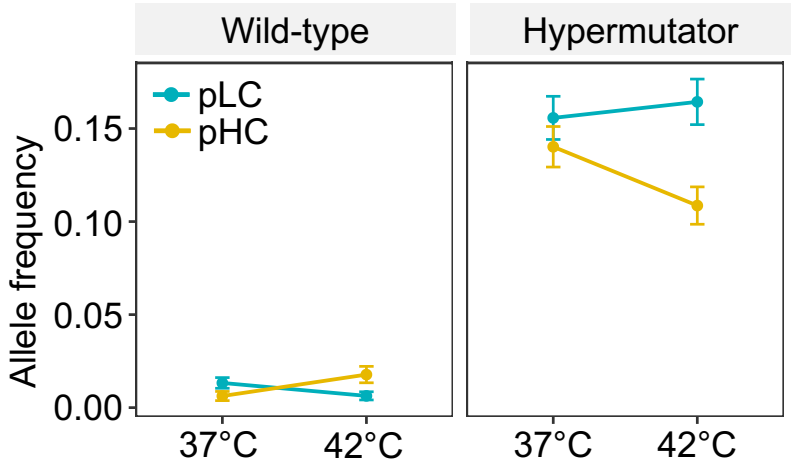

Figure 20. An interaction plot of the main factors in the experiment as calculated from the complete set of allele frequencies of parallel variants (included in Supplementary Table 23). Dots represent means and error bars represent the standard error of the mean. ANOVA demonstrated significant effects for plasmid replicon type and temperature along with significant interactions between the three factors used in the experiment (statistics in Supplementary Table 24).

To further identify variants that are characteristic for specific factor combinations, the effect of the factors and their interaction on the allele frequency of each parallel variant was tested (using ANOVA on aligned rank transformed allele frequencies and FDR). This results in 37 variants whose allele frequency is significantly different among the factor combinations (Figure 21; Supplementary Table 25).

A single variant occurred in all wt-pLC populations evolved at 37°C, where a nonsense mutation of Glutamine into a stop codon occurred in the *rpoS* gene. Hence, that gene is likely non-functionalized in these populations. The *rpoS* encodes the RNA polymerase σ^S-subunit that is the master regulator of the general stress response in *E. coli* (e.g., Antoine and Locht 1992, Patten et al. 2004). Loss of RpoS function was previously reported to occur rapidly in nutrient-limited chemostat populations (Notley-McRobb et al. 2003, Jahn et al. 2016). Two additional non-synonymous substitutions in genes encoding for an integrase (*intA*) of a cryptic prophage and a glycosyl transferase (*wcaA*) are common to all six hypermutator-pLC populations evolved at 42°C (Figure 21, Table 7).

Mutations that are characteristic to hypermutator-pLC populations (Figure 21) are found in genes that belong to four main functional categories, including carbohydrate metabolism, fatty acid metabolism, biofilm formation and stress response. Eleven of the 17 variants identified in protein coding sequences result in a change of the amino acid sequences (Table 7). Notably, the vast majority of these mutations are located in genes whose proteins are involved in the formation of the outer membrane or in biofilm formation.

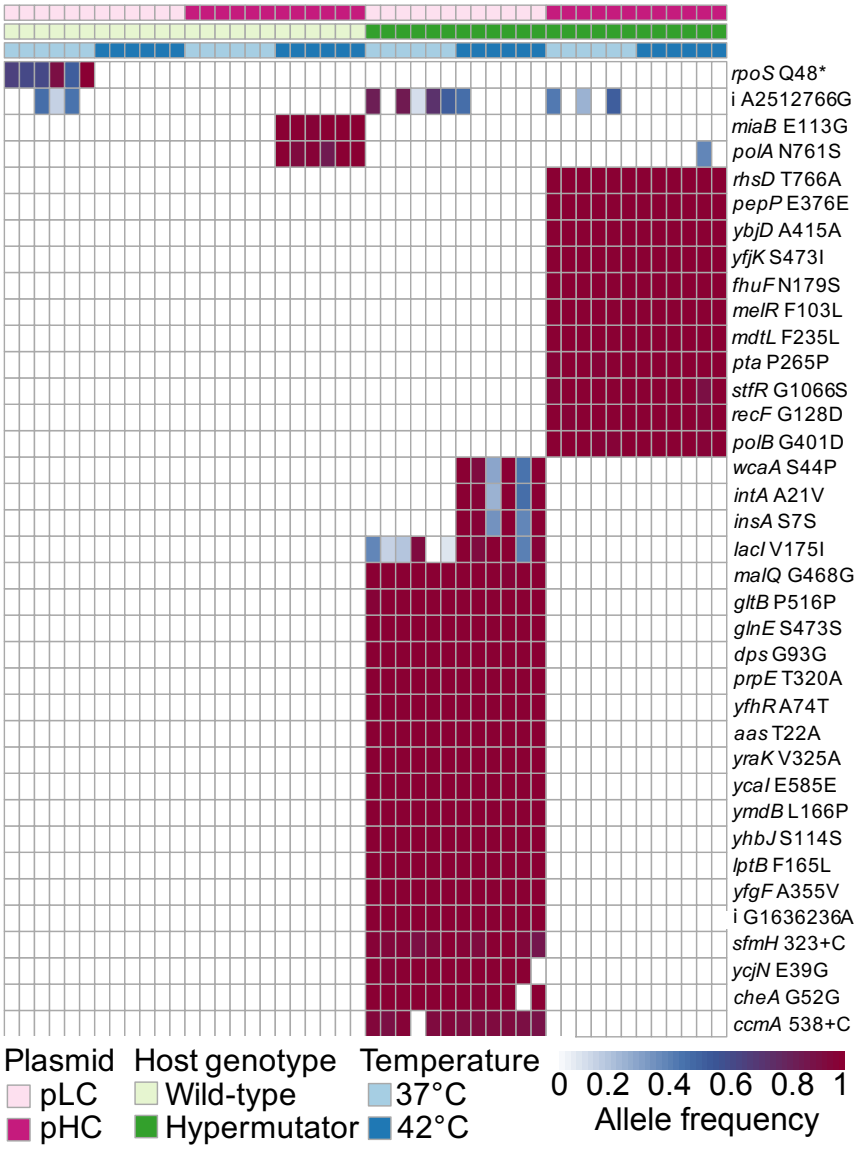

Figure 21. Color-coded matrix of chromosomal variants whose allele frequency is significantly different among the main factors or their combination (using ANOVA on aligned rank transformed allele frequencies and FDR; statistics in Supplementary Table 25). Intragenic variants (11 synonymous and 22 non-synonymous) are indicated by the gene symbol and, in case of a single base substitution, coded as [ancestral amino acid][amino acid position][alternative amino acid]. The two insertion mutations are indicated by a gene symbol and coded as [nucleotide position in gene][+ inserted nucleotide]. [*] indicates a non-sense codon. The two intergenic variants are indicated by [i] coded as [ancestral nucleotide][genomic position][alternative nucleotide].

Example genes that likely contribute to biofilm formation are *sfmH* and *yraK* that code for fimbrial-like adhesin proteins known to promote adhesion in *E. coli* (Vieira and Messing 1982, Korea et al. 2010). The corresponding amino acid changes are located within the fimbrial-type adhesion domains of these proteins. The non-synonymous mutation in the *yraK* gene results in an amino-acid replacement and the insertion mutation located within the *sfmH* gene likely alters the stop codon such that the new polypeptide is

only 123 amino acids long instead of 327 amino acid length. Example genes involved in the formation of the outer membrane are the essential gene *lptB* and an acetyltransferase encoding gene (*aas)* that participates in membrane phospholipid turnover (Hsu et al. 1991). LptB is part of a transporter complex involved in the translocation of lipopolysaccharides from the inner to the outer membrane in *E. coli* (Sperandeo et al. 2006, Rosano and Ceccarelli 2014). The non-synonymous *lptB* mutation observed in all hypermutator-pHC populations results in an amino-acid replacement located within the ABC-transporter like domain of that protein (Table 7). Additional amino acid replacements occurred in a propionyl-CoA synthetase (*prpE*) and the repressor of the lactose operon (*lacI*) where the amino acid replacement is observed in the ligand binding domain (Pfam annotation: periplasmic binding protein-like domain; Table 7). The propionyl-CoA synthetase PrpE catalyzes the first step of propionate catabolism in *E. coli* (Textor et al. 1997, Arjan et al. 1999) and the amino acid replacement is located within a putative AMP binding domain (Table 7).

Table 7. Functional categories of parallel chromosomal mutations observed in pLC-populations. Functions are reported for non-synonymous and frame-shift mutations whose allele frequency is significantly different among the main factors or their combination. Functional categories are assigned according to GO terminology. Putative functional domains are reported for variants located in known functional domains as found in the Pfam database.

Variant	Functional category	Reference	Pfam domains
pLC wild-type 37°C			
rpoS Q48*	regulation of transcription; stress response	Nguyen et al. 1993; Maciag et al. 2011	
pLC hypermutator 42°C			
wcaA S44P	lipopolysaccharide biosynthetic process	Stevenson et al. 1996	glycosyl transferase family 2
intA A21V	provirus excision	Kirby et al. 1994	DNA-binding domain
pLC hypermutator 37°C and 42°C			
lacI V175I	negative regulation of transcription	Hudson and Fried 1990	periplasmic binding protein-like domain
prpE T320A	propionate catabolic process	Guo and Oliver 2012	AMP binding domain
yfhR A74T	uncharacterized protein		
aas T22A	phospholipid biosynthetic process	Hsu et al. 1991	acyltransferase domain
yraK V325A	cell adhesion	Korea et al. 2010	fimbrial domain
ymdB L166P	negative regulation of endoribonuclease activity; regulation of biofilm formation	Kim et al. 2008; Kim et al. 2013	
lptB F165L	lipopolysaccharide transport	Sperandeo et al. 2006	ABC transporter-like domain
yfgF A355V	cellular response to anoxia; regulation of biofilm formation	Lacey et al. 2010	
sfmH 332 +C	cell adhesion; mannose binding	Korea et al. 2010	fimbrial domain
ycjN E39G	lipoprotein; predicted periplasmic binding protein	Moussatova et al. 2008	extracellular solute-binding protein family
ccmA 538 +C	heme transport	Feissner et al. 2006	

The evolution of hypermutator-pHC populations is characterized by a majority of non-synonymous point mutations (Table 8). These variants are fixed (i.e., AF > 0.9) in all hypermutator-pHC populations. The mutated genes are classified into three main categories including carbohydrate metabolism, stress response and DNA replication. Example mutated genes are DNA polymerase II (*polB*) and DNA gap repair protein (*recF*). The amino acid replacement observed in Pol II is located within the putative DNA polymerase domain and according to UniProt database the *polB* G401D variant is a frequently observed a natural variant. RecF is a component of the RecFOR complex that functions in RecA-mediated recombinational DNA-repair (mainly ssDNA gaps; e.g., Handa et al. 2009). The amino acid replacement observed in the RecF protein is not located within any specific functional region.

A single variant located upstream of the *mntH* gene (i A2512766G; Figure 21) a permease that is involved in the uptake of manganese (Haemig and Brooker 2004), was identified in eleven populations evolved at 37°C and one population evolved at 42°C. It was previously suggested that manganese supports the growth of iron-deficient *E. coli* cells and it was shown that *mntH* expression is strongly induced in peroxide-stressed cells (Anjem et al. 2009, Vega and Gore 2014). A promotor prediction revealed that this mutation might results in altered sites involved in the transcriptional regulation of this gene (Supplementary Figure 11).

Table 8. Functional categories of parallel chromosomal mutations observed in pHC-populations. Functions are reported for non-synonymous and frame-shift mutations whose allele frequency is significantly different among the main factors or their combination. Functional categories are assigned according to GO terminology. Pfam domains are reported for variants located in known functional domains as found in the Pfam database.

Variant	Functional category	Reference	Pfam domains
pHC wild-type 42°C			
miaB E113G	tRNA methylation	Esberg et al. 1999	
polA N761S	e.g., DNA replication and repair	Setlow and Kornberg 1972; Sharon et al. 1975	DNA polymerase family A
pHC hypermutator 37°C and 42°C			
rhsD T766A	cellular response to sulfur starvation	van der Ploeg et al. 1996	
yfjK S473I	response to ionizing radiation; defense response to virus	Yasui et al. 2014; Byrne et al. 2014	
fhuF N179S	siderophore-dependent iron import into cell; reductive iron assimilation	Matzanke et al. 2004	
melR F103L	regulation of transcription	Webster et al. 1989	
mdtL F235L	drug transmembrane transport	Nishino and Yamaguchi 2001	
stfR G1066S	structural protein of cryptic prophage	Riley et al. 2006	Phage tail fibre repeat
recF G128D	e.g., DNA repair, double-strand break repair and SOS response	Villarroya et al. 1998	
polB G401D	e.g., DNA replication and repair	Kornberg and Gefter 1971	DNA polymerase family B

A cluster including two non-synonymous substitutions is observed for wt-pHC populations evolved at 42°C. The substitutions occurred in a gene encoding for a tRNA modification enzyme (*miaB*) and the DNA polymerase I encoding gene (*polA*). Overall, 11 different *polA* mutations were identified in 16 pHC-populations and none in pLC-populations (Supplementary Table 23). Mutations in *polA* have been previous reported to decrease the copy number of high copy number ColE1 plasmid mutants in *E. coli* (Yang and Polisky 1993). Most of the *polA* mutations identified here are located in the same region (Klenow fragment), similarly to the previously reported mutants. This suggests that the *polA* mutations observed in the wt-pHC populations evolved as a response to the pHC high copy number. Nonetheless, notably no decrease in pHC copy number in the pHC populations having the *polA* mutation was observed (Supplementary Tables 19 and 22).

Taken together, the differential acquisition of mutations in hypermutator populations carrying plasmid pLC or pHC suggests that the plasmid replicon type had a significant impact on the host chromosome evolution.

5 Discussion

5.1 Evolution of the host chromosome vs. evolution of the plasmid

Previous experimental evolution studies of plasmid-host adaptation noted that evolved variants are mostly observed in the host chromosome rather than the plasmid genome (e.g., Bouma and Lenski 1988, San Millan et al. 2014, San Millan et al. 2016, Santos-Lopez et al. 2016, Loftie-Eaton et al. 2017), and this is indeed the case also for our study. Naturally, the mutational supply of a chromosome of the size of *E. coli* (4.6 Mb) is higher than the mutational supply of our model plasmid genomes. Consequently, more mutations are likely to arise on the chromosome than on the plasmid. Notably, in most studies of plasmid-host coevolution (including ours), the selection pressure is imposed on the maintenance of the plasmid in the host population rather than a specific plasmid allele (e.g., as in San Millan et al. 2016). Because plasmids depend on the host machinery for their replication and persistence, the selection for plasmid maintenance is, in practice, imposed on the host machinery rather than on the plasmid itself. Moreover, the potential adaptive responses to the selective pressure for the plasmid maintenance are numerous in the complex host chromosomes (e.g., San Millan et al. 2014, Harrison et al. 2015), but are very limited in the genetically compact plasmid genome. This, in combination with the higher mutational supply of the chromosome, implies that most adaptive variants are expected to occur on the chromosome. This can explain the high frequency of genetic variants observed on the chromosome in our experiment, as well as others (e.g., San Millan et al. 2014, Harrison et al. 2015, Loftie-Eaton et al. 2017).

The significant effect of plasmid type on the chromosomal allele frequency observed in the experiment (Figure 21) suggests that evolution of the host chromosome depends on the replicon type of the model plasmids, with the origin of replication being a prominent characteristic thereof. The evolutionary scenario portrayed here is highly relevant for plasmid-mediated evolution of antibiotics resistant strains (e.g., Stoesser et al. 2016, Jechalke et al. 2014, Sandegren et al. 2011) as in such incidents, the antibiotics impose a selection pressure for the plasmid maintenance in the population. These findings suggest that the evolution of plasmid-mediated antibiotics resistance is expected mostly to involve the host adaptation to the plasmid replicon type rather than evolution of the plasmid encoded trait.

The results from the experimental evolution of model plasmids demonstrate that the low-copy replicon has accumulated more point mutations in comparison to the high-copy replicon (Table 5). This observation is in contrary to the expectation according to the

mutational supply on the plasmid genome. This deviation from the expectation can be explained by the inverse correlation between population size and the impact of genetic drift on allele dynamics in the population. The low-copy plasmid constitutes a small replicon population within the cell. The dynamics of allele frequency due to drift in small populations are expected to have large fluctuations such that novel alleles are quickly lost or fixed (Bodmer and Cavalli-Sforza 1976). In contrast, the high copy plasmid constitutes a large replicon population within the cell where fluctuations in allele frequency over time are expected to be small (Bodmer and Cavalli-Sforza 1976).

Notably, plasmids are physically linked to their host and therefore, the fate of plasmid genotypes strictly depend on their host fitness. In other words, the plasmid genotypes observed at the end of the evolution experiment are likely linked with evolutionary successful host genotype. Previous experimental evolution studies using a chemostat system showed that the largest fitness improvement (i.e., adaptation to the chemostat conditions) was reached after 150 to 200 generations (e.g., Wick et al. 2002, Dykhuizen and Hartl 1981). Thus we speculate that evolutionary successful genotypes have swiped through the population early on in the experiment. Considering that our experiment was conducted with 800 generations, we hypothesize that most of the genetic variation we observe has emerged later on during the experiment. This would explain the fixation of chromosomal mutations that seem to be related to adaptation to chemostat conditions. Accordingly, we suggest that the plasmid diversification occurred later on within these co-existing chromosomal genotypes. Further time series analysis of the evolved populations will elucidate the rise of plasmid mutations over time.

5.2 Impact of population size and consideration of the experimental system

In addition to differences in plasmid copy number, the accumulation of mutations on the plasmid is affected also by the size of the (cell) population. In the hypermutator pHC populations, where an observable number of plasmid mutations was expected to be observed, the frequency of plasmid carrying cells was between 35% and 98% at the end of the evolution experiment. For neutral mutations residing on a chromosome or plasmid of copy number of one per cell, theory predicts that the rate of substitution is equal to the rate of mutation and is independent of the population size. On the other hand, for advantageous mutations, theory predicts that the mean number of mutant cells is a product of the population size, the mutation rate and the selection coefficient (Graur 2015). The average estimated substitution rates for pLC and pHC are almost identical (Table 5). Furthermore, assuming the selection regime was similar in all evolve populations, leaves the population size as the main difference between the pLC and pHC

populations. Hence, one could hypothesize that the observed differences in the number of mutations are the result of difference in the population size. Nonetheless, while the total population size was not different among populations in the chemostat system, the proportion of plasmid hosts – i.e., the host population size – was different between the pLC and pHC populations. While pLC-Hypermutator populations comprised ca. 100% hosts, the lowest fraction of hosts in pHC-Hypermutator populations was only 35%. Therefore, without the impact of segregational drift, the number of adaptive point mutations *K* on the pHC plasmid, is expected to be roughly three times larger than for plasmid pLC. Given an average PCN of 10 for plasmid pLC and an average PCN of 100 for plasmid pHC, the ratio of the expected number of point mutations is calculated as:

$$K = 2Nsu$$

$$\frac{K_{pLC}}{K_{pHC}} = \frac{2N_{pLC}su \times PCN_{pLC}}{2N_{pHC}su \times PCN_{pHC}}$$

$$= \frac{N_{pLC} \times PCN_{pLC}}{N_{pHC} \times PCN_{pHC}} = \frac{3}{1} \times \frac{10}{100} = \frac{3}{10}$$

where *N* is the population size, *s* is the selection coefficient and *u* is the mutation rate. Consequently, even considering the differences in the number of plasmid carrying cells, an increased number of mutations is expected for plasmid pHC. Note, that this is a simplistic estimation that does not take into account the structured plasmid population (see Appendix Section 6.1 and discussion below).

The choice of the experimental evolution system in this study deserved a special consideration. Most of the experimental evolution studies published in the literature in the last decade used the method of serial transfer experiments (see review in Barrick and Lenski 2013). In comparison to serial batch experiments, where the evolved populations experience serial bottlenecks, the population size in a chemostat system is kept constant over time. This difference constitutes a significant advantage when studying population genetics since most theoretical models of allele dynamics assume a constant population size. In addition, the fluctuating population size in serial batch experiments is expected to reduce the rate of molecular and phenotypic adaptation by reducing genetic diversity due to a stochastic elimination of rare alleles (de Visser und Rozen 2005, Colegrave 2002). Furthermore, in comparison to serial transfer experiments, the bacterial population size is kept at a much larger size in chemostats (usually 10^8-10^{11} cells). Population genetic theory predicts that genetic diversity increases with the population size and the mutation rate. Therefore, the larger population size that can be achieved in a chemostat system allows

for the emergence of a higher genetic diversity in comparison to population sizes usually used in serial batch experiments. Since our hypothesis predicted a paucity of observable plasmid alleles (due to segregational drift) the latter property of the chemostat system added an important component to our decision to establish and use a chemostat system in this study.

5.3 Segregational drift

The impact of segregational drift on plasmid alleles is best understood in comparison to the chromosomal alleles. While novel chromosomal alleles emerging on a haploid chromosome are inherited to all daughter cells in the population, the inheritance of plasmid alleles depends on the segregation pattern of plasmid copies. Indeed, simulated evolution (Section 6.1) demonstrated that the frequency of neutral mutations emerging on a multicopy plasmid is higher in comparison to a haploid chromosome, which is in agreement with the higher mutational supply of multicopy plasmids (San Millan et al. 2016). Nevertheless, the simulation also showed that median allele frequency of mutations arising on multicopy plasmids is lower than that of chromosomal mutations in a comparable population size (i.e., number of replicons). Hence, the allele frequency of mutations residing on multicopy plasmids is increasing slower in comparison to chromosomal alleles. Following the emergence of a novel plasmid allele, plasmid segregation during cell division has three potential outcomes for the plasmid genotype of the daughter cells: 1) loss of the novel plasmid allele, 2) the presence of polymorphic plasmid alleles in the cell, or 3) fixation of the novel plasmid allele in the cell (see illustration in Figure 22).

The expected effect of plasmid copy number on the allele dynamics was observed in the simulated evolution of beneficial alleles (i.e., $s > 0$; Section 6.1): on the low-copy plasmid (p10), the loss of plasmid alleles occurs more frequently in comparison to the chromosome, but the median fixation time is nearly the same as that of the chromosome. Indeed, previous studies showed that under strong selective conditions, beneficial mutations on multicopy plasmids can rise quickly to fixation (San Millan et al. 2016). Notably, the simulation of beneficial alleles (Section 6.1) revealed that alleles on the high copy plasmid (p100) remain polymorphic over a longer time scale and have a higher median fixation time. For neutral alleles, segregational drift of multicopy plasmids hinders the increase of plasmid allele frequency; it leads to frequent and rapid mutant allele loss on the one hand, and to longer fixation time on the other hand. Altogether, these simulations demonstrated that the effect of segregational drift on plasmid allele dynamics counteracts the effect of higher mutational supply accompanying increased copy number.

Consequently, the evolvability of low-copy plasmids is higher than that of high copy plasmids despite the latter higher mutational supply.

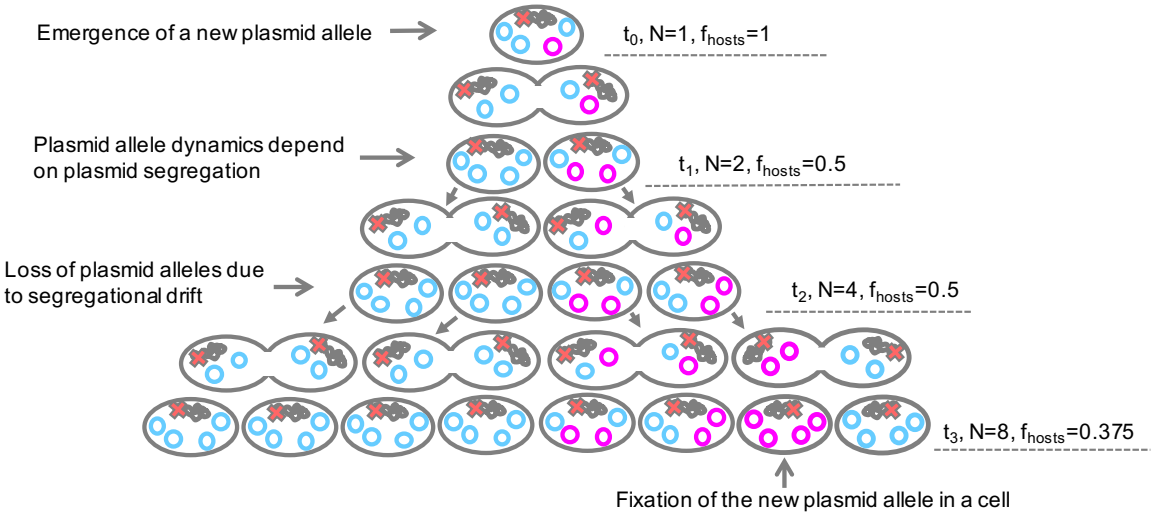

Figure 22. An illustration of the consequences of segregational drift to plasmid allele dynamics. The illustrated plasmid copy number is four and its segregation into daughter cells is balanced (i.e., the daughter cells inherit an equal number of plasmids). In the depicted scenario, one allele emerges on the chromosome (red X) and another allele emerges on the plasmid (magenta) at t_0. Both alleles are considered neutral (i.e., s = 0). The population size (N) and the frequency of hosts (f_{hosts}) over three generations are presented. The chromosomal allele is inherited into all daughter cells, such that it is present in the total population. Random segregation of the plasmid genotypes leads to decrease in the number of hosts. At t_3, only a small minority in the population harbors the new plasmid allele. In the absence of selection for the plasmid allele presence, the new plasmid allele is deemed to remain at a very low frequency within the population (or be lost). Note: this is a simplistic example that does not include loss of host cells due to drift and it does not include consideration of recombination among plasmids.

The expected effect of plasmid copy number on the allele dynamics was observed in the simulated evolution of beneficial alleles (i.e., s > 0; Section 6.1): on the low-copy plasmid (p10), the loss of plasmid alleles occurs more frequently in comparison to the chromosome, but the median fixation time is nearly the same as that of the chromosome. Indeed, previous studies showed that under strong selective conditions, beneficial mutations on multicopy plasmids can rise quickly to fixation (San Millan et al. 2016). Notably, the simulation of beneficial alleles (Section 6.1) revealed that alleles on the high copy plasmid (p100) remain polymorphic over a longer time scale and have a higher median fixation time. For neutral alleles, segregational drift of multicopy plasmids hinders the increase of plasmid allele frequency; it leads to frequent and rapid mutant allele loss on the one hand, and to longer fixation time on the other hand. Altogether, these simulations demonstrated that the effect of segregational drift on plasmid allele dynamics counteracts the effect of higher mutational supply accompanying increased copy number.

Consequently, the evolvability of low-copy plasmids is higher than that of high copy plasmids despite the latter higher mutational supply.

The impact of segregational drift is not expected to be limited to non-mobile plasmids as mobile (or conjugative) plasmids are also found in multicopy state (e.g., Figurski and Helinski 1979). Moreover, plasmid copy number may be heterogeneous within the population, especially for plasmids that were modified towards a high copy number such as the pUC origin (e.g., Münch et al. 2015). Furthermore, plasmid copy number can be variable during evolution (e.g., San Millan et al. 2016, Santos-Lopez et al. 2016). Using simulations (Section 6.1) it was demonstrated that segregational drift during the evolution of plasmids having a constant copy number has an effect on their evolutionary rate. This scenario is relevant for naturally occurring plasmids having a tightly controlled copy number and segregation mechanisms. Variable plasmid copy number within the population, and over time, is expected to have implications for the effect of segregational drift on plasmid evolution and may thus lead to evolutionary rate heterogeneity in plasmid genomes. The evolution of multicopy plasmids entails time spans of intra-cellular heterogeneity, which is a situation also encountered by mitochondrial genomes within single cells. Thus, within this study, the operation of analogous evolutionary processes in bacterial plasmids and eukaryotic organelles was highlighted. In summary, a realistic portrayal and modelling of plasmid genome evolution requires deeper understanding of segregational drift.

6 Appendices

6.1 Simulations

To further test the segregational hypothesis I designed a simulation study in collaboration with Dr. Anne Kupczok and Tal Dagan. This chapter of my thesis presents the results of the simulations. The scripts were programmed by Anne Kupczok and analyzed by the three of us.

6.1.1 Plasmid population dynamics.

What are the theoretical expectations for the impact of segregational drift on the dynamics of plasmid alleles in comparison to chromosomal alleles? To address this question we simulated plasmid and chromosome allele dynamics. For this purpose, we applied the standard haploid Wright-Fisher model to simulate forward-time evolution of a population of cells that is subject to random genetic drift (Gillespie 2010). In the simulation, the cell population size remains constant throughout evolution. To simulate plasmid evolution, we added an additional layer of random genetic drift by applying a Wright-Fisher model to the plasmid inheritance (similarly to mitochondria simulated evolution (Peng and Kimmel 2005). Thus, during cell division, plasmid alleles are selected randomly into the daughter cells of the next generation. In terms of population genetics, the plasmid population in the simulated evolution has a substructure within the population. This implies that plasmid allele dynamics have two hierarchical levels: within the cell and within the total population.

We compared the allele frequency dynamics of neutral variants emerging in a population of $N = 10^5$ cells on a haploid chromosome (termed $Cx10^5$) and two multicopy plasmids: one plasmid has a copy number of 10 plasmids per cell (termed $p10x10^5$), while the second plasmid has 100 copies per cell (termed $p100x10^5$). The plasmid copy number remains constant throughout the simulation, hence, a population of 10^5 cells harbors a total of 10^6 p10 replicons. The total number of p100 replicon in such a population is 10^7. In order to examine the effect of the increased total number of plasmid replicons, we simulated in addition the allele dynamics of a haploid chromosome with two additional population sizes. In the first population, the number of cells equals the total p10 replicons, i.e., $N = 10^6$ (termed $Cx10^6$). In the second population the number of cells matches the total $p100x10^5$ replicons, i.e., $N = 10^7$ (termed $Cx10^7$). In addition, we eliminate the effect of replicon size on the probability of mutation by defining the plasmids and chromosomes to have an equal size of 500 loci. The evolution of all replicons was simulated over 1,000 generations in 100 replicate populations. The simulation results reveal that the number of accumulated mutations on the plasmids is higher in comparison to $Cx10^5$ and lower in comparison to chromosomes with the respective population size (i.e., $p10x10^5$ vs. $Cx10^6$

and p100x10^5 vs. Cx10^7; Supplementary Figure 1A). These results demonstrate that the number of accumulating plasmid mutations is lower than the expected number according to plasmid mutational supply (i.e., total plasmid replicons). This discrepancy indicates that most plasmid mutations are lost rapidly after their emergence. Further comparison of the allele frequency distribution among replicons shows that the median AF of p10x10^5 and p100x10^5 is smaller in comparison to Cx10^5 and in comparison to the chromosome of the respective population size (Supplementary Figure 1B). This demonstrates that the increase in allele frequency of plasmid mutations is generally slower in comparison to the mutations emerging on a haploid chromosome.

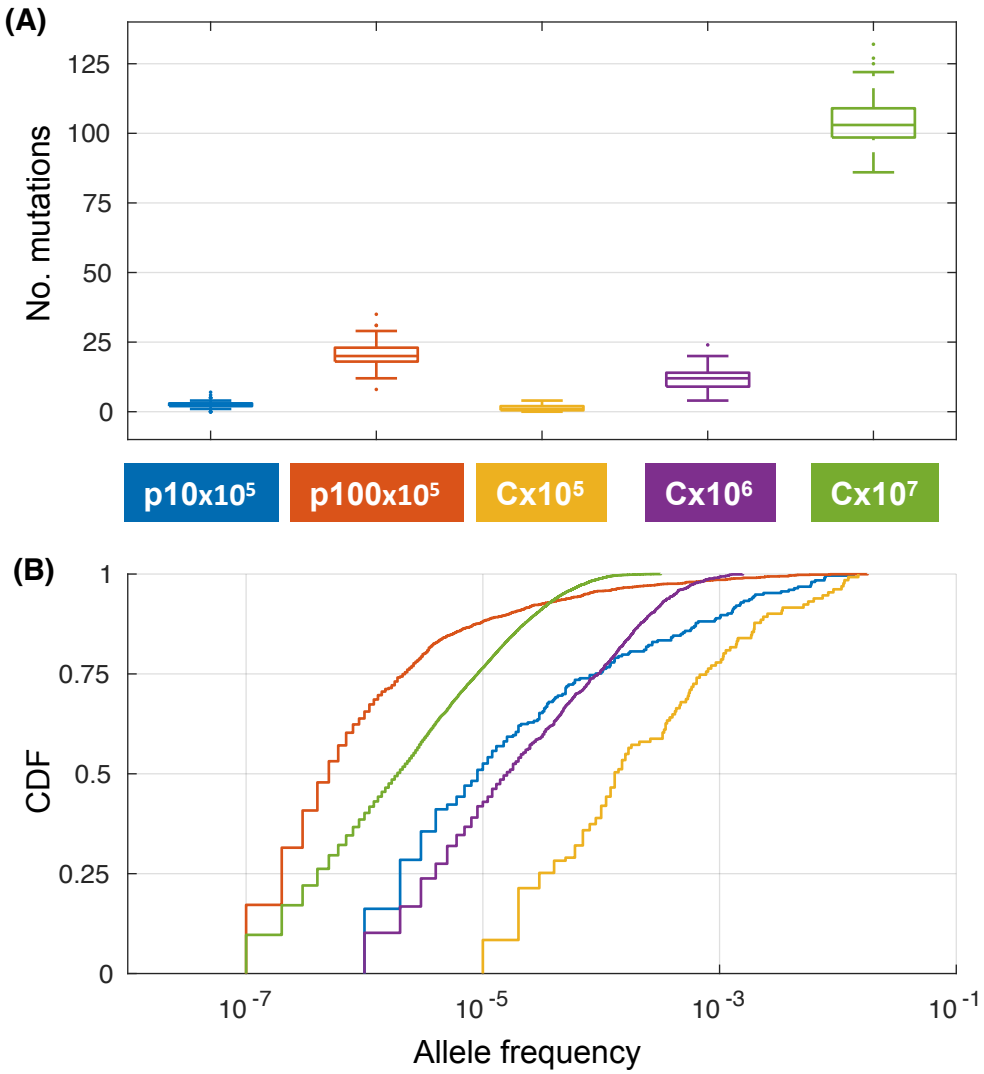

Supplementary Figure 1. Simulated evolution of plasmids and chromosomes under neutrality with mutation (500 loci, mutation rate 2 × 10^{-9} per locus per generation). (**A**) Distribution of the number of mutations after 1,000 generations in 100 replicates. The color of the boxes corresponds to the combination of replicon and population size as in the legend. (**B**) Joint cumulative distribution function (CDF) of the allele frequency of all mutations present in the replicates after 1,000 generations.

To compare the dynamics of mutant alleles residing on the plasmid or chromosome while excluding the effect of mutational supply, we simulated the inheritance of a mutant allele already present in the population at a specified initial frequency (*f*). Thus, the allele dynamics in the population are determined by the combination of the initial mutant allele frequency, random genetic drift and the mutant allele selection coefficient (*s*). The simulation of an initially low-frequency mutant allele (*f* = 0.0001) that is neutral to the fitness of the cell (i.e., selection coefficient *s* = 0) shows that the majority of mutant alleles on plasmids are lost quickly in comparison to mutant alleles on chromosomes (Supplementary Figure 2). For example, the loss of the mutant allele in 20% of the replicates was observed at generation 22 for $p10x10^5$ and at generation 76 for $p100x10^5$. The chromosomal replicons lost 20% of the mutant allele much later: generation 128 in $Cx10^5$, generation 139 in $Cx10^6$ and generation 1,136 in $Cx10^7$ (Supplementary Figure 2A). Increasing the initial mutant allele frequency 10-fold (*f* = 0.001) results in a similar rate of allele loss between the plasmids and $Cx10^5$ populations. Nonetheless, loss rates of plasmid mutant alleles remain higher in comparison to chromosomal mutant alleles in simulations with the equivalent total number of replicons (Supplementary Figure 2, *s* = 0, *f* = 0.001; Supplementary Table 1). Overall, our results indicate that the loss dynamics of plasmid alleles due to segregational drift depend on the initial mutant allele frequency in the total population and the distribution of the mutant allele among plasmid hosts. Notably, the initial allele frequencies used in the simulation may be encountered upon the acquisition of a new plasmid variant in the population, e.g., by conjugation or transformation. In the case of *de novo* plasmid mutations, the initial allele frequency of the mutant plasmid is expected to be extremely low. Hence, according to our simulations, in the absence of a strong benefit for the cell, a mutation on a plasmid will be quickly lost.

Performing the simulations where the allele has a positive selection advantage (*s* = 0.01) reveals a higher loss rate of the mutant allele in $p10x10^5$ in comparison to $p100x10^5$, yet the median fixation time is lower for $p10x10^5$ than for $p100x10^5$. Notably, the median fixation time of plasmid mutant alleles that are not lost is smaller in comparison to chromosome populations of comparable total replicon numbers when the initial frequency is low albeit the majority of plasmid populations lost the mutant allele under these conditions (Supplementary Figure 2, *s* = 0.01, *f* = 0.0001; Supplementary Table 1). The median fixation time of plasmid mutant alleles is similar to the chromosomal one when the initial frequency is increased (Supplementary Figure 2, *s* = 0.01, *f* = 0.001; Supplementary Table 1). With a high selection coefficient (*s* = 0.1), mutant allele loss is smaller than for *s* = 0.01 and the median fixation time of $p10x10^5$ is similar to the chromosome populations. Notably, the median fixation time in $p100x10^5$ is substantially higher in comparison to all

other replicons under these conditions (Supplementary Figure 2, s = 0.1, f = 0.0001 and f = 0.001; Supplementary Table 1).

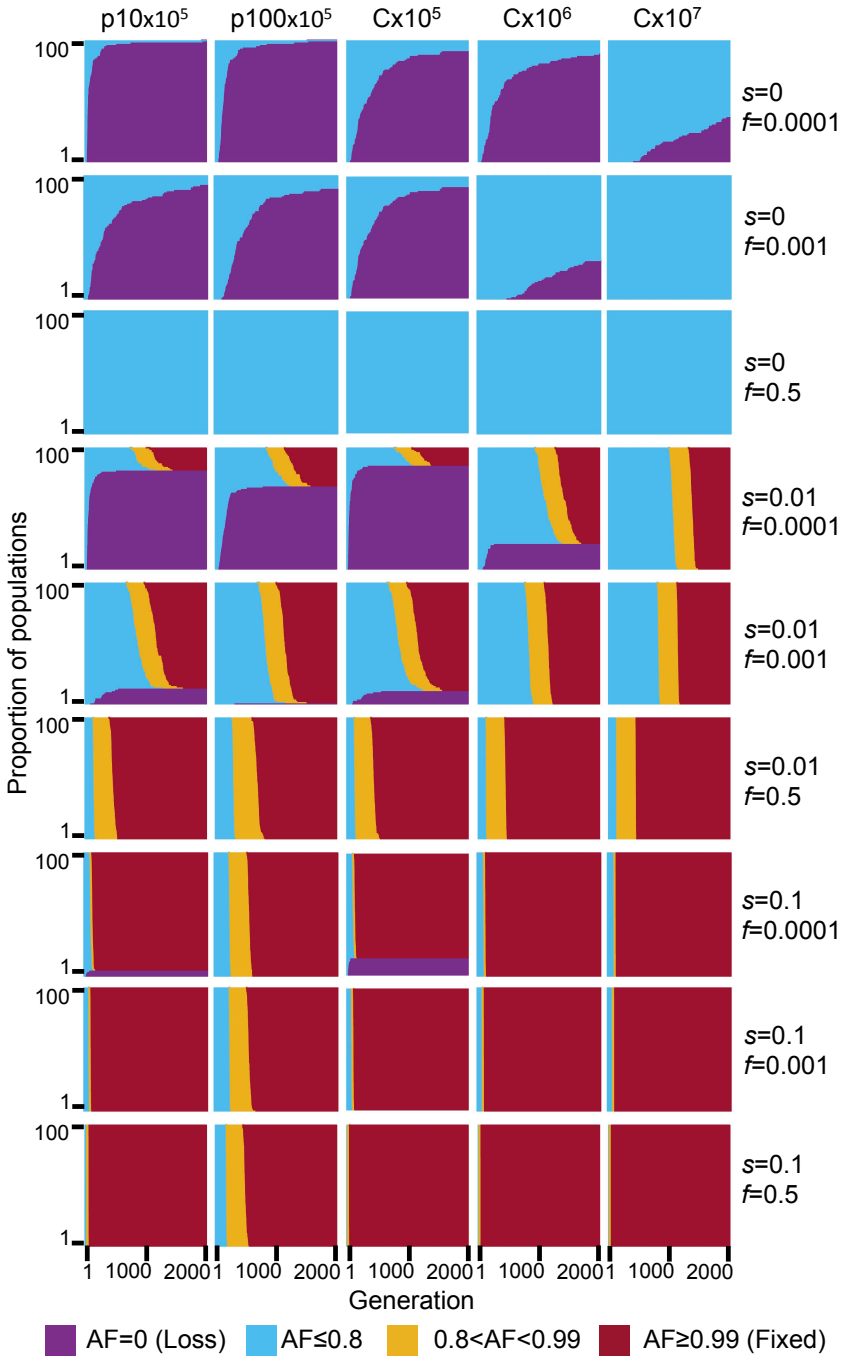

Supplementary Figure 2. Simulated evolutionary dynamics of mutant alleles on plasmids and chromosomes. Allele frequency dynamics over 2,000 generations in 100 replicate simulated populations. (**A**) Columns are the five combinations of simulated replicon type and population size, and rows are the different combinations of selective coefficient (s) and initial allele frequency (f). Generations are on the x-axis, proportion of AF of replicates are stacked along the y-axis, population allele frequency is color coded. For f=0.001 and f=0.0001, the starting frequency of mutant alleles is randomly sampled with the respective frequencies. For f=0.5, the starting frequency of the mutant allele is exactly 0.5 for the chromosome and exactly 0.5 inside each cell for the plasmids. Note that, the initial frequency of cells with a mutant allele in the population is higher in the plasmid simulations compared to chromosome simulations (see Supplementary Table 1 for expected number of mutant cells).

Supplementary Table 1. Loss frequency and median fixation time during simulated evolution of mutant alleles on plasmids and chromosomes. **(A)** The number of populations where the mutant allele went extinct during the simulation is presented for each combination of simulated replicon type and populations size, initial allele frequency (*f*) and selection coefficient (*s*) with 100 replicate populations for each combination. The median fixation time across the 100 simulated replicate populations is calculated as the medium number of generations where a) at least 1 plasmid per cell is present in 80% of the cells, or where b) 80% of the cells harbor plasmid mutants only, or where c) 80% of all replicons is of mutant type (i.e., mutant alleles in the population). **(B)** Expected number of cells having a mutant allele in the initial population. The expected number of cells is calculated by $(1-(1-f)^{cp})\times c$ with initial mutant allele frequency *f*, plasmid copy number *cp* and number of cells *c*.

(A)

		Loss (no. of populations out of 100)					Median fixation time (excluding loss)								
							a) At least 1 plasmid in cell		b) Cells with mutant plasmids only		c) Mutatant alleles in the population				
s	***f***	**p10**	**p100**	**Chr10^5**	**Chr10^6**	**Chr10^7**	**p10**	**p100**	**p10**	**p100**	**p10**	**p100**	**Chr10^5**	**Chr10^6**	**Chr10^7**
0	0.0001	99	99	91	89	37	–	–	–	–	–	–	–	–	–
0	0.001	92	89	91	32	0	–	–	–	–	–	–	–	–	–
0	0.01	34	39	40	0	0	–	–	–	–	–	–	–	–	–
0.01	0.0001	81	68	85	21	0	862	969	862	971	862	969	932	1089	1071
0.01	0.001	13	1	11	0	0	853	836	853	836	853	836	852	842	833
0.01	0.01	0	0	0	0	0	600	620	600	627	600	622	604	602	602
0.1	0.0001	5	0	14	0	0	114	110	114	330	114	258	111	113	112
0.1	0.001	0	0	0	0	0	88	87	88	332	88	259	88	88	88
0.1	0.01	0	0	0	0	0	64	70	65	328	65	256	63	63	63

(B) Average initial frequency in number of cells

f	**p10**	**p100**	**Chr10^5**	**Chr10^6**	**Chr10^7**
0.0001	100	995	10	100	1000
0.001	996	9521	100	1000	10000
0.01	9562	63397	1000	10000	100000

In the presence of balancing selection for multiple plasmid alleles (e.g., alleles supplying resistance for different antibiotics), plasmid loci may remain polymorphic over a long time-scale. Previous studies showed that when the balancing selection is replaced by selection for only one of the plasmid alleles, alternative plasmid alleles may remain polymorphic in the population for a certain time (Bedhomme et al. 2017, Rodriguez-Beltran et al. 2018). We hypothesize that the persistence of alternative plasmid alleles in the population in the absence of selection for the allele, is affected by segregational drift. To test our hypothesis, we performed simulations of plasmid allele dynamics post balancing selection. Thus, the initial mutant allele frequency is set to exactly $f = 0.5$ (i.e., each cell has equal proportions of the ancestral and mutant allele). Here we compare the dynamics of plasmid alleles to chromosomal alleles with the same total replicons as in the above simulations. Our results show that in the absence of selection for the mutant allele, both the ancestral and the mutant allele remain in the population in equilibrium as expected (Supplementary Figure 2, $s = 0$, $f = 0.5$; Supplementary Figure 3A, $s = 0$, $f = 0.5$). When the mutant allele is beneficial ($s = 0.01$ or $s = 0.1$), the ancestral allele persists in the population when it is on the plasmid for a longer time scale in comparison to a chromosomal allele of the same total replicon population (Supplementary Figure 2, s = 0.01 and s = 0.1, f = 0.5). Nonetheless, the proportion of mutant cells in the population

declines at the beginning of the simulation, hence, the beneficial mutant allele is tends to be lost in cells – also when the mutant allele is beneficial (Supplementary Figure 3A, s = 0.01 and s = 0.1, f = 0.5). Furthermore, the consequences of segregational drift to the loss of the mutant (beneficial) allele are more pronounced in the low copy plasmid (p10) simulations. The simulations of the high copy plasmid (p100) with s = 0.1 show that the ancestral allele may persist in the population four-fold longer than the expected for a chromosomal allele with the same total number of replicons (i.e., Cx10^7; Supplementary Figure 2; Supplementary Figure 3B).

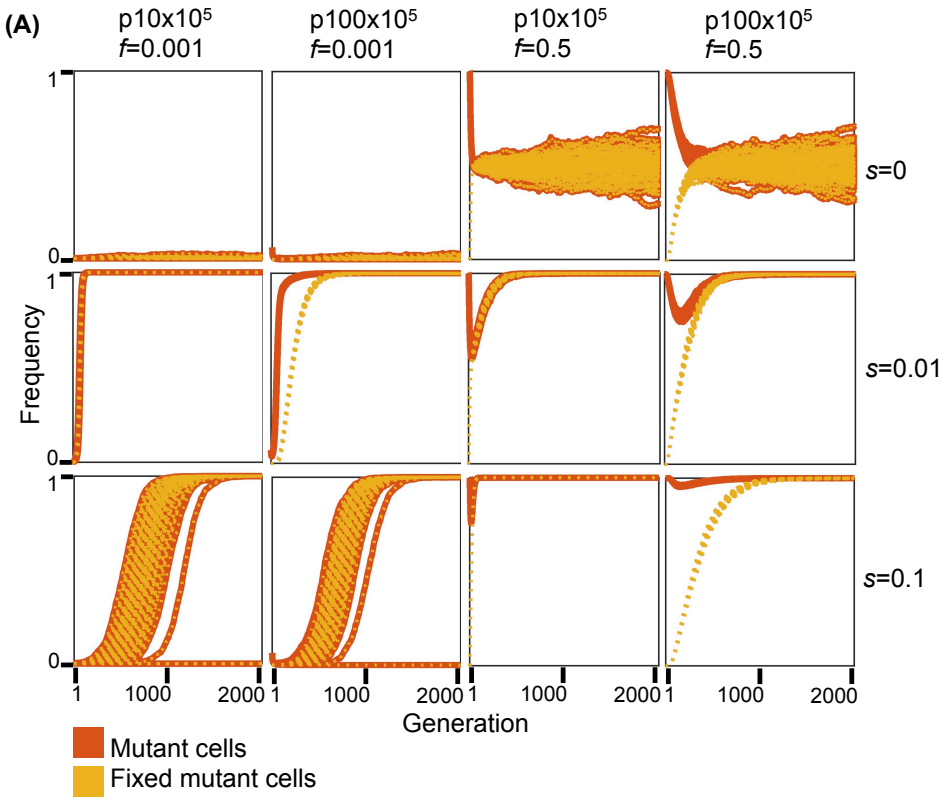

(B) Loss of the ancestral allele (median no. generations; f=0.5)

s	p10x10^5	p100x10^5	Cx10^5	Cx10^6	Cx10^7
0	–	–	–	–	–
0.01	811	1086	775	1019	1285
0.1	131	876	108	129	157

Supplementary Figure 3. Frequency trajectories of plasmid alleles per cell in the plasmid simulations. **(A)** Data shown for with initial allele frequencies f = 0.001, and f = 0.5. The frequency of mutant cells is calculated as the proportion of cells with at least one mutant plasmid allele within the population. The frequency of fixed mutant cells is the proportion of cells in which all plasmids loci contain the mutant allele (i.e., the plasmid allele is fixed in the cell). Starting with a low initial allele frequency (f = 0.001), the difference between mutant plasmid allele dynamics and mutant cells in the population is most pronounced with s = 0.01. The results of the simulation where s = 0.1 are presented for comparison; in this setting, the dynamics of mutant plasmid alleles and mutant cells are similar. In the simulation of plasmid allele dynamics post balancing selection (f = 0.5) the ancestral and mutant alleles are set to an equal ratio within all cells at the beginning of the simulation. **(B)** Ancestral allele loss is calculated as the median number of generation where the ancestral allele was lost across all simulated populations.

The longer fixation time of p100x10^5 alleles under the simulated conditions of strong selection (s = 0.1) are well explained by the effect of segregational drift on the rate of plasmid allele fixation within the host cell. The high selection coefficient acts in favor of cells harboring at least one plasmid mutant, such that those cells rise quickly to fixation within the population. In comparison, the increase of the plasmid allele in the total population is slower due to the effect of random genetic drift of plasmid alleles during cell division, which hinders the increase of plasmid allele frequency in daughter cells. In other words, when the plasmid copy number is high, plasmid alleles within the cell remain polymorphic (i.e., heterogeneous) over a longer time scale, also when the mutant allele is beneficial. This is also observed for the post balancing selection simulation where the loss of the non-mutant (less beneficial) alleles is prolonged for higher copy numbers.

Notably, a plasmid copy number of 100 is within the range of PCNs observed in natural isolates (Projan et al. 1987, Zhong et al. 2011), hence, the extended fixation (and loss) time observed for p100x10^5 is likely to occur also under natural conditions. Since our simulations do not include intra-host plasmid recombination, the observed differences in allele dynamics between plasmids and chromosomes are solely due to inheritance and segregational drift. Overall, the results of the simulation demonstrate that segregational drift of multicopy plasmids has a considerable impact on plasmid allele dynamics in the population by increasing the loss rate and fixation time of plasmid alleles.

6.1.2 Methodology

Forward-time simulations based non non-overlapping generations with a constant cell population size were performed with python3.4 and the module simuPOP v1.1.8.3 (Chiang and Bremer 1988, Peng and Kimmel 2005). Two types of cells were simulated independently. Cells with chromosomes have `L` haploid loci (`ploidy=1`). Cells with plasmids have a predefined plasmid copy number `cp` that stays constant throughout the simulation. Each plasmid has `L` loci, resulting in a total number of `L×cp` loci in each cell. This was implemented based on `cp` customized chromosomes (`chromTypes=[sim.CUSTOMIZED]*cp`), each with `L` haploid loci. Alleles were simulated as binary (`alleleType='binary'`). Inheritance mode for the chromosome corresponds to a Wright-Fisher model (operator `RandomSelection()`). Inheritance mode for the plasmid corresponds to a Wright Fisher model with mitochondrial inheritance of organelles (operator `RandomSelection(ops=[sim.MitochondrialGenoTransmitter()])`).

For the simulations with mutation, initial populations (t=0) were homogenous, i.e., all loci had state 0. The mutation rate in the simulation was constant with 2×10^{-9} per locus per generation (operator `SNPmutator(u=2e-9)`). For the simulated evolutionary dynamics

of mutant alleles, we simulated the evolution of one binary locus (`L=1`) having a mutant allele already present in the initial population at a specified initial frequency (*f*) and no new mutation is applied during simulated evolution. Initial populations were randomly generated with a particular mutant frequency `f` (parameter `freq=[1-f,f]` for the method `initGenotype`). Note that this assigns the mutant allele randomly to each locus, independent of the state of the other loci in the same cell for plasmid simulations. For the simulated evolution with selection, the probability to be inherited to the next generation is proportional to the fitness value of the cell. For cells with a chromosome, a fitness value of 1+s was assigned to allele state 1 and fitness value 1 was assigned to allele state 0. For cells with plasmids, a fitness value of 1+s was assigned if at least one plasmid has allele state 1, otherwise the fitness is 1 (i.e., dominant selection mode). Selection was applied using a fitness field (`infoFields="fitness"`) and the operator `PySelector`. Simulations were run for a particular number of generations using the `evolve` method.

6.2 Supplementary Figures

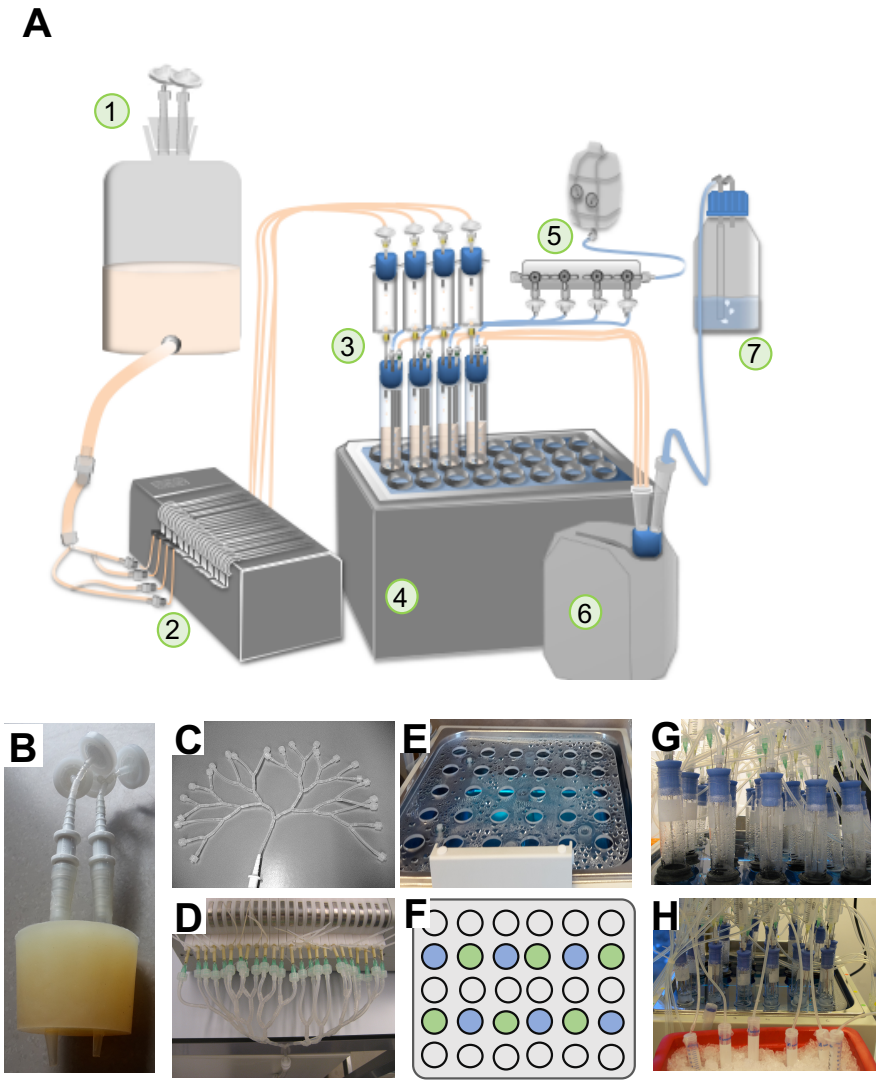

Supplementary Figure 4. (A) Illustration of the chemostat system as it was used in the evolution experiment. The culturing system includes 1) media supply, 2) peristaltic pump with 24 channels, 3) culturing units, 4) water bath, 5) air supply, 6) effluent module including 7) a gas washing bottle. **(B)** Assembled stopper for venting of the media carboy. **(C)** Media supply hose that splits into 24 ports for the flow of media to the culture vessels regulated through a peristaltic pump. **(D)** Media supply hose with its 24 channels connected to the peristaltic pump. **(E)** Custom-made rack for the culturing units placed into a water bath. **(F)** Example for the arrangement of culture vessels inoculated with bacteria (blue) and control vessels without bacteria inoculated (green) used during chemostat establishment to test for contamination. **(G)** Chemostat vessels showing evaporation. **(H)** Sampling of chemostat culture. Note, that all photos were taken during culturing tests.

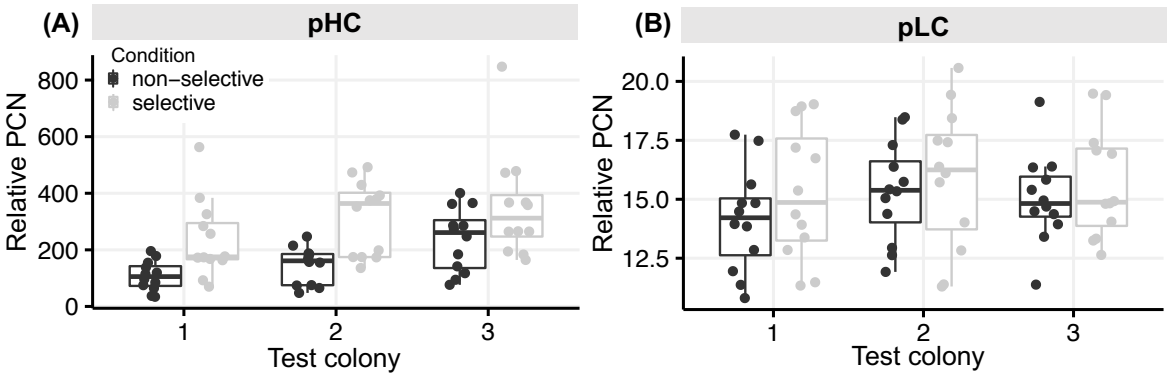

Supplementary Figure 5. Relative PCN of single colonies after regrowth on selective and non-selective media. Three test colonies grown on M9 agar plates were restreaked on non-selective and selective (M9/amp$_{100}$) media to obtain single colonies. PCNs were determined for each test-colony (progenitor) and for twelve colonies obtained after restreak and ON growth at 37°C (descendants). **(A)** Relative PCNs of pHC-wt colonies. PCNs of progenitor colonies were as following: 1: 222.63, 2: 300.45, 3: 404.4. **(B)** Relative PCNs of pLC-wt colonies. PCNs of progenitor colonies were as following: 1: 15.12, 2:17.27, 3: 13.55.

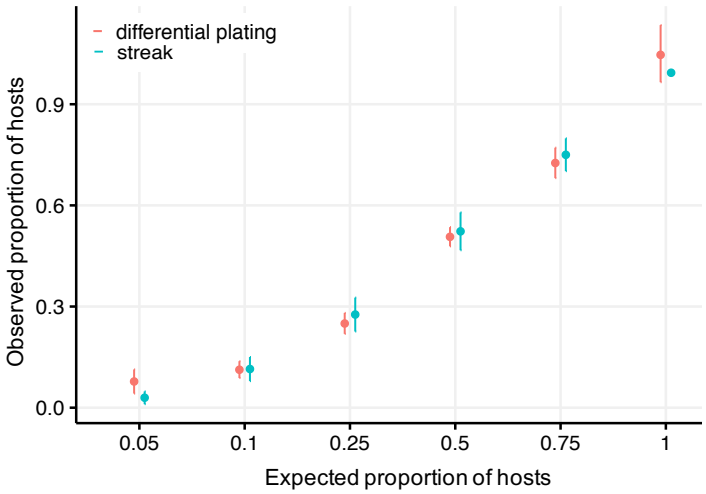

Supplementary Figure 6. Confidence intervals (confidence level = 95%) for two methods used to determine the host proportion of chemostat populations. Confidence intervals for the differential plating method were calculated using the mean as for each constructed test sample 15 independent samples were analyzed. Confidence intervals for the streak method were calculated using the adjusted Wald method for binomial proportions (Agresti and Coull 1998). The raw data is given in Supplementary Table 16.

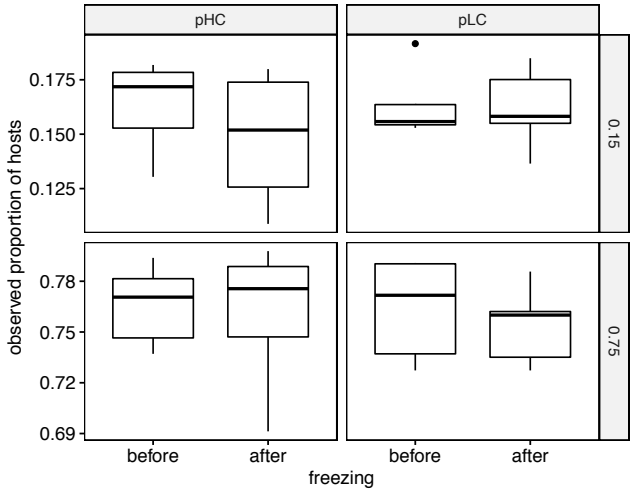

Supplementary Figure 7. Effect of freezing and reviving on proportion of hosts. The effect of freezing and reving on the proportion of hosts in pLC-wt and pHC-wt populations with an expected proportion of hosts of 0.15 and 0.75 was examined by estimating the proportions before and after freezing at -80°C for six weeks. Five technical replicates were used per test group. Raw data is reported in Supplementary Table 17.

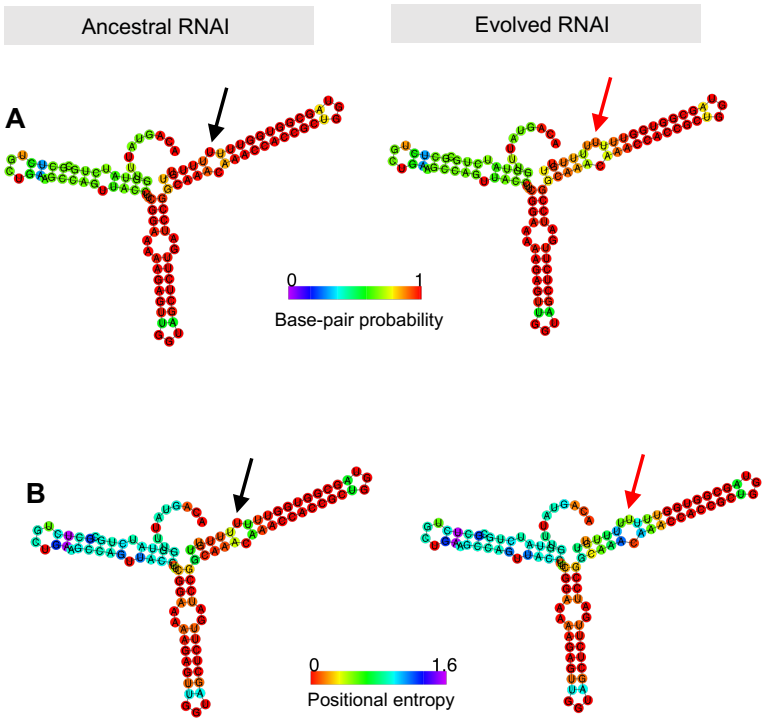

Supplementary Figure 8. Ancestral and evolved predicted secondary structures of RNAI encoded on plasmid pHC. Secondary structures were predicted using RNAfold (Lorenz et al. 2011, Gruber et al. 2008). The evolved structures include a single nucleotide insertion mutation. Black arrows indicate the ancestral state, red arrows indicate the evolved state. **(A)** The structures are colored by base-pairing probabilities. For unpaired regions the color denotes the probability of being unpaired. **(B)** The structures are colored by positional entropy.

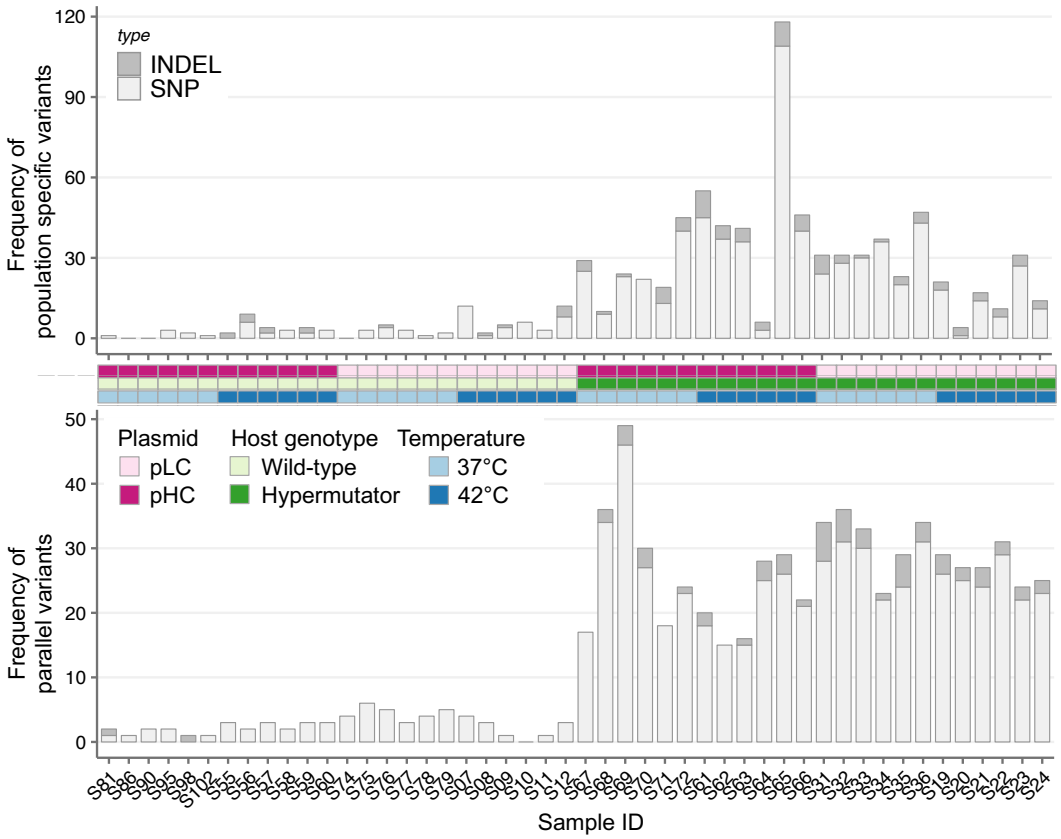

Supplementary Figure 9. Frequency of population specific and parallel variants. Frequency of point mutations (SNPs) and indels were calculated for each of the 48 evolved populations. Parallel variants are defined as variants occurring in more than one population.

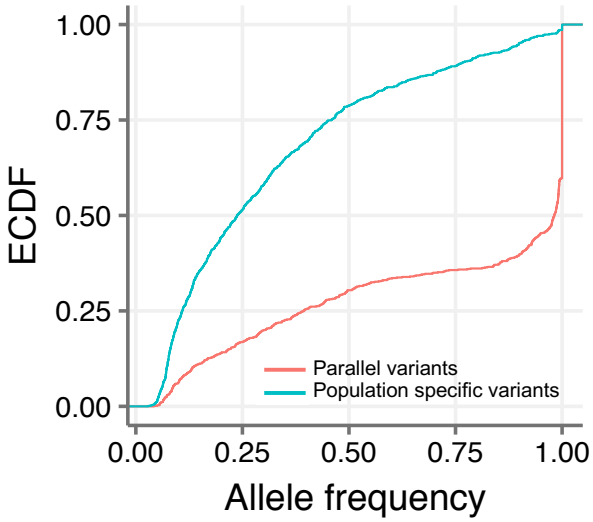

Supplementary Figure 10. Joint allele frequency plot of chromosomal variants detected in more than one population (parallel variants) and in one population only (populations specific variants).

Supplementary Figure 11. Effect of an intergenic mutation observed on the chromosome in multiple evolved populations. Promotor sequences upstream the *mntH* gene were predicted using BProm with default settings (Solovyev and Salamov 2011). A single nucleotide substitution observed in 11 evolved populations is predicted to result in new promotor regulatory boxes (indicated in orange). The log-likelihood scores for the predicted elements were as following: ancestral –10-box (grey): 27, ancestral –35-box (grey): 41, evolved sample's –10-box: 42, evolved sample's –35-box: 32, evolved sample's *rpoD* transcription factor binding site: 6.

6.3 Supplementary Tables

Supplementary Table 2. Oligonucleotides used in this study.

Name	DNA sequence (5'->3')
Plasmid construction	
inv1_R	CGGAGGCTTTTCCCCAGAGA
inv2_F	CCAGACTATCGGCTGTAGCC
pUC_ori_F	CCACTGAGCGTCAGACCC
pUC_ori_R	TGCGTTGCGCTCACTGCC
Strain construction	
art3_F	GCTAAGGAGACAGCGCACATC
art3_R	GCTGCAGGACGGTACAAGAAATG
attTn7_F	GCACATCATCGAGATGCCG
attTn7_R	ATTTGGCATACACCGGCGCAG
mutS_KO_F	**AATAAAAACCATCACACCCCATTTAATATCAGG** **GAACCGGACATAACCCC**AATTAACCCTCACTAA AGGGCG
mutS_KO_R	**TCAGTTGTCGTTAATATTCCCGATAGCAAAAGA** **CTATCGGGAATTGTTA**TAATACGACTCACTATAG GGCTC
PGK_F	CGAGACTAGTGAGACGTGCTAC
mutS_test_R	CACCAACGACCCATATATGGCG
mutS_test_F	GAAGAAGGGTTAGCCAACCGATAC
qPCR	
q_idnT_F	GTGGGTTTTGTCCTGCTGTT
q_idnT_R	ACAGAGAGCGCTGCTACCAT
q_bla_F	GAAGTAAGTTGGCCGCAGTGT
q_bla_R	GTCGCCGCATACACTATTCTC
q_mutS_F	CGGGCTATAACGAAGAGCTG
q_mutS_R	AAAGCCAACTTTCAGCGTGT
q_pUC_ori_F	CCACTGAGCGTCAGACCC
q_pUC_ori_R	GTTGGTAGCTCTTGATCCGGC
q_pBB_rep_F	CACGAGGTGATGCAGCAG
q_pBB_rep_R	GGCCACGCAGTCCAGAG

Supplementary Table 3 (part 1). Materials and equipment used to build the chemostat system for the evolution experiment.

Media supply						
No	Item	Specification	Article no.	Quantity	Vendor	Note
1	Media carboys	Carboy Nalgene PP 10 L, with PP screw and tube connector (ID 13 mm)	215-0118	2	VWR	Filled with medium under sterile conditions
2	Stopper for carboy (and venting)	Rotilabo stoppers made of silicone rubber, bottom D 60 mm, top D 70 mm	TL37.1	2	ROTH	70 mm stoppers with holes commercially not available. Therefore, 2 holes were drilled into each stopper, 5 ml pipet tips and universal tubing connectors inserted and connected to gas filters; see Supplementary Figure 1.
3	Medium carboy outlet tubing	Biocompatible silicone tubing, platinum cured, Versilic, ID 10 mm	HC72.2	10 m	ROTH	
4	Hose clamp	For tubes with OD up to 19 mm, acetal	229-0321	1 pack of 6	VWR	
5	Hose clamp	For tubes with OD 3.2 mm - 11 mm, acetal	229-0320	1 pack of 12	VWR	
6	Universal tubing connectors	For tubes with ID from 4/8 mm - 17 mm, PP	Y523.1	1 pack of 10	ROTH	
7	Tubing that connects carboy outlet with quick	Biocompatible silicone tubing, platinum cured, Versilic, ID 6 mm	HC67.2	10 m	ROTH	Also used in other parts of the chemostat
8	Quick connect coupling female	PP with barrier, tubing ID 6.4 mm	2-1863	2	neoLab	
9	Quick connect coupling male	PP with barrier, tubing ID 6.4 mm	2-1865	2	neoLab	
10	Tube reducing connectors	PP, Rotilabo, connector I OD 8-12 mm, connector II OD 4-8 mm	E801.1	2	ROTH	
11	Hose that connects carboy outlet tubing with pump tubing	Biocompatible silicone tubing, platinum cured, Versilic, ID 2 mm	HC62.1	50 m	ROTH	Also used in other parts of the chemostat
12	Y-shape tubing connector	Rotilabo Y-pieces, for hoses with ID 3 mm	E770.1	5 packs of 10	ROTH	Used to split main media carboy outlet hose into 24 channels; see Supplementary Figure 1.
13	Tubing connector with Luer Lock male	Rotilabo Luer-tubing connectors, male, for hoses with ID 3.2 mm	CT60.1	10 packs of 10	ROTH	Connects pump tubing with adjacent hoses via Luer Lock male connector; see Supplementary Figure 1.
14	Needle to connect pump tubing with adjacent hoses	Disposable needles Sterican, blunt edge, 21G, length 22 mm	X134.1	2 packs of 100	ROTH	
15	Peristaltic pump	24-channel tubing pump ISMATEC IPC-N ISM939D	224-1031	2	VWR	
16	Pump tubing	2-stop tubing ISMATEC PharMed Ismaprene, ID 0.38 mm	ISMCSC0321	8 packs of 6	VWR	New or autoclaved tubing requires running-in time (at least 1 hour)
17	Hose connecting pump tubing with air break	Biocompatible silicone tubing, platinum cured, Versilic, ID 2 mm	HC62.1	included in no. 11	ROTH	
Air supply						
No	Item	Specification	Article no.	Quantity	Vendor	Note
18	Air pump	Eheim air pump 400, pump capacity 400 L h^{-1}	3704010	4	REBIE Online	
19	Hose connecting air pump with manifold	Biocompatible silicone tubing, platinum cured, Versilic, ID 2 mm	HC62.1	included in no. 11	ROTH	
20	Manifold	5-port manifold, 7x Luer Lock female	2-6357	8	neoLab	
21	Tubing connector with Luer Lock male	Rotilabo Luer-tubing connectors, male, for hoses with ID 3.2 mm	CT60.1	5 packs of 10	ROTH	Used to connect manifold and hose (ID 2 mm)
22	Gas filter	Syringe filter, PTFE membrane, 0.2 µm, D 25 mm	514-0070	1 pack of 100	VWR	
23	Hose connecting gas filter and canula in culturing unit	Biocompatible silicone tubing, platinum cured, Versilic, ID 2 mm	HC62.1	included in no. 11	ROTH	
24	Culture vessel inlet needle	Cannulas Luer-Lock connection, 1.2 × 150 mm	2-3118	16 packs of 3	NeoLab	
Air break						
No	Item	Specification	Article no.	Quantity	Vendor	Note
25	Tubing connector with Luer Lock male	Rotilabo Luer-tubing connectors, male, for hoses with ID 3.2 mm	CT60.1	5 packs of 10	ROTH	Used to connect hose (ID 2 mm) and syringe filter
26	Syringe filter	Filtropur L 0.2 µm, AC membrane	83.1827.001	1 pack of 50	SARSTEDT	
27	Syringe filter	Filtropur S 0.2 µm, PES membrane	83.1826.001	1 pack of 50	SARSTEDT	Used in case no. 25 not available, exchanged every day
28	Stopper	Silicone sponge stopper, 30 × 19 × 25 mm	2-4254	5 packs of 10	NeoLab	Used to plug syringe (air break)
29	Stopper	Rotilabo stoppers made of natural rubber, bottom D 21 mm, top D 27 mm	C381.2	2 packs of 25	ROTH	Used to plug syringe (air break)
30	Syringe	Disposable syringe Omnifix, Luer-Lock fitting, PP	T550.1	1 pack of 100	ROTH	Autoclavable cylinder part used as air break
31	Culture vessel inlet needle	Disposable needles Sterican, long edge, 20 G, length 70 mm	C722.1	1 pack of 100	ROTH	Used as inlet to culture vessel, connected to syringe

Supplementary Table 3 (part 2). Materials and equipment used to build the chemostat system for the evolution experiment.

Culturing unit						
No.	Item	Specification	Article no.	Quantity	Vendor	Note
32	Culture vessel	Test tube, beaded rim, borosilicate glass, 150 × 25 mm, 50 mL, autoclavable	9010620	1 pack of 100	EYDAM	
33	Stopper	Silicone sponge stopper, 30 ×19 × 25 mm	2-4254	5 packs of 10	NeoLab	Used to plug culture vessel, holds 4 needles for delivery of air (1x), delivery of medium (1x), and to remove effluent (2x)
Culturing chamber						
No.	Item	Specification	Article no.	Quantity	Vendor	Note
34	Water baths	Water baths for 4-12 L up to 100°C, inner dimensions 306×281×125 mm (wide×length×height)	462-0242	2	VWR	
35	Rack	Rack for test tubes, with 24 slots, D 25 mm, temperature stable to 100°C, polymethylmethacrylate, 300×270×130 mm	n/a	2	custom-made	see Supplementary Figure 1
36	Water baths protect agent	with color indicator	AN93.1	1	1×100 mL	
37	Tube holder	O-ring, ID 25 mm	n/a	48	Hardware store	
Effluent						
No.	Item	Specification	Article no.	Quantity	Vendor	Note
38	Culture vessel effluent needle	Disposable needles Sterican, long edge, 21 G, length 120 mm	C722.1	1 pack of 100	ROTH	Used as effluent port; two needles per culturing vessel
39	Tubing connector with Luer Lock male	Rotilabo Luer-tubing connectors, male, for hoses with ID 3.2 mm	CT60.1	10 packs of 10	ROTH	Used to connect manifold and hose (ID 2 mm)
40	Hose connecting effluent needle with effluent collection vessel	Biocompatible silicone tubing, platinum cured, Versilic, ID 2 mm	HC62.1	included in no. 11	ROTH	Kept as short as possible; transferred into hose with larger diameter to ensure stable efflux; end of hose equipped with tip of a pipette tip (2.5 µl)
41	Pipet tip	5 mL pipet tip	n/a	24	n/a	Used to connect effluent hoses of six chemostat vessels with large diameter hose; sealed with parafilm and end piece of effluent hose are pushed through
42	Effluent collection hose	Biocompatible silicone tubing, platinum cured, Versilic, ID 10 mm	HC72.2	included in no. 3	ROTH	Facultatively used to connect chemostat vessel effluent hoses and effluent collection vessels; holds 5 ml pipette tip
43	Stopper for effluent collection vessel	Silicone sponge stopper, 48 × 44 × 52 mm (height × D bottom × D top)	2-4259	8	NeoLab	Insert two 5 mL pipette tips to connect (1.) effluent collection hose with collection vessel and (2.) to connect collection vessel with gas washing bottle ; see Supplementary Figure 1
44	Tubing that connects collection vessel gas washing	Biocompatible silicone tubing, platinum cured, Versilic, ID 6 mm	HC67.2	included in no. 7	ROTH	
45	Gas washing bottle	Laboratory bottle, 1000 mL, borosilicate glass	215-1595	2	VWR	
46	Screw cap with two connectors	Screw cap GL 45 with twin connectors, PP	PY86.1	2	ROTH	One connector used as inlet, the other connector used as outlet of gas passed through $_{dd}$H20 supplemented with biocide agent (no. 36)

Supplementary Table 4. List of samples and sequencing information.

Sample ID	Plasmid type	Host genotype	T °C	Repli-cate	Sample type	Library preparation type	Sequencing platform	BioSample accession	SRA run accession
S74	pLC	Wt	37	1	total population	Nextera	HiSeq2500	SAMN08956166	SRR7040486
S75	pLC	Wt	37	2	total population	Nextera	HiSeq2500	SAMN08956166	SRR7040488
S76	pLC	Wt	37	3	total population	Nextera	HiSeq2500	SAMN08956166	SRR7040489
S77	pLC	Wt	37	4	total population	Nextera	HiSeq2500	SAMN08956166	SRR7040490
S78	pLC	Wt	37	5	total population	Nextera	HiSeq2500	SAMN08956166	SRR7040491
S79	pLC	Wt	37	6	total population	Nextera	HiSeq2500	SAMN08956166	SRR7040492
S07	pLC	Wt	42	1	total population	NexteraXT	NextSeq500	SAMN08956168	SRR7040479
S08	pLC	Wt	42	2	total population	NexteraXT	NextSeq500	SAMN08956168	SRR7040480
S09	pLC	Wt	42	3	total population	NexteraXT	NextSeq500	SAMN08956168	SRR7040473
S10	pLC	Wt	42	4	total population	NexteraXT	NextSeq500	SAMN08956168	SRR7040474
S11	pLC	Wt	42	5	total population	NexteraXT	NextSeq500	SAMN08956168	SRR7040475
S12	pLC	Wt	42	6	total population	NexteraXT	NextSeq500	SAMN08956168	SRR7040476
S31	pLC	Hypermutator	37	1	total population	NexteraXT	NextSeq500	SAMN08956170	SRR7040507
S32	pLC	Hypermutator	37	2	total population	NexteraXT	NextSeq500	SAMN08956170	SRR7040506
S33	pLC	Hypermutator	37	3	total population	NexteraXT	NextSeq500	SAMN08956170	SRR7040509
S34	pLC	Hypermutator	37	4	total population	NexteraXT	NextSeq500	SAMN08956170	SRR7040508
S35	pLC	Hypermutator	37	5	total population	NexteraXT	NextSeq500	SAMN08956170	SRR7040500
S36	pLC	Hypermutator	37	6	total population	NexteraXT	NextSeq500	SAMN08956170	SRR7040499
S19	pLC	Hypermutator	42	1	total population	NexteraXT	NextSeq500	SAMN08956169	SRR7040471
S20	pLC	Hypermutator	42	2	total population	NexteraXT	NextSeq500	SAMN08956169	SRR7040472
S21	pLC	Hypermutator	42	3	total population	NexteraXT	NextSeq500	SAMN08956169	SRR7040503
S22	pLC	Hypermutator	42	4	total population	NexteraXT	NextSeq500	SAMN08956169	SRR7040502
S23	pLC	Hypermutator	42	5	total population	NexteraXT	NextSeq500	SAMN08956169	SRR7040505
S24	pLC	Hypermutator	42	6	total population	NexteraXT	NextSeq500	SAMN08956169	SRR7040504
S81	pHC	Wt	37	1	pooled hosts	Nextera	HiSeq2500	SAMN08956167	SRR7040494
S86	pHC	Wt	37	2	pooled hosts	Nextera	HiSeq2500	SAMN08956167	SRR7040487
S90	pHC	Wt	37	3	pooled hosts	Nextera	HiSeq2500	SAMN08956167	SRR7040484
S95	pHC	Wt	37	4	pooled hosts	Nextera	HiSeq2500	SAMN08956167	SRR7040493
S98	pHC	Wt	37	5	pooled hosts	Nextera	HiSeq2500	SAMN08956167	SRR7040478
S102	pHC	Wt	37	6	pooled hosts	Nextera	HiSeq2500	SAMN08956167	SRR7040477
S55	pHC	Wt	42	1	pooled hosts	NexteraXT	NextSeq500	SAMN08956175	SRR7040496
S56	pHC	Wt	42	2	pooled hosts	NexteraXT	NextSeq500	SAMN08956175	SRR7040458
S57	pHC	Wt	42	3	pooled hosts	NexteraXT	NextSeq500	SAMN08956175	SRR7040498
S58	pHC	Wt	42	4	pooled hosts	NexteraXT	NextSeq500	SAMN08956175	SRR7040501
S59	pHC	Wt	42	5	pooled hosts	NexteraXT	NextSeq500	SAMN08956175	SRR7040469
S60	pHC	Wt	42	6	pooled hosts	NexteraXT	NextSeq500	SAMN08956175	SRR7040470
S67	pHC	Hypermutator	37	1	pooled hosts	NexteraXT	NextSeq500	SAMN08956177	SRR7040462
S68	pHC	Hypermutator	37	2	pooled hosts	NexteraXT	NextSeq500	SAMN08956177	SRR7040461
S69	pHC	Hypermutator	37	3	pooled hosts	NexteraXT	NextSeq500	SAMN08956177	SRR7040460
S70	pHC	Hypermutator	37	4	pooled hosts	NexteraXT	NextSeq500	SAMN08956177	SRR7040459
S71	pHC	Hypermutator	37	5	pooled hosts	NexteraXT	NextSeq500	SAMN08956177	SRR7040481
S72	pHC	Hypermutator	37	6	pooled hosts	NexteraXT	NextSeq500	SAMN08956177	SRR7040482
S61	pHC	Hypermutator	42	1	pooled hosts	NexteraXT	NextSeq500	SAMN08956176	SRR7040468
S62	pHC	Hypermutator	42	2	pooled hosts	NexteraXT	NextSeq500	SAMN08956176	SRR7040467
S63	pHC	Hypermutator	42	3	pooled hosts	NexteraXT	NextSeq500	SAMN08956176	SRR7040466
S64	pHC	Hypermutator	42	4	pooled hosts	NexteraXT	NextSeq500	SAMN08956176	SRR7040465
S65	pHC	Hypermutator	42	5	pooled hosts	NexteraXT	NextSeq500	SAMN08956176	SRR7040464
S66	pHC	Hypermutator	42	6	pooled hosts	NexteraXT	NextSeq500	SAMN08956176	SRR7040463
S81	pHC	Wt	37	1	total population	Nextera	HiSeq2500	SAMN08956167	SRR7535018
S86	pHC	Wt	37	2	total population	Nextera	HiSeq2500	SAMN08956167	SRR7535017
S90	pHC	Wt	37	3	total population	Nextera	HiSeq2500	SAMN08956167	SRR7535020
S95	pHC	Wt	37	4	total population	Nextera	HiSeq2500	SAMN08956167	SRR7535019
S98	pHC	Wt	37	5	total population	Nextera	HiSeq2500	SAMN08956167	SRR7535014
S102	pHC	Wt	37	6	total population	Nextera	HiSeq2500	SAMN08956167	SRR7535013
S55	pHC	Wt	42	1	total population	NexteraXT	NextSeq500	SAMN08956175	SRR7535016
S56	pHC	Wt	42	2	total population	NexteraXT	NextSeq500	SAMN08956175	SRR7535015
S57	pHC	Wt	42	3	total population	NexteraXT	NextSeq500	SAMN08956175	SRR7535012
S58	pHC	Wt	42	4	total population	NexteraXT	NextSeq500	SAMN08956175	SRR7535011
S59	pHC	Wt	42	5	total population	NexteraXT	NextSeq500	SAMN08956175	SRR7535010
S60	pHC	Wt	42	6	total population	NexteraXT	NextSeq500	SAMN08956175	SRR7535009
S67	pHC	Hypermutator	37	1	total population	NexteraXT	NextSeq500	SAMN08956177	SRR7535008
S68	pHC	Hypermutator	37	2	total population	NexteraXT	NextSeq500	SAMN08956177	SRR7535007
S69	pHC	Hypermutator	37	3	total population	NexteraXT	NextSeq500	SAMN08956177	SRR7535006
S70	pHC	Hypermutator	37	4	total population	NexteraXT	NextSeq500	SAMN08956177	SRR7535005
S71	pHC	Hypermutator	37	5	total population	NexteraXT	NextSeq500	SAMN08956177	SRR7535004
S72	pHC	Hypermutator	37	6	total population	NexteraXT	NextSeq500	SAMN08956177	SRR7535003
S61	pHC	Hypermutator	42	1	total population	NexteraXT	NextSeq500	SAMN08956176	SRR7535002
S62	pHC	Hypermutator	42	2	total population	NexteraXT	NextSeq500	SAMN08956176	SRR7535001
S63	pHC	Hypermutator	42	3	total population	NexteraXT	NextSeq500	SAMN08956176	SRR7534999
S64	pHC	Hypermutator	42	4	total population	NexteraXT	NextSeq500	SAMN08956176	SRR7535000
S65	pHC	Hypermutator	42	5	total population	NexteraXT	NextSeq500	SAMN08956176	SRR7534997
S66	pHC	Hypermutator	42	6	total population	NexteraXT	NextSeq500	SAMN08956176	SRR7534998
S52	pLC	Wt	37		ancestor	NexteraXT	NextSeq500	SAMN08956172	SRR7040497
S54	pLC	Hypermutator	37		ancestor	NexteraXT	NextSeq500	SAMN08956174	SRR7040483
S51	pHC	Wt	37		ancestor	NexteraXT	NextSeq500	SAMN08956171	SRR7040495
S53	pHC	Hypermutator	37		ancestor	NexteraXT	NextSeq500	SAMN08956173	SRR7040485

Supplementary Table 5. R packages used in this study.

	package	version
interface	rmarkdown	1.8
	RStudio	1.1.383
data handling and manipulation	broom	0.4.3
	data.table	1.10.4-3
	dplyr	0.7.4
	reshape2	1.4.3
	stringr	1.3.1
	tidyr	0.7.2
statistics	ARTool	0.10.4
	factoextra	1.0.5
	FactoMineR	1.39
	growthcurver	0.2.1
	growthrates	0.7.1
	matrixStats	0.52.2
	stats	3.4.3
	vegan	3.4.3
	moments	0.14
visualization	colormap	0.1.9
	corrplot	0.84
	ggthemes	3.4.0
	ggplot2	3.0.0
	ggpubr	0.1.6
	Hmisc	4.0-3
	NMF	0.20.6
	RColorBrewer	1.1-2
	scales	0.5.0
	viridis	0.4.0

Supplementary Table 6. Test for evaporation of media in the chemostat system. To test for the level of evaporating liquid, flow rates of four chemostat units operated with and without the air hydration module were measured twice a day (sample). Flow rates are reported in µl per unit time (10 min). Note, that there was no significant difference between flow rates obtained from cultures cultivated in a chemostat system with an air hydration module and without an air hydration module ($t(109.48) = 0.084$, $P = 0.933$, using independent sample t-test).

	sample	unit	day 1	2	3	4	5	6	7	*M*	*SD*
including air hydration module	1	1	828	816	815	827	785	822	796	812.71	16.27
		2	814	784	814	841	806	779	813	807.29	20.83
		3	794	821	815	829	769	802	825	807.86	21.22
		4	825	832	779	832	818	827	814	818.14	18.52
	2	1	815	793	825	805	830	825	810	814.71	13.12
		2	824	804	789	801	806	879	816	817.00	29.51
		3	804	815	803	822	818	802	822	812.29	9.03
		4	817	834	816	786	780	817	832	811.71	21.01
		M	815.1	812.4	807	818	802	819	816		
		SD	11.44	17.72	15.6	18.6	21.3	29	10.8		
without air hydration module	1	1	841	784	820	841	833	809	826	822.00	20.31
		2	810	826	785	830	812	785	811	808.43	17.77
		3	828	807	796	804	799	816	793	806.14	12.29
		4	781	805	819	790	827	819	814	807.86	16.84
	2	1	823	815	835	815	834	828	830	825.71	8.32
		2	805	793	828	823	816	794	833	813.14	16.12
		3	811	814	816	802	820	792	819	810.57	10.16
		4	782	817	785	816	817	849	773	805.57	26.76
		M	810.1	807.6	811	815	820	812	812		
		SD	21.06	13.63	19.3	16.4	11.6	21.2	20.3		

Supplementary Table 7. Cell densities obtained during test cultivation using the chemostat system established in this study. Over a culturing period of 21 days, cell densities were assesed from twelve chemostat cultures by colony-count method (presented as CFU $mL^{-1} \times 10^{-8}$).

T		Generation												
°C	Unit	1	18	34	51	67	84	101	117	134	151	167	*M*	*SD*
37	1	1.84	1.83	1.78	1.82	1.69	1.76	1.80	1.87	1.59	1.68	1.81	1.77	0.08
37	2	1.88	1.81	1.80	1.81	1.84	1.92	1.81	1.96	1.86	1.75	1.74	1.83	0.07
37	3	1.93	1.92	1.92	1.72	1.83	1.91	2.04	1.83	1.82	1.97	1.84	1.88	0.09
37	4	1.92	1.91	1.86	1.73	1.75	1.82	1.76	1.82	1.88	1.70	1.57	1.79	0.10
37	5	1.98	1.87	1.75	1.84	1.94	1.72	1.89	1.69	1.79	1.71	1.95	1.83	0.10
37	6	1.89	1.88	1.82	1.91	1.90	1.84	1.84	1.85	1.67	1.93	1.48	1.82	0.13
42	7	1.83	1.82	1.81	1.89	1.77	1.79	1.88	1.98	1.91	1.90	1.78	1.85	0.07
42	8	1.83	1.84	1.87	1.82	1.93	1.72	1.91	1.66	1.71	1.72	1.89	1.81	0.09
42	9	1.84	1.80	1.76	1.96	1.91	1.90	1.94	1.82	1.59	1.83	1.81	1.83	0.10
42	10	1.94	1.91	1.90	1.94	1.99	1.84	1.65	1.76	1.95	1.98	1.96	1.89	0.10
42	11	1.92	1.91	1.88	1.75	1.73	1.89	1.79	1.53	1.73	1.73	1.95	1.80	0.12
42	12	1.92	1.91	1.78	1.79	1.85	1.71	1.86	1.91	1.90	1.84	1.73	1.84	0.07
	M	1.89	1.87	1.83	1.83	1.84	1.82	1.85	1.81	1.78	1.81	1.79		
	SD	0.05	0.04	0.06	0.08	0.09	0.08	0.10	0.13	0.12	0.11	0.15		

Supplementary Table 8. Transcription levels of the chaperonin *groEL* and reference gene *idnT* in *E. coli* MG1655, pLC. Transcript levels of *groEL* gene were determined for a total of six independent chemostat cultures (1-6) grown at 37°C or 42°C. Samples were collected at four consecutive days after 144 hours of steady-state growth in the chemostat system established here. Normalized *groEL* transcript levels are calculated using ΔCt-method.

			Mean(Ct)		normalized
day	culturing unit	T (°C)	*groEL*	*idnT*	transcript level
1	1	37	19.87	27.54	203.35
1	2	37	20.04	28.09	264.84
1	3	37	19.51	27.54	262.67
2	1	37	19.74	27.81	268.77
2	2	37	20.00	28.16	285.84
2	3	37	19.48	27.68	294.99
3	1	37	20.17	28.20	260.88
3	2	37	22.00	30.00	257.46
3	3	37	20.26	28.36	275.51
4	1	37	20.08	28.08	255.80
4	2	37	20.11	27.96	231.63
4	3	37	20.10	28.14	263.96
1	4	42	18.68	27.56	471.39
1	5	42	18.18	27.17	508.10
1	6	42	19.01	27.98	503.94
2	4	42	18.31	27.10	442.71
2	5	42	18.10	27.35	608.49
2	6	42	19.13	28.19	535.43
3	4	42	18.19	27.15	497.06
3	5	42	18.13	27.45	642.79
3	6	42	18.49	27.87	669.05
4	4	42	19.18	28.22	525.98
4	5	42	18.22	27.12	479.60
4	6	42	18.26	27.64	668.22

Supplementary Table 9. Comparison of growth rates between plasmid-free and plasmid-carrying strains grown at 37°C and 42°C. Growth rates were determined in batch culture as described in Section 3.7. Pairwise Wilcoxon rank sum tests with FDR correction were performed independently for the two temperature datasets. FDR-corrected *P*-vales are reported.

37°C	pHC-Wt	pLC-Wt	pHC-Hm	pLC-Hm	Hm
pLC-Wt	0.863	-	-	-	-
pHC-Hm	0.206	0.015	-	-	-
pLC-Hm	1.000	0.015	0.015	-	-
Hm	0.997	0.078	0.029	0.914	-
Wt	0.015	0.015	0.015	0.015	0.015

42°C	pHC-Wt	pLC-Wt	pHC-Hm	pLC-Hm	Hm
pLC-Wt	0.005	-	-	-	-
pHC-Hm	0.005	0.005	-	-	-
pLC-Hm	0.005	0.009	0.005	-	-
Hm	0.005	0.005	0.005	0.537	-
Wt	0.005	0.005	0.005	0.005	0.005

Supplementary Table 10. Density of pLC-populations in the chemostat vessels throughout the evolution experiment. Population densities (CFU/ml) were estimated by colony count analyses (*) or optical density measurements (**) and are represented as means ± *SD* of two replicate sample for each evolutionary line.

				Generation										
				1	90	200	280	400	480	600	680	800		
Host genotype	Plasmid type	Temp. °C	Replicate	*M** ± *SD*	*M*** ± *SD*	*M** ± *SD*	*M*** ± *SD*	*M** ± *SD*	*M*** ± *SD*	*M** ± *SD*	*M*** ± *SD*	*M** ± *SD*	*M* ± *SD*	CV %
Wild-type	pLC	37	1	1.84E+08 ± 6.36E+06	1.77E+08 ± 3.49E+05	1.87E+08 ± 1.34E+07	1.89E+08 ± 1.98E+06	2.10E+08 ± 9.90E+06	1.83E+08 ± 6.40E+06	1.87E+08 ± 9.19E+06	1.83E+08 ± 6.23E+06	1.85E+08 ± 6.36E+06	1.87E+08 ± 9.22E+06	4.93
Wild-type	pLC	37	2	2.05E+08 ± 7.78E+06	1.91E+08 ± 6.98E+05	2.16E+08 ± 4.24E+06	1.84E+08 ± 5.18E+06	1.87E+08 ± 9.90E+06	1.85E+08 ± 4.07E+06	1.94E+08 ± 1.41E+07	1.84E+08 ± 6.58E+06	1.86E+08 ± 1.56E+07	1.92E+08 ± 1.11E+07	5.75
Wild-type	pLC	37	3	2.15E+08 ± 3.82E+07	1.85E+08 ± 2.09E+06	1.87E+08 ± 1.27E+07	1.85E+08 ± 5.99E+06	1.98E+08 ± 1.56E+07	1.83E+08 ± 1.75E+06	1.95E+08 ± 3.04E+07	1.83E+08 ± 5.82E+04	1.97E+08 ± 6.36E+06	1.92E+08 ± 1.06E+07	5.50
Wild-type	pLC	37	4	2.04E+08 ± 1.77E+07	1.90E+08 ± 1.45E+06	1.92E+08 ± 2.19E+07	1.79E+08 ± 1.16E+05	1.95E+08 ± 9.19E+06	1.83E+08 ± 9.31E+05	1.83E+08 ± 5.66E+06	1.85E+08 ± 7.45E+06	1.89E+08 ± 1.48E+07	1.89E+08 ± 7.40E+06	3.92
Wild-type	pLC	37	5	2.04E+08 ± 9.90E+06	1.88E+08 ± 1.69E+06	1.98E+08 ± 1.84E+07	1.86E+08 ± 7.10E+06	1.95E+08 ± 2.47E+07	1.84E+08 ± 3.03E+06	1.97E+08 ± 2.19E+07	1.82E+08 ± 5.64E+06	1.96E+08 ± 3.68E+07	1.92E+08 ± 7.44E+06	3.87
Wild-type	pLC	37	6	1.96E+08 ± 7.07E+06	1.90E+08 ± 1.40E+06	1.97E+08 ± 9.19E+06	1.79E+08 ± 1.16E+05	1.92E+08 ± 1.13E+07	1.79E+08 ± 7.56E+05	1.76E+08 ± 7.07E+06	1.87E+08 ± 2.91E+05	1.87E+08 ± 7.07E+06	1.87E+08 ± 7.52E+06	4.02
			M	2.01E+08	1.87E+08	1.96E+08	1.84E+08	1.96E+08	1.83E+08	1.88E+08	1.84E+08	1.90E+08		
			σ	9.62E+06	4.73E+06	9.96E+06	3.68E+06	7.09E+06	1.80E+06	7.31E+06	1.86E+06	4.75E+06		
			CV %	4.78	2.53	5.09	2.00	3.62	0.99	3.88	1.01	2.50		

				Generation										
				1	90	200	280	400	480	600	680	800		
Host genotype	Plasmid type	Temp. °C	Replicate	*M** ± *SD*	*M*** ± *SD*	*M** ± *SD*	*M*** ± *SD*	*M** ± *SD*	*M*** ± *SD*	*M** ± *SD*	*M*** ± *SD*	*M** ± *SD*	*M* ± *SD*	CV %
Wild-type	pLC	42	1	2.14E+08 ± 1.06E+07	1.87E+08 ± 2.91E+05	2.10E+08 ± 1.48E+07	1.78E+08 ± 1.16E+05	1.94E+08 ± 7.07E+05	1.83E+08 ± 9.89E+05	1.93E+08 ± 5.66E+06	1.82E+08 ± 5.41E+06	1.99E+08 ± 6.36E+06	1.93E+08 ± 1.24E+07	6.41
Wild-type	pLC	42	2	2.00E+08 ± 5.66E+06	1.87E+08 ± 1.11E+06	2.05E+08 ± 1.13E+07	1.82E+08 ± 9.31E+05	2.12E+08 ± 1.06E+07	1.84E+08 ± 4.07E+05	2.05E+08 ± 2.19E+07	1.81E+08 ± 2.33E+05	1.89E+08 ± 0.00E+00	1.94E+08 ± 1.15E+07	5.95
Wild-type	pLC	42	3	2.11E+08 ± 5.66E+06	1.86E+08 ± 6.98E+05	1.93E+08 ± 6.36E+06	1.82E+08 ± 4.66E+06	1.98E+08 ± 4.24E+06	1.86E+08 ± 3.37E+06	1.81E+08 ± 7.78E+06	1.85E+08 ± 7.68E+06	2.03E+08 ± 1.98E+07	1.92E+08 ± 1.05E+07	5.46
Wild-type	pLC	42	4	1.83E+08 ± 7.07E+06	1.87E+08 ± 6.40E+05	2.05E+08 ± 1.41E+06	1.84E+08 ± 4.36E+06	1.97E+08 ± 7.07E+06	1.87E+08 ± 3.43E+06	1.96E+08 ± 3.68E+07	1.83E+08 ± 1.69E+06	1.86E+08 ± 1.48E+07	1.90E+08 ± 7.75E+06	4.09
Wild-type	pLC	42	5	2.01E+08 ± 5.66E+06	1.92E+08 ± 1.11E+06	1.97E+08 ± 4.24E+06	1.81E+08 ± 7.56E+05	1.84E+08 ± 3.54E+06	1.80E+08 ± 2.97E+06	2.02E+08 ± 3.18E+07	1.84E+08 ± 5.59E+06	2.22E+08 ± 1.41E+07	1.93E+08 ± 1.37E+07	7.06
Wild-type	pLC	42	6	1.91E+08 ± 8.49E+06	1.88E+08 ± 7.56E+05	1.96E+08 ± 2.12E+06	1.89E+08 ± 9.31E+05	2.11E+08 ± 9.90E+06	1.88E+08 ± 2.21E+06	2.15E+08 ± 7.07E+06	1.81E+08 ± 5.06E+06	1.99E+08 ± 1.63E+07	1.95E+08 ± 1.14E+07	5.82
			M	2.00E+08	1.88E+08	2.01E+08	1.83E+08	1.99E+08	1.85E+08	1.98E+08	1.82E+08	1.99E+08		
			σ	1.06E+07	1.86E+06	6.09E+06	3.35E+06	9.80E+06	2.80E+06	1.06E+07	1.51E+06	1.17E+07		
			CV %	5.30	0.99	3.03	1.84	4.92	1.51	5.36	0.83	5.89		

				Generation										
				1	100	200	300	400	500	600	700	800		
Host genotype	Plasmid type	Temp. °C	Replicate	*M** ± *SD*	*M*** ± *SD*	*M** ± *SD*	*M*** ± *SD*	*M** ± *SD*	*M*** ± *SD*	*M** ± *SD*	*M*** ± *SD*	*M** ± *SD*	*M* ± *SD*	CV %
Hypermutator	pLC	37	1	1.86E+08 ± 1.98E+07	1.82E+08 ± 6.92E+06	2.05E+08 ± 3.61E+07	1.80E+08 ± 8.73E+05	2.13E+08 ± 1.27E+07	1.85E+08 ± 1.16E+05	2.11E+08 ± 2.40E+07	1.80E+08 ± 3.49E+05	1.95E+08 ± 4.24E+06	1.93E+08 ± 1.34E+07	6.94
Hypermutator	pLC	37	2	2.00E+08 ± 2.12E+07	1.81E+08 ± 4.66E+05	2.03E+08 ± 3.75E+07	1.86E+08 ± 5.82E+05	2.19E+08 ± 4.24E+06	1.87E+08 ± 1.80E+06	1.80E+08 ± 1.06E+07	1.85E+08 ± 3.72E+06	1.95E+08 ± 1.20E+07	1.93E+08 ± 1.26E+07	6.54
Hypermutator	pLC	37	3	2.22E+08 ± 9.19E+06	1.85E+08 ± 7.27E+06	1.81E+08 ± 1.56E+07	1.87E+08 ± 3.55E+06	1.90E+08 ± 9.90E+06	1.82E+08 ± 3.84E+06	1.87E+08 ± 8.49E+06	1.88E+08 ± 2.97E+06	1.94E+08 ± 2.62E+07	1.90E+08 ± 1.23E+07	6.45
Hypermutator	pLC	37	4	1.84E+08 ± 2.12E+06	1.88E+08 ± 1.51E+06	1.89E+08 ± 2.05E+07	1.81E+08 ± 1.98E+06	2.00E+08 ± 3.11E+07	1.88E+08 ± 3.96E+06	2.00E+08 ± 2.83E+07	1.84E+08 ± 6.23E+06	2.00E+08 ± 2.40E+07	1.90E+08 ± 7.74E+06	4.07
Hypermutator	pLC	37	5	2.03E+08 ± 0.00E+00	1.88E+08 ± 2.04E+06	1.87E+08 ± 2.19E+07	1.87E+08 ± 5.47E+06	2.02E+08 ± 3.54E+06	1.86E+08 ± 4.83E+06	1.91E+08 ± 2.12E+06	1.86E+08 ± 7.04E+06	1.98E+08 ± 4.24E+07	1.92E+08 ± 7.07E+06	3.69
Hypermutator	pLC	37	6	2.09E+08 ± 2.55E+07	1.85E+08 ± 6.23E+06	1.99E+08 ± 2.76E+07	1.88E+08 ± 4.48E+06	2.08E+08 ± 2.90E+07	1.83E+08 ± 2.79E+06	1.91E+08 ± 1.84E+07	1.85E+08 ± 1.28E+06	1.91E+08 ± 3.25E+07	1.93E+08 ± 9.76E+06	5.06
			M	2.01E+08	1.85E+08	1.94E+08	1.85E+08	2.05E+08	1.85E+08	1.93E+08	1.85E+08	1.95E+08		
			σ	1.30E+07	2.45E+06	8.73E+06	3.19E+06	9.38E+06	2.30E+06	1.00E+07	2.29E+06	2.94E+06		
			CV %	6.50	1.32	4.51	1.73	4.57	1.24	5.18	1.24	1.50		

				Generation										
				1	100	200	300	400	500	600	700	800		
Host genotype	Plasmid type	Temp. °C	Replicate	*M** ± *SD*	*M*** ± *SD*	*M** ± *SD*	*M*** ± *SD*	*M** ± *SD*	*M*** ± *SD*	*M** ± *SD*	*M*** ± *SD*	*M** ± *SD*	*M* ± *SD*	CV %
Hypermutator	pLC	42	1	1.82E+08 ± 3.54E+06	1.86E+08 ± 5.59E+06	1.93E+08 ± 1.84E+07	1.81E+08 ± 5.24E+05	2.01E+08 ± 2.83E+06	1.83E+08 ± 7.74E+06	1.99E+08 ± 3.46E+07	1.84E+08 ± 7.22E+06	1.98E+08 ± 3.32E+07	1.89E+08 ± 8.01E+06	4.23
Hypermutator	pLC	42	2	2.11E+08 ± 2.33E+07	1.82E+08 ± 4.42E+06	1.80E+08 ± 4.24E+06	1.82E+08 ± 1.63E+06	2.04E+08 ± 3.89E+07	1.86E+08 ± 3.43E+06	2.19E+08 ± 9.90E+06	1.86E+08 ± 4.01E+06	1.95E+08 ± 3.75E+07	1.94E+08 ± 1.42E+07	7.33
Hypermutator	pLC	42	3	2.20E+08 ± 4.95E+06	1.84E+08 ± 7.56E+06	1.78E+08 ± 4.24E+06	1.85E+08 ± 2.04E+06	2.12E+08 ± 2.19E+07	1.88E+08 ± 3.37E+06	1.92E+08 ± 2.33E+07	1.84E+08 ± 6.34E+06	1.95E+08 ± 2.12E+06	1.93E+08 ± 1.39E+07	7.21
Hypermutator	pLC	42	4	2.06E+08 ± 0.00E+00	1.82E+08 ± 5.12E+06	2.07E+08 ± 1.91E+07	1.84E+08 ± 3.37E+06	2.00E+08 ± 2.33E+07	1.87E+08 ± 4.31E+06	1.80E+08 ± 1.34E+07	1.81E+08 ± 2.68E+06	1.83E+08 ± 1.13E+07	1.90E+08 ± 1.10E+07	5.78
Hypermutator	pLC	42	5	2.00E+08 ± 3.75E+07	1.86E+08 ± 1.86E+06	1.94E+08 ± 1.13E+07	1.84E+08 ± 3.96E+06	2.02E+08 ± 3.25E+07	1.89E+08 ± 2.79E+06	1.90E+08 ± 2.76E+07	1.88E+08 ± 2.91E+06	1.74E+08 ± 2.12E+06	1.89E+08 ± 8.49E+06	4.48
Hypermutator	pLC	42	6	2.02E+08 ± 3.68E+07	1.82E+08 ± 2.79E+06	2.26E+08 ± 2.12E+06	1.87E+08 ± 4.89E+06	1.84E+08 ± 6.36E+06	1.86E+08 ± 3.32E+06	1.84E+08 ± 1.98E+07	1.86E+08 ± 5.82E+04	2.07E+08 ± 3.39E+07	1.94E+08 ± 1.49E+07	7.67
			M	2.03E+08	1.83E+08	1.96E+08	1.84E+08	2.00E+08	1.86E+08	1.94E+08	1.85E+08	1.92E+08		
			σ	1.16E+07	1.73E+06	1.62E+07	2.03E+06	8.38E+06	1.89E+06	1.28E+07	2.10E+06	1.07E+07		
			CV %	5.73	0.94	8.25	1.10	4.19	1.01	6.60	1.14	5.60		

Supplementary Table 11. Density of pHC-populations in the chemostat vessels throughout the evolution experiment. Population densities (CFU/ml) were estimated by colony count analyses (*) or optical density measurements (**) and are represented as means ± *SD* of two replicate samples for each evolutionary line. Summary statistics are reported for each replicate (last two columns) and for each time point (at the bottom of each sub-table).

				Generation										
				1	90	200	280	400	480	600	680	800		
Host genotype	Plasmid type	Temp. °C	Replicate	*M** ± *SD*	*M*** ± *SD*	*M** ± *SD*	*M*** ± *SD*	*M** ± *SD*	*M*** ± *SD*	*M** ± *SD*	*M*** ± *SD*	*M** ± *SD*	*M* ± *SD*	CV %
Wild-type	pHC	37	1	1.84E+08 ± 6.36E+06	1.81E+08 ± 2.85E+06	1.80E+08 ± 4.95E+06	1.82E+08 ± 1.22E+06	1.97E+08 ± 1.41E+07	1.81E+08 ± 3.49E+05	2.16E+08 ± 1.06E+07	1.91E+08 ± 3.14E+06	1.93E+08 ± 1.98E+07	1.89E+08 1.17E+07	6.18
Wild-type	pHC	37	2	2.05E+08 ± 7.78E+06	1.86E+08 ± 5.59E+06	2.09E+08 ± 6.36E+06	1.81E+08 ± 5.82E+04	2.07E+08 ± 1.27E+07	1.86E+08 ± 2.91E+05	2.06E+08 ± 1.41E+07	1.87E+08 ± 2.85E+06	2.11E+08 ± 2.05E+07	1.97E+08 1.19E+07	6.04
Wild-type	pHC	37	3	2.15E+08 ± 3.82E+07	1.95E+08 ± 5.24E+05	2.05E+08 ± 1.13E+07	1.83E+08 ± 3.49E+05	2.04E+08 ± 1.20E+07	1.85E+08 ± 3.49E+05	1.95E+08 ± 1.48E+07	1.85E+08 ± 6.40E+05	1.89E+08 ± 7.07E+05	1.95E+08 1.10E+07	5.65
Wild-type	pHC	37	4	2.04E+08 ± 1.77E+07	1.80E+08 ± 4.07E+05	2.25E+08 ± 2.55E+07	1.81E+08 ± 4.66E+05	1.98E+08 ± 1.41E+07	1.80E+08 ± 6.40E+05	1.96E+08 ± 7.07E+06	1.80E+08 ± 1.22E+06	2.10E+08 ± 7.07E+05	1.95E+08 1.62E+07	8.30
Wild-type	pHC	37	5	2.04E+08 ± 9.90E+06	1.81E+08 ± 6.40E+05	1.93E+08 ± 2.83E+06	1.89E+08 ± 3.49E+05	1.98E+08 ± 1.27E+07	1.91E+08 ± 2.91E+05	2.08E+08 ± 1.91E+07	1.90E+08 ± 1.98E+06	1.96E+08 ± 2.62E+07	1.94E+08 7.96E+06	4.09
Wild-type	pHC	37	6	1.96E+08 ± 7.07E+06	1.99E+08 ± 2.91E+05	2.04E+08 ± 1.41E+07	1.81E+08 ± 4.07E+05	2.03E+08 ± 2.55E+07	1.88E+08 ± 1.57E+06	1.92E+08 ± 5.66E+06	1.91E+08 ± 5.24E+05	2.08E+08 ± 9.90E+06	1.96E+08 8.58E+06	4.38
			M	2.01E+08	1.87E+08	2.03E+08	1.83E+08	2.01E+08	1.85E+08	2.02E+08	1.87E+08	2.01E+08		
			σ	9.62E+06	7.41E+06	1.40E+07	2.99E+06	3.66E+06	3.96E+06	8.37E+06	3.88E+06	8.77E+06		
			CV %	4.78	3.96	6.90	1.63	1.82	2.14	4.15	2.07	4.37		

				Generation										
				1	90	200	280	400	480	600	680	800		
Host genotype	Plasmid type	Temp. °C	Replicate	*M** ± *SD*	*M*** ± *SD*	*M** ± *SD*	*M*** ± *SD*	*M** ± *SD*	*M*** ± *SD*	*M** ± *SD*	*M*** ± *SD*	*M** ± *SD*	*M* ± *SD*	CV %
Wild-type	pHC	42	1	2.14E+08 ± 1.06E+07	1.84E+08 ± 1.05E+06	1.89E+08 ± 1.77E+07	1.82E+08 ± 6.98E+05	1.88E+08 ± 1.20E+07	1.87E+08 ± 6.40E+05	1.92E+08 ± 4.95E+06	1.87E+08 ± 6.40E+05	2.11E+08 ± 1.13E+07	1.92E+08 1.15E+07	6.00
Wild-type	pHC	42	2	2.00E+08 ± 5.66E+06	1.76E+08 ± 7.62E+06	2.04E+08 ± 1.20E+07	1.83E+08 ± 2.33E+05	2.08E+08 ± 4.24E+06	1.90E+08 ± 6.98E+05	1.98E+08 ± 5.66E+06	1.88E+08 ± 1.11E+06	1.96E+08 ± 1.27E+07	1.94E+08 1.02E+07	5.27
Wild-type	pHC	42	3	2.11E+08 ± 5.66E+06	1.84E+08 ± 6.98E+06	2.00E+08 ± 8.49E+06	1.84E+08 ± 5.82E+05	2.00E+08 ± 9.90E+06	1.96E+08 ± 9.31E+05	2.05E+08 ± 1.13E+07	2.12E+08 ± 1.16E+05	1.92E+08 ± 3.54E+06	1.98E+08 1.04E+07	5.24
Wild-type	pHC	42	4	1.83E+08 ± 7.07E+06	1.78E+08 ± 6.40E+05	1.99E+08 ± 1.56E+07	1.87E+08 ± 8.73E+05	2.08E+08 ± 4.95E+06	1.86E+08 ± 2.62E+06	2.06E+08 ± 1.48E+07	1.80E+08 ± 1.34E+06	1.98E+08 ± 1.13E+07	1.92E+08 1.11E+07	5.78
Wild-type	pHC	42	5	2.01E+08 ± 5.66E+06	1.83E+08 ± 2.33E+05	1.94E+08 ± 1.84E+07	1.85E+08 ± 6.98E+05	1.99E+08 ± 9.90E+06	1.90E+08 ± 1.22E+06	2.05E+08 ± 7.78E+06	1.84E+08 ± 1.34E+06	1.90E+08 ± 3.25E+07	1.92E+08 7.98E+06	4.15
Wild-type	pHC	42	6	1.91E+08 ± 8.49E+06	1.81E+08 ± 1.11E+06	1.92E+08 ± 1.41E+07	1.83E+08 ± 6.40E+05	2.09E+08 ± 1.13E+07	1.83E+08 ± 1.57E+06	1.89E+08 ± 5.66E+06	1.91E+08 ± 6.40E+05	2.14E+08 ± 9.90E+06	1.93E+08 1.16E+07	6.00
			M	2.00E+08	1.81E+08	1.96E+08	1.84E+08	2.02E+08	1.89E+08	1.99E+08	1.90E+08	2.00E+08		
			σ	1.06E+07	2.97E+06	5.12E+06	1.59E+06	7.51E+06	3.86E+06	6.65E+06	1.02E+07	9.21E+06		
			CV %	5.30	1.64	2.61	0.86	3.72	2.04	3.35	5.36	4.60		

				Generation										
				1	100	200	300	400	500	600	700	800		
Host genotype	Plasmid type	Temp. °C	Replicate	*M** ± *SD*	*M*** ± *SD*	*M** ± *SD*	*M*** ± *SD*	*M** ± *SD*	*M*** ± *SD*	*M** ± *SD*	*M*** ± *SD*	*M** ± *SD*	*M* ± *SD*	CV %
Hypermutator	pHC	37	1	2.20E+08 ± 7.07E+06	1.78E+08 ± 6.40E+05	2.18E+08 ± 3.54E+06	1.86E+08 ± 7.56E+06	1.98E+08 ± 1.13E+07	1.78E+08 ± 8.73E+05	1.99E+08 ± 2.83E+07	1.85E+08 ± 6.75E+06	1.88E+08 ± 1.77E+07	1.94E+08 1.57E+07	8.10
Hypermutator	pHC	37	2	2.11E+08 ± 2.76E+07	1.80E+08 ± 5.82E+05	1.94E+08 ± 1.48E+07	1.87E+08 ± 5.30E+06	2.03E+08 ± 2.83E+07	1.87E+08 ± 1.69E+06	2.13E+08 ± 1.27E+07	1.86E+08 ± 5.47E+06	2.03E+08 ± 1.13E+07	1.96E+08 1.19E+07	6.07
Hypermutator	pHC	37	3	2.14E+08 ± 1.98E+07	1.84E+08 ± 9.43E+06	2.10E+08 ± 1.41E+06	1.87E+08 ± 8.15E+05	2.16E+08 ± 2.83E+06	1.82E+08 ± 5.70E+06	1.98E+08 ± 2.90E+07	1.81E+08 ± 4.36E+06	1.79E+08 ± 1.20E+07	1.94E+08 1.52E+07	7.84
Hypermutator	pHC	37	4	2.22E+08 ± 1.34E+07	1.80E+08 ± 3.20E+06	1.86E+08 ± 1.70E+07	1.86E+08 ± 2.73E+06	1.81E+08 ± 1.56E+07	1.86E+08 ± 4.36E+06	2.09E+08 ± 7.07E+05	1.82E+08 ± 3.14E+06	1.99E+08 ± 1.41E+06	1.92E+08 1.44E+07	7.52
Hypermutator	pHC	37	5	1.97E+08 ± 2.76E+07	1.85E+08 ± 6.05E+06	2.16E+08 ± 4.24E+06	1.81E+08 ± 3.67E+06	1.97E+08 ± 2.69E+07	1.83E+08 ± 1.57E+06	2.00E+08 ± 7.78E+06	1.88E+08 ± 1.16E+06	1.90E+08 ± 2.40E+07	1.93E+08 1.09E+07	5.65
Hypermutator	pHC	37	6	1.83E+08 ± 2.26E+07	1.84E+08 ± 6.81E+06	1.77E+08 ± 1.34E+07	1.85E+08 ± 2.62E+06	1.99E+08 ± 1.91E+07	1.81E+08 ± 4.71E+06	1.98E+08 ± 2.26E+07	1.79E+08 ± 1.11E+06	2.08E+08 ± 3.11E+07	1.88E+08 1.08E+07	5.76
			M	2.08E+08	1.82E+08	2.00E+08	1.85E+08	1.99E+08	1.83E+08	2.03E+08	1.83E+08	1.94E+08		
			σ	1.37E+07	2.75E+06	1.56E+07	2.16E+06	1.03E+07	3.09E+06	5.95E+06	3.10E+06	1.00E+07		
			CV %	6.60	1.51	7.78	1.16	5.17	1.69	2.94	1.69	5.15		

				Generation										
				1	100	200	300	400	500	600	700	800		
Host genotype	Plasmid type	Temp. °C	Replicate	*M** ± *SD*	*M*** ± *SD*	*M** ± *SD*	*M*** ± *SD*	*M** ± *SD*	*M*** ± *SD*	*M** ± *SD*	*M*** ± *SD*	*M** ± *SD*	*M* ± *SD*	CV %
Hypermutator	pHC	42	1	2.00E+08 ± 1.77E+07	1.81E+08 ± 5.70E+06	1.98E+08 ± 1.41E+06	1.84E+08 ± 6.63E+06	2.07E+08 ± 1.70E+07	1.88E+08 ± 3.20E+06	1.84E+08 ± 1.27E+07	1.81E+08 ± 2.85E+06	2.16E+08 ± 1.27E+07	1.93E+08 1.26E+07	6.50
Hypermutator	pHC	42	2	1.93E+08 ± 2.83E+07	1.82E+08 ± 6.69E+06	1.91E+08 ± 1.70E+07	1.89E+08 ± 3.43E+06	2.10E+08 ± 3.04E+07	1.79E+08 ± 1.80E+06	1.95E+08 ± 6.36E+06	1.85E+08 ± 5.12E+06	1.95E+08 ± 3.54E+07	1.91E+08 8.90E+06	4.66
Hypermutator	pHC	42	3	1.95E+08 ± 1.48E+07	1.83E+08 ± 1.86E+06	1.90E+08 ± 3.18E+07	1.81E+08 ± 3.61E+06	2.08E+08 ± 1.27E+07	1.84E+08 ± 8.44E+06	1.83E+08 ± 1.98E+07	1.82E+08 ± 6.17E+06	2.05E+08 ± 3.75E+07	1.90E+08 1.02E+07	5.36
Hypermutator	pHC	42	4	2.11E+08 ± 7.07E+05	1.88E+08 ± 1.63E+06	1.74E+08 ± 9.90E+06	1.81E+08 ± 1.51E+06	2.00E+08 ± 4.31E+07	1.83E+08 ± 1.45E+06	1.75E+08 ± 4.95E+06	1.86E+08 ± 5.82E+06	1.97E+08 ± 7.07E+06	1.88E+08 1.21E+07	6.45
Hypermutator	pHC	42	5	2.18E+08 ± 1.27E+07	1.85E+08 ± 3.03E+06	2.02E+08 ± 9.90E+06	1.83E+08 ± 8.26E+06	2.14E+08 ± 1.84E+07	1.83E+08 ± 5.06E+06	2.21E+08 ± 7.78E+06	1.82E+08 ± 3.55E+06	2.10E+08 ± 6.36E+06	2.00E+08 1.64E+07	8.22
Hypermutator	pHC	42	6	1.94E+08 ± 1.63E+07	1.83E+08 ± 8.44E+06	2.07E+08 ± 7.78E+06	1.86E+08 ± 1.57E+06	1.70E+08 ± 3.54E+06	1.87E+08 ± 4.36E+06	1.86E+08 ± 1.91E+07	1.80E+08 ± 1.05E+06	1.92E+08 ± 4.24E+06	1.87E+08 1.01E+07	5.40
			M	2.02E+08	1.84E+08	1.94E+08	1.84E+08	2.01E+08	1.84E+08	1.90E+08	1.83E+08	2.02E+08		
			σ	9.51E+06	2.35E+06	1.05E+07	2.72E+06	1.48E+07	2.80E+06	1.47E+07	2.02E+06	8.48E+06		
			CV %	4.72	1.28	5.44	1.48	7.37	1.52	7.72	1.11	4.19		

Supplementary Table 12. Independent-samples *t*-test for the comparison of population densities between chemostat cultures belonging to different groups of experimenal factors. Individual population densities are reported in Supplementary Table 10 and Supplementary Table 11.

Experimental Factor Group	*N*	*M*	*SD*	t	*df*	p	95% Confidence Interval of the Difference	
							lower	upper
37°C	216	1.92E+08	1.10E+07	-0.03	429.80	0.976	2.08E+06	2.14E+06
42°C	216	1.92E+08	1.13E+07					
pLC	216	1.92E+08	1.05E+07	-1.43	425.06	0.153	3.64E+06	5.71E+05
pHC	216	1.93E+08	1.17E+07					
Wild-type	216	1.93E+08	1.05E+07	-0.59	424.27	0.554	2.74E+06	1.47E+06
Hypermutator	216	1.92E+08	1.18E+07					

Supplementary Table 13. Descriptive statistics for PCNs of single colonies.

	n	Min.	1st Qu.	Med	M	3rd Qu.	Max.
pLC	35	6.52	11.26	14.41	14.10	16.36	23.16
pHC	91	0.00	104.70	399.80	1214.60	2209.20	7609.80

Supplementary Table 14. Plasmid copy numbers of pLC-populations in the chemostats. Mean plasmid copy numbers (*M*) and standard deviations (SD) of two sample dilutions are presented for each evolutionary line. Summary statistics are reported consecutively for biological replicates sampled at a time (below each experimental group) and for each replicate in the last two columns.

				Generation						
				1	200	400	600	800		
Host genotype	Plasmid type	Temp. °C	Replicate	*M* ± *SD*	*M* ± *SD*	*M* ± *SD*	*M* ± *SD*	*M* ± *SD*	*M* ± *SD*	CV %
Wild-type	pLC	37	1	8.30 ± 0.14	15.26 ± 0.34	21.44 ± 1.63	10.21 ± 0.66	7.16 ± 0.34	12.47 5.89	47.22
Wild-type	pLC	37	2	8.56 ± 1.98	25.37 ± 1.72	20.96 ± 2.28	18.74 ± 1.68	21.33 ± 0.89	18.99 6.30	33.19
Wild-type	pLC	37	3	7.24 ± 0.02	14.39 ± 0.10	18.79 ± 0.01	12.81 ± 0.00	9.41 ± 0.61	12.53 4.49	35.81
Wild-type	pLC	37	4	6.03 ± 0.03	14.12 ± 1.10	22.28 ± 0.92	14.48 ± 1.72	10.12 ± 0.61	13.41 6.03	44.99
Wild-type	pLC	37	5	7.81 ± 0.04	23.85 ± 0.28	24.58 ± 1.79	12.42 ± 0.99	8.35 ± 0.62	15.40 8.25	53.54
Wild-type	pLC	37	6	7.44 ± 0.11	20.93 ± 1.93	24.70 ± 2.20	15.38 ± 0.83	12.88 ± 0.94	16.27 6.76	41.58
			M	7.56	18.99	22.12	14.01	11.54		
			σ	0.82	4.60	2.07	2.67	4.72		
			CV %	10.88	24.22	9.34	19.09	40.89		
Wild-type	pLC	42	1	7.52 ± 1.23	11.66 ± 1.56	19.51 ± 0.55	9.97 ± 0.77	17.24 ± 1.22	13.18 5.03	38.16
Wild-type	pLC	42	2	8.09 ± 0.60	7.83 ± 1.61	15.65 ± 0.11	8.99 ± 0.88	15.78 ± 0.51	11.27 4.08	36.21
Wild-type	pLC	42	3	8.93 ± 0.41	7.20 ± 0.69	8.91 ± 0.43	9.26 ± 0.88	10.76 ± 0.61	9.01 1.27	14.07
Wild-type	pLC	42	4	7.10 ± 1.16	13.17 ± 1.02	15.34 ± 0.25	12.28 ± 2.00	12.79 ± 0.11	12.14 3.04	25.08
Wild-type	pLC	42	5	8.98 ± 0.17	7.83 ± 0.77	13.13 ± 0.65	11.66 ± 1.57	12.50 ± 0.37	10.82 2.30	21.25
Wild-type	pLC	42	6	9.19 ± 0.12	10.73 ± 1.33	14.58 ± 1.45	11.97 ± 0.39	18.07 ± 1.39	12.91 3.50	27.10
			M	8.30	9.74	14.52	10.69	14.52		
			σ	0.79	2.24	3.17	1.33	2.67		
			CV %	9.50	23.03	21.82	12.41	18.39		
Hypermutator	pLC	37	1	9.89 ± 0.24	15.45 ± 0.67	12.36 ± 0.58	10.49 ± 0.90	10.72 ± 0.74	11.78 2.25	19.07
Hypermutator	pLC	37	2	10.69 ± 0.60	12.58 ± 0.99	12.16 ± 0.76	10.02 ± 0.45	9.00 ± 0.47	10.89 1.48	13.63
Hypermutator	pLC	37	3	9.50 ± 1.85	9.17 ± 0.13	8.28 ± 0.85	7.33 ± 0.45	12.47 ± 0.47	9.35 1.94	20.74
Hypermutator	pLC	37	4	9.76 ± 0.26	10.77 ± 0.22	20.35 ± 0.17	12.51 ± 1.03	7.58 ± 0.39	12.19 4.90	40.16
Hypermutator	pLC	37	5	10.48 ± 0.06	5.35 ± 0.42	14.57 ± 0.26	8.58 ± 0.16	13.01 ± 0.11	10.40 3.64	35.03
Hypermutator	pLC	37	6	9.37 ± 0.53	7.11 ± 0.46	22.04 ± 1.06	10.17 ± 1.02	9.39 ± 0.66	11.62 5.94	51.10
			M	9.95	10.07	14.96	9.85	10.36		
			σ	0.49	3.36	4.81	1.61	1.92		
			CV %	4.88	33.33	32.13	16.36	18.51		
Hypermutator	pLC	42	1	8.90 ± 0.35	10.77 ± 0.19	10.10 ± 1.23	13.23 ± 0.59	13.38 ± 0.42	11.28 1.97	17.48
Hypermutator	pLC	42	2	9.53 ± 0.69	7.46 ± 0.16	8.23 ± 0.26	7.54 ± 0.65	11.79 ± 0.31	8.91 1.81	20.33
Hypermutator	pLC	42	3	11.13 ± 0.93	7.31 ± 0.18	10.13 ± 0.27	6.80 ± 0.39	13.28 ± 0.34	9.73 2.70	27.75
Hypermutator	pLC	42	4	8.11 ± 0.66	7.73 ± 0.47	9.27 ± 0.84	6.88 ± 0.71	8.95 ± 0.35	8.19 0.96	11.73
Hypermutator	pLC	42	5	9.78 ± 0.92	9.19 ± 0.57	11.68 ± 1.45	8.48 ± 0.27	10.49 ± 0.68	9.92 1.23	12.36
Hypermutator	pLC	42	6	7.74 ± 0.38	8.11 ± 0.85	13.39 ± 0.62	12.00 ± 0.29	11.99 ± 0.11	10.64 2.55	23.96
			M	9.20	8.43	10.47	9.16	11.65		
			σ	1.12	1.21	1.67	2.53	1.55		
			CV %	12.22	14.40	15.92	27.65	13.30		

Supplementary Table 15. Plasmid copy numbers of pHC-populations in the chemostats. The mean plasmid copy numbers and standard deviations of two sample dilutions are presented for each evolutionary line.

				Generation						
				1	200	400	600	800		
Host genotype	Plasmid type	Temp. °C	Evol. line	*M* ± *SD*	*M* ± *SD*	*M* ± *SD*	*M* ± *SD*	*M* ± *SD*	*M* ± *SD*	CV %
Wild-type	pHC	37	1	677.94 ± 1.48	39.61 ± 1.58	18.75 ± 0.25	1.07 ± 0.02	3.80 ± 0.18	148.24 296.51	200.03
Wild-type	pHC	37	2	725.68 ± 14.82	5.99 ± 0.44	4.03 ± 0.35	1.08 ± 0.03	14.58 ± 0.47	150.27 321.70	214.08
Wild-type	pHC	37	3	677.64 ± 17.04	36.76 ± 0.32	38.99 ± 1.09	37.10 ± 1.15	37.86 ± 2.22	165.67 286.20	172.76
Wild-type	pHC	37	4	688.52 ± 42.79	37.24 ± 2.16	14.47 ± 1.12	4.83 ± 0.34	10.15 ± 0.17	151.04 300.71	199.09
Wild-type	pHC	37	5	694.36 ± 26.21	153.22 ± 3.47	11.34 ± 0.60	10.37 ± 0.42	0.70 ± 0.08	174.00 297.69	171.09
Wild-type	pHC	37	6	576.76 ± 28.42	64.12 ± 4.70	16.80 ± 0.92	17.46 ± 1.51	18.40 ± 1.70	138.71 245.71	177.14
			M	673.48	56.16	17.40	11.99	14.25		
			σ	46.15	46.56	10.74	12.60	12.14		
			CV %	6.85	82.92	61.74	105.14	85.21		

				Generation						
				1	200	400	600	800		
Host genotype	Plasmid type	Temp. °C	Evol. line	*M* ± *SD*	*M* ± *SD*	*M* ± *SD*	*M* ± *SD*	*M* ± *SD*	*M* ± *SD*	CV %
Wild-type	pHC	42	1	719.87 ± 37.83	5.66 ± 0.46	24.85 ± 1.53	12.53 ± 1.22	39.02 ± 1.30	160.39 313.02	195.17
Wild-type	pHC	42	2	667.69 ± 27.81	2.15 ± 0.20	6.63 ± 1.73	2.02 ± 0.09	50.92 ± 0.59	145.88 292.42	200.45
Wild-type	pHC	42	3	710.94 ± 26.46	1.03 ± 0.01	8.31 ± 0.01	12.49 ± 1.47	28.50 ± 0.88	152.25 312.48	205.23
Wild-type	pHC	42	4	704.96 ± 22.64	1.21 ± 0.01	5.38 ± 0.42	5.28 ± 0.32	37.54 ± 1.74	150.87 310.09	205.53
Wild-type	pHC	42	5	659.55 ± 21.87	13.24 ± 1.01	15.96 ± 0.07	1.70 ± 0.00	3.69 ± 0.10	138.83 291.15	209.72
Wild-type	pHC	42	6	701.15 ± 18.75	2.01 ± 0.06	21.03 ± 1.05	12.96 ± 0.18	53.25 ± 2.26	158.08 304.19	192.43
			M	694.03	4.22	13.69	7.83	35.49		
			σ	22.39	4.32	7.43	4.96	16.48		
			CV %	3.23	102.41	54.28	63.41	46.45		

				Generation						
				1	200	400	600	800		
Host genotype	Plasmid type	Temp. °C	Evol. line	*M* ± *SD*	*M* ± *SD*	*M* ± *SD*	*M* ± *SD*	*M* ± *SD*	*M* ± *SD*	CV %
Hypermutator	pHC	37	1	991.92 ± 31.85	1030.45 ± 25.28	397.06 ± 4.35	537.91 ± 9.58	444.94 ± 22.11	680.46 306.43	45.03
Hypermutator	pHC	37	2	912.07 ± 10.00	512.68 ± 3.94	229.49 ± 26.49	228.55 ± 9.56	240.56 ± 4.99	424.67 298.23	70.23
Hypermutator	pHC	37	3	747.49 ± 5.63	1037.48 ± 49.27	415.69 ± 23.34	155.89 ± 14.07	145.36 ± 7.34	500.38 387.76	77.49
Hypermutator	pHC	37	4	1053.02 ± 41.15	545.77 ± 20.69	305.54 ± 2.30	293.24 ± 29.76	184.22 ± 10.19	476.36 348.36	73.13
Hypermutator	pHC	37	5	847.60 ± 16.05	968.08 ± 19.29	434.68 ± 27.01	198.61 ± 7.02	121.70 ± 9.78	514.13 379.85	73.88
Hypermutator	pHC	37	6	917.84 ± 28.03	966.24 ± 35.64	422.99 ± 5.29	174.41 ± 15.89	113.12 ± 9.25	518.92 403.67	77.79
			M	911.66	843.45	367.58	264.77	208.32		
			σ	97.91	224.07	74.91	129.82	114.12		
			CV %	10.74	26.57	20.38	49.03	54.78		

				Generation						
				1	200	400	600	800		
Host genotype	Plasmid type	Temp. °C	Evol. line	*M* ± *SD*	*M* ± *SD*	*M* ± *SD*	*M* ± *SD*	*M* ± *SD*	*M* ± *SD*	CV %
Hypermutator	pHC	42	1	1014.37 ± 13.10	102.98 ± 1.20	33.46 ± 0.34	28.03 ± 0.42	23.95 ± 1.14	240.56 433.79	180.33
Hypermutator	pHC	42	2	997.74 ± 15.29	212.32 ± 0.48	128.89 ± 6.06	151.01 ± 0.82	72.77 ± 8.85	312.55 386.28	123.59
Hypermutator	pHC	42	3	846.64 ± 24.80	14.18 ± 0.70	18.50 ± 0.18	31.76 ± 1.06	14.29 ± 0.71	185.07 369.90	199.86
Hypermutator	pHC	42	4	1010.20 ± 60.15	7.59 ± 0.52	25.82 ± 2.92	25.54 ± 1.07	26.53 ± 1.91	219.14 442.29	201.84
Hypermutator	pHC	42	5	916.79 ± 27.55	13.62 ± 1.51	154.26 ± 14.24	24.51 ± 1.48	45.02 ± 2.68	230.84 387.52	167.87
Hypermutator	pHC	42	6	940.22 ± 23.14	24.42 ± 0.80	22.20 ± 1.15	57.12 ± 3.61	29.19 ± 0.42	214.63 405.86	189.10
			M	954.33	62.52	63.86	52.99	35.29		
			σ	60.30	74.47	55.62	45.21	19.08		
			CV %	6.32	119.12	87.11	85.31	54.05		

Supplementary Table 16. Test results for the differential plating method and the streak method used to determine host proportions. Six test samples with different proportions of pLC plasmid bearing cells (expected proportion) were constructed to evaluate both methods. The number of colonies grown on selective media (*n*(amp+)) and non-selective media (*n*(amp-)) are reported for both methods. **(A)** For the differential plating method, the number of colonies counted on selective media (*n*(amp+)) and non-selective media (*n*(amp-)) are reported along with 95% confidence intervals calculated for the mean estimated proportion. **(B)** For the streak method, the total number of tested colonies grown on non-selective media (*n*(amp-)) and the total number of colonies grown on selective media (*n*(amp+)) are reported along with 95% confidence intervals and adjusted proportions calculated using the adjusted Wald method (Agresti and Coull 1998).

A)

expected proportion	sample	*n*(amp-)	*n*(amp+)	observed proportion		
1	1	148	165	1.11		
1	2	171	166	0.97		
1	3	152	160	1.05		
1	4	124	137	1.10		
1	5	176	187	1.06		
1	6	132	101	0.77	*M*	1.05
1	7	115	154	1.34	*SD*	0.15
1	8	166	145	0.87	*CV (%)*	14.62
1	9	188	167	0.89	*CI* - low	0.97
1	10	126	154	1.22	*CI* - upper	1.00
1	11	242	205	0.85		
1	12	177	189	1.07		
1	13	223	244	1.09		
1	14	215	244	1.13		
1	15	176	204	1.16		
0.75	1	167	133	0.80		
0.75	2	154	96	0.62		
0.75	3	187	114	0.61		
0.75	4	203	161	0.79		
0.75	5	178	126	0.71		
0.75	6	98	63	0.64	*M*	0.73
0.75	7	178	132	0.74	*SD*	0.08
0.75	8	254	178	0.70	*CV (%)*	11.23
0.75	9	233	154	0.66	*CI* - low	0.68
0.75	10	185	132	0.71	*CI* - upper	0.77
0.75	11	191	166	0.87		
0.75	12	237	177	0.75		
0.75	13	241	182	0.76		
0.75	14	154	101	0.66		
0.75	15	190	165	0.87		
0.5	1	431	215	0.50		
0.5	2	422	201	0.48		
0.5	3	513	255	0.50		
0.5	4	427	235	0.55		
0.5	5	398	186	0.47		
0.5	6	276	112	0.41	*M*	0.51
0.5	7	260	152	0.58	*SD*	0.05
0.5	8	249	122	0.49	*CV (%)*	10.16
0.5	9	279	147	0.53	*CI* - low	0.48
0.5	10	215	131	0.61	*CI* - upper	0.54
0.5	11	217	101	0.47		
0.5	12	236	127	0.54		
0.5	13	244	125	0.51		
0.5	14	209	96	0.46		
0.5	15	279	145	0.52		
0.25	1	289	75	0.26		
0.25	2	267	61	0.23		
0.25	3	258	85	0.33		
0.25	4	278	57	0.21		
0.25	5	288	63	0.22		
0.25	6	163	47	0.29	*M*	2.35
0.25	7	187	45	0.24	*SD*	4.37
0.25	8	213	63	0.30	*CV (%)*	186.35
0.25	9	139	21	0.15	*CI* - low	0.22
0.25	10	172	41	0.24	*CI* - upper	0.28
0.25	11	325	114	0.35		
0.25	12	285	84	0.29		
0.25	13	276	71	0.26		
0.25	14	269	43	0.16		
0.25	15	255	58	0.23		
0.1	1	291	32	0.11		
0.1	2	256	22	0.09		
0.1	3	221	21	0.10		
0.1	4	198	36	0.18		
0.1	5	108	7	0.06		
0.1	6	188	24	0.13	*M*	0.11
0.1	7	179	15	0.08	*SD*	0.05
0.1	8	158	29	0.18	*CV (%)*	40.10
0.1	9	83	11	0.13	*CI* - low	0.09
0.1	10	197	28	0.14	*CI* - upper	0.14
0.1	11	310	24	0.08		
0.1	12	250	32	0.13		
0.1	13	354	37	0.10		
0.1	14	402	63	0.16		
0.1	15	136	2	0.01		
0.05	1	372	16	0.04		
0.05	2	268	33	0.12		
0.05	3	176	17	0.10		
0.05	4	282	15	0.05		
0.05	5	254	2	0.01		
0.05	6	263	64	0.24	*M*	0.08
0.05	7	372	43	0.12	*SD*	0.06
0.05	8	259	9	0.03	*CV (%)*	83.10
0.05	9	265	2	0.01	*CI* - low	0.04
0.05	10	329	19	0.06	*CI* - upper	0.11
0.05	11	246	39	0.16		
0.05	12	261	14	0.05		
0.05	13	184	16	0.09		
0.05	14	428	36	0.08		
0.05	15	138	0	0.00		

B)

expected proportion	*n*(amp-)	*n*(amp+)	observed adjusted proportion	*CI* lower bound	upper bound
1	298	298	0.99	0.99	1.00
0.75	226	300	0.75	0.70	0.80
0.5	157	300	0.52	0.47	0.58
0.25	82	300	0.28	0.23	0.33
0.1	33	301	0.11	0.08	0.15
0.05	7	300	0.03	0.01	0.05

Supplementary Table 17. Effect of freezing and reviving on proportion of hosts. The effect of freezing and reving on the proportion of hosts in pLC-wt and pHC-wt populations with an expected proportion of hosts of 0.15 and 0.75 was examined by estimating the proportions before and after freezing at -80°C for six weeks using the streak method. **A)** Five technical replicates were used per test group and the number of colonies grown selective media (*n*(amp+)) and non-selective media are reported. **B)** Paired t-tests revealed no significant differences in observed proportions of hosts before and after freezing and reviving.

A)		pLC-wt				pHC-wt			
		p_{exp} = 0.15		p_{exp} = 0.75		p_{exp} = 0.15		p_{exp} = 0.75	
sample		before	after	before	after	before	after	before	after
1	n(amp-)	167	129	253	206	241	237	213	149
	n(amp+)	32	20	184	157	43	36	159	103
	p_{obs}	0.19	0.16	0.73	0.76	0.18	0.15	0.75	0.69
2	n(amp-)	214	177	248	185	264	289	194	557
	n(amp+)	35	31	196	136	48	52	143	432
	p_{obs}	0.16	0.18	0.79	0.74	0.18	0.18	0.74	0.78
3	n(amp-)	430	265	219	253	489	167	109	194
	n(amp+)	67	49	169	184	84	21	84	153
	p_{obs}	0.16	0.18	0.77	0.73	0.17	0.13	0.77	0.79
4	n(amp-)	242	158	153	168	386	294	389	174
	n(amp+)	37	25	121	132	59	32	304	130
	p_{obs}	0.15	0.16	0.79	0.79	0.15	0.11	0.78	0.75
5	n(amp-)	337	271	175	150	184	138	194	361
	n(amp+)	52	37	129	114	24	24	154	288
	p_{obs}	0.15	0.14	0.74	0.76	0.13	0.17	0.79	0.80

B)					*M* of the	95% CI of the difference			
genotype	expected p		*M*	*SD*	difference	Lower	Upper	*t*	*df*
pLC-wt	0.15	before	0.16	1.62E-02	1.70E-03	-3.03E-02	3.37E-02	*0.148*	*4*
		after	0.16	1.88E-02					
	0.75	before	0.76	2.97E-02	9.40E-03	-4.00E-02	5.88E-02	0.528	4
		after	0.75	2.33E-02					
pHC-wt	0.15	before	0.16	2.14E-02	1.50E-02	-3.12E-02	6.12E-02	0.902	4
		after	0.15	3.06E-02					
	0.75	before	0.77	2.37E-02	5.80E-03	-4.18E-02	5.34E-02	0.338	4
		after	0.76	4.30E-02					

Supplementary Table 18. Host proportions in chemostat cultures at generation 1 and generation 800. Proportion of hosts were estimated using the streak method (Section 3.8) and the tested number of colonies (*n*(amp-)) and resistant colonies (*n*(amp+)) is reported. Confidence intervals were calculated using the adjusted Wald method (Agresti and Coull 1998).

				Generation 1					Generation 800				
Plasmid	Host	T	Repli-			Proportion	CI 95%				Proportion	CI 95%	
type	genotype	°C	cate	*n*(amp-)	*n*(amp+)	of hosts	Lower	Upper	*n*(amp-)	*n*(amp+)	of hosts	Lower	Upper
pLC	Wt	37	1	102	102	1.00	0.95	1.00	224	224	1.00	0.98	1.00
pLC	Wt	37	2	101	101	1.00	0.95	1.00	218	218	1.00	0.98	1.00
pLC	Wt	37	3	105	105	1.00	0.96	1.00	216	216	1.00	0.98	1.00
pLC	Wt	37	4	105	105	1.00	0.96	1.00	226	226	1.00	0.98	1.00
pLC	Wt	37	5	102	102	1.00	0.95	1.00	220	220	1.00	0.98	1.00
pLC	Wt	37	6	106	106	1.00	0.96	1.00	212	212	1.00	0.98	1.00
pLC	Wt	42	1	100	100	1.00	0.95	1.00	139	139	1.00	0.97	1.00
pLC	Wt	42	2	104	104	1.00	0.96	1.00	108	108	1.00	0.96	1.00
pLC	Wt	42	3	102	102	1.00	0.95	1.00	139	136	0.98	0.93	1.00
pLC	Wt	42	4	101	101	1.00	0.95	1.00	141	140	0.99	0.96	1.00
pLC	Wt	42	5	101	101	1.00	0.95	1.00	141	140	0.99	0.96	1.00
pLC	Wt	42	6	110	110	1.00	0.96	1.00	141	138	0.98	0.94	1.00
pLC	Hypermutator	37	1	112	112	1.00	0.96	1.00	147	147	1.00	0.97	1.00
pLC	Hypermutator	37	2	110	110	1.00	0.96	1.00	146	146	1.00	0.97	1.00
pLC	Hypermutator	37	3	101	101	1.00	0.95	1.00	141	141	1.00	0.97	1.00
pLC	Hypermutator	37	4	106	106	1.00	0.96	1.00	142	142	1.00	0.97	1.00
pLC	Hypermutator	37	5	124	124	1.00	0.96	1.00	147	147	1.00	0.97	1.00
pLC	Hypermutator	37	6	113	113	1.00	0.96	1.00	148	148	1.00	0.97	1.00
pLC	Hypermutator	42	1	109	109	1.00	0.96	1.00	128	126	0.98	0.94	1.00
pLC	Hypermutator	42	2	104	104	1.00	0.96	1.00	118	115	0.97	0.92	0.99
pLC	Hypermutator	42	3	105	105	1.00	0.96	1.00	126	112	0.89	0.82	0.93
pLC	Hypermutator	42	4	111	111	1.00	0.96	1.00	120	120	1.00	0.96	1.00
pLC	Hypermutator	42	5	107	107	1.00	0.96	1.00	123	123	1.00	0.96	1.00
pLC	Hypermutator	42	6	105	105	1.00	0.96	1.00	133	133	1.00	0.96	1.00
pHC	Wt	37	1	127	120	0.94	0.89	0.98	481	31	0.06	0.05	0.09
pHC	Wt	37	2	123	116	0.94	0.88	0.97	460	35	0.08	0.05	0.10
pHC	Wt	37	3	117	114	0.97	0.92	0.99	723	173	0.24	0.21	0.27
pHC	Wt	37	4	105	101	0.96	0.90	0.99	436	11	0.03	0.01	0.05
pHC	Wt	37	5	102	99	0.97	0.91	0.99	457	4	0.01	0.00	0.02
pHC	Wt	37	6	220	163	0.74	0.68	0.80	550	19	0.03	0.02	0.05
pHC	Wt	42	1	128	125	0.98	0.93	1.00	188	146	0.78	0.71	0.83
pHC	Wt	42	2	154	145	0.94	0.89	0.97	147	28	0.19	0.13	0.26
pHC	Wt	42	3	134	128	0.96	0.90	0.98	153	9	0.06	0.03	0.11
pHC	Wt	42	4	176	167	0.95	0.90	0.97	165	61	0.37	0.30	0.45
pHC	Wt	42	5	157	151	0.96	0.92	0.98	157	32	0.20	0.15	0.28
pHC	Wt	42	6	139	131	0.94	0.89	0.97	172	9	0.05	0.03	0.10
pHC	Hypermutator	37	1	158	146	0.92	0.87	0.96	180	176	0.98	0.94	0.99
pHC	Hypermutator	37	2	163	154	0.94	0.90	0.97	172	168	0.98	0.94	0.99
pHC	Hypermutator	37	3	157	146	0.93	0.88	0.96	179	170	0.95	0.90	0.98
pHC	Hypermutator	37	4	149	139	0.93	0.88	0.97	175	171	0.98	0.94	0.99
pHC	Hypermutator	37	5	142	135	0.95	0.90	0.98	232	81	0.35	0.29	0.41
pHC	Hypermutator	37	6	143	131	0.92	0.86	0.95	183	177	0.97	0.93	0.99
pHC	Hypermutator	42	1	144	131	0.91	0.85	0.95	157	118	0.75	0.68	0.81
pHC	Hypermutator	42	2	127	116	0.91	0.85	0.95	172	153	0.89	0.83	0.93
pHC	Hypermutator	42	3	165	156	0.95	0.90	0.97	157	126	0.80	0.73	0.86
pHC	Hypermutator	42	4	143	128	0.90	0.83	0.94	176	80	0.45	0.38	0.53
pHC	Hypermutator	42	5	155	142	0.92	0.86	0.95	165	67	0.41	0.33	0.48
pHC	Hypermutator	42	6	136	128	0.94	0.89	0.97	170	139	0.82	0.75	0.87

Supplementary Table 19. Sequencing information and coverage statistics for evolved and ancestral samples. Mean read coverage for plasmids and chromosomes were calculated before and after deduplication. The sample type is either of type 'total population' (TP) or 'pooled hosts' (PH). Wt: wild-type; Hm: Hypermutator.

						Mean read coverage					
						Plasmid		Chromosome		Relative PCN	
Plasmid type	Host geno-type	T °C	Repli-cate	Samp-le type	ID	before dedup.	after dedup.	before dedup.	after dedup.	before dedup.	after dedup.
pLC	Wt	37	1	TP	S74	4410.64	2742.4	223.19	209.78	19.76	13.07
pLC	Wt	37	2	TP	S75	6159.45	3452.5	269.38	251.10	22.87	13.75
pLC	Wt	37	3	TP	S76	4178.63	2613.8	209.08	197.44	19.99	13.24
pLC	Wt	37	4	TP	S77	4823.04	2906.9	287.35	268.67	16.78	10.82
pLC	Wt	37	5	TP	S78	4162.12	2592.1	255.59	239.20	16.28	10.84
pLC	Wt	37	6	TP	S79	7786.16	4017.9	264.01	244.78	29.49	16.41
pLC	Wt	42	1	TP	S07	1289.16	1022.1	274.69	254.58	4.69	4.01
pLC	Wt	42	2	TP	S08	844.59	701.78	270.72	250.95	3.12	2.80
pLC	Wt	42	3	TP	S09	442.24	390.21	246.21	227.31	1.80	1.72
pLC	Wt	42	4	TP	S10	1345.52	1063	262.98	244.70	5.12	4.34
pLC	Wt	42	5	TP	S11	803.75	673.14	254.68	236.97	3.16	2.84
pLC	Wt	42	6	TP	S12	3553.52	2396.6	326.87	299.74	10.87	8.00
pLC	Hm	37	1	TP	S31	1174.83	945.99	171.6	161.36	6.85	5.86
pLC	Hm	37	2	TP	S32	1629.70	1267.1	178.95	167.75	9.11	7.55
pLC	Hm	37	3	TP	S33	1199.32	985.13	209.04	194.82	5.74	5.06
pLC	Hm	37	4	TP	S34	2178.17	1652.8	229.99	212.94	9.47	7.76
pLC	Hm	37	5	TP	S35	2201.21	1669.8	277.11	256.05	7.94	6.52
pLC	Hm	37	6	TP	S36	905.10	764.25	243.7	225.64	3.71	3.39
pLC	Hm	42	1	TP	S19	885.58	737.15	264.91	244.91	3.34	3.01
pLC	Hm	42	2	TP	S20	1348.00	1061.9	308.01	283.30	4.38	3.75
pLC	Hm	42	3	TP	S21	976.25	787.71	295.2	270.44	3.31	2.91
pLC	Hm	42	4	TP	S22	609.40	521.04	175.37	164.01	3.47	3.18
pLC	Hm	42	5	TP	S23	1025.63	833.31	150.77	141.82	6.80	5.88
pLC	Hm	42	6	TP	S24	457.43	404.22	150.71	140.47	3.04	2.88
pHC	Wt	37	1	PH	S81	44159.67	12987	152.49	145.42	289.59	89.31
pHC	Wt	37	2	PH	S86	102191.02	20168	109.03	104.59	937.27	192.83
pHC	Wt	37	3	PH	S90	46936.97	12901	195.83	184.46	239.68	69.94
pHC	Wt	37	4	PH	S95	3342.90	2229.3	189.49	180.00	17.64	12.39
pHC	Wt	37	5	PH	S98	133088.64	24599	162.74	155.92	817.80	157.77
pHC	Wt	37	6	PH	S102	272010.80	28054	204.82	193.14	1328.05	145.25
pHC	Wt	42	1	PH	S55	31635.19	15604	216.94	201.43	145.82	77.47
pHC	Wt	42	2	PH	S56	49034.84	17840	149.66	140.28	327.64	127.17
pHC	Wt	42	3	PH	S57	53003.22	11386	163.05	153.47	325.07	74.19
pHC	Wt	42	4	PH	S58	38356.17	18495	171.21	160.66	224.03	115.12
pHC	Wt	42	5	PH	S59	59583.85	13844	123.05	116.72	484.22	118.61
pHC	Wt	42	6	PH	S60	18209.37	11462	141.38	133.70	128.80	85.73
pHC	Hm	37	1	PH	S67	17533.87	7912	170.4	160.81	102.90	49.20
pHC	Hm	37	2	PH	S68	24036.51	9605.2	120.42	114.50	199.61	83.89
pHC	Hm	37	3	PH	S69	33257.60	11996	152.3	144.23	218.37	83.17
pHC	Hm	37	4	PH	S70	18674.53	8337.9	209.15	196.15	89.29	42.51
pHC	Hm	37	5	PH	S71	16997.19	7691.4	171.76	161.51	98.96	47.62
pHC	Hm	37	6	PH	S72	31500.25	11275	144.6	136.79	217.84	82.43
pHC	Hm	42	1	PH	S61	31635.19	12318	168.97	158.76	187.22	77.59
pHC	Hm	42	2	PH	S62	49034.84	15965	160.16	150.43	306.16	106.13
pHC	Hm	42	3	PH	S63	53003.22	16430	144.4	136.23	367.06	120.60
pHC	Hm	42	4	PH	S64	38356.17	13917	178.02	166.70	215.46	83.48
pHC	Hm	42	5	PH	S65	59583.85	16990	171.31	161.46	347.81	105.23
pHC	Hm	42	6	PH	S66	18209.37	8099.5	198.26	186.41	91.85	43.45

Supplementary Table 20. Frequency of variants detected on chromosome and plasmid. For each sequenced population, the number of detected variants, coverage statistics, estimated chromosomal substitution rate, expected and observed number of variants on the plasmid replicons are reported. Unless otherwise stated, reported statistics are derived from sequencing data subsampled to a common mean coverage of 104x. The sample type is either of type 'total population' (TP) or 'pooled hosts' (PH). Wt: wild-type; Hm: hypermutator.

						Chromosome								Plasmids						
Sample ID	Plasmid type	Host geno-type	T °C	Replicate	Sample type	# indels	# point mutations	# intergen. point mutations	# synon. point mutations	# non-synon. point mutations	# nonsense point mutations	# intergen. and synon. sites covered ≥10	Substitution rate /site/generation	# intergen. and synon. sites covered ≥10	Expected number of point mutations (using PCN calculated after deduplication)	Expected number of point mutations (using PCN calculated before deduplication)	Observed number of point mutations	Observed number of point mutations (using full coverage information)	Observed number of indels	Observed number of indels (using full coverage information)
S74	pLC	Wt	37	1	TP	0	4	2	0	1	1	1.44E+06	1.73E-09	4049.00	0.06	0.11	0	0	0	0
S75	pLC	Wt	37	2	TP	0	9	4	0	3	2	1.44E+06	3.47E-09	4049.00	0.14	0.26	0	0	0	0
S76	pLC	Wt	37	3	TP	1	9	3	0	5	1	1.44E+06	2.60E-09	4049.00	0.13	0.17	0	0	0	0
S77	pLC	Wt	37	4	TP	0	6	2	1	2	1	1.44E+06	2.60E-09	4049.00	0.07	0.14	0	0	0	0
S78	pLC	Wt	37	5	TP	0	5	3	0	1	1	1.44E+06	2.60E-09	4049.00	0.06	0.14	0	0	0	0
S79	pLC	Wt	37	6	TP	0	7	2	0	3	2	1.44E+06	1.73E-09	4049.00	0.13	0.17	0	0	0	0
S07	pLC	Wt	42	1	TP	0	16	4	2	10	0	1.43E+06	5.25E-09	4049.00	0.07	0.08	0	1	0	0
S08	pLC	Wt	42	2	TP	1	4	1	0	3	0	1.40E+06	8.91E-10	4049.00	0.01	0.01	0	0	0	0
S09	pLC	Wt	42	3	TP	1	5	1	0	4	0	1.36E+06	9.20E-10	4049.00	0.01	0.01	0	0	0	0
S10	pLC	Wt	42	4	TP	0	6	2	1	3	0	1.41E+06	2.65E-09	4049.00	0.03	0.04	0	0	0	0
S11	pLC	Wt	42	5	TP	0	4	1	0	3	0	1.40E+06	8.90E-10	4049.00	0.01	0.01	0	0	0	0
S12	pLC	Wt	42	6	TP	4	11	4	0	6	1	1.42E+06	3.53E-09	4049.00	0.10	0.12	0	0	0	0
S31	pLC	Hm	37	1	TP	13	52	8	17	27	0	1.42E+06	2.21E-08	4049.00	0.35	0.49	0	0	0	0
S32	pLC	Hm	37	2	TP	8	59	8	18	32	1	1.41E+06	2.31E-08	4049.00	0.51	0.68	1	1	0	0
S33	pLC	Hm	37	3	TP	4	60	9	18	31	2	1.35E+06	2.50E-08	4033.00	0.35	0.46	0	1	0	0
S34	pLC	Hm	37	4	TP	2	58	6	20	32	0	1.37E+06	2.38E-08	4049.00	0.52	0.73	0	0	0	0
S35	pLC	Hm	37	5	TP	8	44	6	8	28	2	1.39E+06	1.25E-08	4049.00	0.33	0.32	0	1	0	0
S36	pLC	Hm	37	6	TP	7	74	7	23	43	1	1.36E+06	2.76E-08	4049.00	0.29	0.33	0	1	0	0
S19	pLC	Hm	42	1	TP	6	44	7	11	26	0	1.40E+06	1.61E-08	4049.00	0.15	0.17	0	1	0	0
S20	pLC	Hm	42	2	TP	5	26	2	8	16	0	1.40E+06	8.96E-09	4049.00	0.11	0.13	0	0	0	0
S21	pLC	Hm	42	3	TP	6	38	2	11	25	0	1.39E+06	1.17E-08	4049.00	0.13	0.13	1	1	0	0
S22	pLC	Hm	42	4	TP	5	37	4	8	24	1	1.37E+06	1.10E-08	4049.00	0.14	0.12	0	1	0	0
S23	pLC	Hm	42	5	TP	6	49	4	16	29	0	1.39E+06	1.79E-08	4049.00	0.33	0.39	0	0	0	0
S24	pLC	Hm	42	6	TP	5	34	2	12	20	0	1.30E+06	1.34E-08	4034.00	0.12	0.13	0	0	0	0
S81	pHC	Wt	37	1	PH	1	2	1	0	1	0	1.44E+06	8.67E-10	4201.33	0.19	0.84	0	0	0	0
S86	pHC	Wt	37	2	PH	0	1	1	0	0	0	1.44E+06	8.67E-10	4201.33	0.20	2.73	0	0	0	0
S90	pHC	Wt	37	3	PH	0	2	0	0	2	0	1.44E+06	0	4201.33	0.15	0.00	0	0	0	0
S95	pHC	Wt	37	4	PH	0	5	1	0	4	0	1.44E+06	8.67E-10	4181.33	0.07	0.05	0	0	0	0
S98	pHC	Wt	37	5	PH	1	2	1	1	0	0	1.44E+06	1.73E-09	4199.33	0.33	4.76	0	0	0	0
S102	pHC	Wt	37	6	PH	0	2	1	0	1	0	1.44E+06	8.68E-10	4201.33	0.31	3.87	0	0	0	0
S55	pHC	Wt	42	1	PH	2	3	0	0	3	0	1.44E+06	0	4201.33	0.25	0.00	0	0	0	0
S56	pHC	Wt	42	2	PH	3	8	1	0	6	1	1.41E+06	8.83E-10	4201.33	1.08	1.34	0	0	0	0
S57	pHC	Wt	42	3	PH	2	5	2	0	3	0	1.43E+06	1.74E-09	4201.33	0.39	1.03	0	0	0	0
S58	pHC	Wt	42	4	PH	0	5	0	0	5	0	1.44E+06	0	4201.33	0.61	0.00	0	0	0	0
S59	pHC	Wt	42	5	PH	2	5	2	0	3	0	1.44E+06	1.73E-09	4201.33	0.63	1.80	0	0	0	0
S60	pHC	Wt	42	6	PH	0	6	1	0	5	0	1.43E+06	8.73E-10	4201.33	0.54	0.59	0	0	0	0
S67	pHC	Hm	37	1	PH	4	42	5	10	26	1	1.44E+06	1.31E-08	4201.33	2.18	4.52	0	0	0	2
S68	pHC	Hm	37	2	PH	3	43	6	10	27	0	1.43E+06	1.40E-08	4201.33	3.82	9.36	0	0	1	1
S69	pHC	Hm	37	3	PH	4	69	8	13	47	1	1.43E+06	1.83E-08	4201.33	6.06	13.43	0	0	0	1
S70	pHC	Hm	37	4	PH	3	49	6	7	35	1	1.44E+06	1.13E-08	4201.33	2.20	3.39	0	1	0	0
S71	pHC	Hm	37	5	PH	6	31	7	4	20	0	1.43E+06	9.60E-09	4201.33	1.56	3.19	0	0	0	0
S72	pHC	Hm	37	6	PH	6	63	5	17	41	0	1.43E+06	1.93E-08	4201.33	5.51	14.12	0	0	1	1
S61	pHC	Hm	42	1	PH	12	63	9	18	36	0	1.43E+06	2.36E-08	4201.33	5.18	14.87	0	0	0	1
S62	pHC	Hm	42	2	PH	5	52	4	9	39	0	1.43E+06	1.13E-08	4201.33	5.83	11.65	0	0	0	0
S63	pHC	Hm	42	3	PH	6	51	5	17	29	0	1.44E+06	1.91E-08	4201.33	6.49	23.56	0	0	0	1
S64	pHC	Hm	42	4	PH	6	28	2	11	15	0	1.40E+06	1.16E-08	4201.33	2.51	8.42	0	0	0	0
S65	pHC	Hm	42	5	PH	12	135	25	24	81	5	1.44E+06	4.26E-08	4201.33	15.00	49.79	0	0	0	0
S66	pHC	Hm	42	6	PH	7	61	9	14	38	0	1.43E+06	2.01E-08	4201.33	2.80	6.19	0	0	0	0

Supplementary Table 21. Comparison of the number of variants detected in pooled hosts and total population pHC sequencing samples. For each sequenced population, the number of detected variants, coverage statistics, estimated chromosomal substitution rate, expected and observed number of variants on the plasmid replicons are reported. Unless otherwise stated, reported statistics are derived from sequencing data subsampled to a common mean coverage of 104x. The sample type is either of type 'total population' (TP) or 'pooled hosts' (PH). Wt: wild-type; Hm: hypermutator.

						# point mutations			# indels			Sequencing information on total population				Proportion of hosts at generation 800			
Plasmid type	Host geno-type	T °C	Repli-cate	Sample ID – PH	Sample ID – TP	PH	TP	detected in both samples	PH	TP	detected in both samples	Library preparation type	Sequencing platform	BioSample accession	SRA run accession	Number of colonies tested	Proportion of hosts	Lower limit at a 95% confidence interval	Upper limit at a 95% confidence interval
pHC	Wt	37	1	S81	S84	1	2	0	1	0	0	Nextera	HiSeq2500	SAMN08956167	SRR7535018	481	0.06	0.05	0.09
pHC	Wt	37	2	S86	S89	1	1	0	0	0	0	Nextera	HiSeq2500	SAMN08956167	SRR7535017	460	0.08	0.05	0.10
pHC	Wt	37	3	S90	S93	2	3	1	0	0	0	Nextera	HiSeq2500	SAMN08956167	SRR7535020	723	0.24	0.21	0.27
pHC	Wt	37	4	S95	S97	4	5	4	0	0	0	Nextera	HiSeq2500	SAMN08956167	SRR7535019	436	0.03	0.01	0.05
pHC	Wt	37	5	S98	S101	2	8	0	1	1	0	Nextera	HiSeq2500	SAMN08956167	SRR7535014	457	0.01	0.00	0.02
pHC	Wt	37	6	S102	S105	2	11	1	0	1	0	Nextera	HiSeq2500	SAMN08956167	SRR7535013	550	0.03	0.02	0.05
pHC	Wt	42	1	S55	S01	4	5	4	2	2	2	NexteraXT	NextSeq500	SAMN08956175	SRR7535016	188	0.78	0.71	0.83
pHC	Wt	42	2	S56	S02	7	6	3	2	1	0	NexteraXT	NextSeq500	SAMN08956175	SRR7535015	147	0.19	0.13	0.26
pHC	Wt	42	3	S57	S03	4	5	3	1	1	1	NexteraXT	NextSeq500	SAMN08956175	SRR7535012	153	0.06	0.03	0.11
pHC	Wt	42	4	S58	S04	5	6	2	0	0	0	NexteraXT	NextSeq500	SAMN08956175	SRR7535011	165	0.37	0.30	0.45
pHC	Wt	42	5	S59	S05	4	6	2	2	1	0	NexteraXT	NextSeq500	SAMN08956175	SRR7535010	157	0.20	0.15	0.27
pHC	Wt	42	6	S60	S06	7	9	3	0	1	0	NexteraXT	NextSeq500	SAMN08956175	SRR7535009	172	0.05	0.03	0.10
pHC	Hm	37	1	S67	S25	42	39	36	4	4	4	NexteraXT	NextSeq500	SAMN08956177	SRR7535008	180	0.98	0.94	0.99
pHC	Hm	37	2	S68	S26	40	29	14	2	6	2	NexteraXT	NextSeq500	SAMN08956177	SRR7535007	172	0.98	0.94	0.99
pHC	Hm	37	3	S69	S27	66	29	23	4	3	2	NexteraXT	NextSeq500	SAMN08956177	SRR7535006	179	0.95	0.91	0.97
pHC	Hm	37	4	S70	S28	44	44	36	3	3	3	NexteraXT	NextSeq500	SAMN08956177	SRR7535005	175	0.98	0.94	0.99
pHC	Hm	37	5	S71	S29	32	8	7	5	5	5	NexteraXT	NextSeq500	SAMN08956177	SRR7535004	232	0.35	0.29	0.41
pHC	Hm	37	6	S72	S30	61	60	52	2	5	2	NexteraXT	NextSeq500	SAMN08956177	SRR7535003	183	0.97	0.93	0.99
pHC	Hm	42	1	S61	S13	60	47	29	9	14	1	NexteraXT	NextSeq500	SAMN08956176	SRR7535002	157	0.75	0.68	0.81
pHC	Hm	42	2	S62	S14	49	40	22	5	6	0	NexteraXT	NextSeq500	SAMN08956176	SRR7535001	172	0.89	0.83	0.93
pHC	Hm	42	3	S63	S15	49	57	38	6	9	4	NexteraXT	NextSeq500	SAMN08956176	SRR7534999	157	0.80	0.73	0.86
pHC	Hm	42	4	S64	S16	27	33	26	7	6	5	NexteraXT	NextSeq500	SAMN08956176	SRR7535000	176	0.45	0.38	0.53
pHC	Hm	42	5	S65	S17	106	48	26	5	7	1	NexteraXT	NextSeq500	SAMN08956176	SRR7534997	165	0.41	0.33	0.48
pHC	Hm	42	6	S66	S18	53	29	24	8	8	3	NexteraXT	NextSeq500	SAMN08956176	SRR7534998	170	0.82	0.75	0.87

Supplementary Table 22. Number of chromosomal mutations detected in both samples of pooled hosts and corresponding total population samples of evolved pHC populations. As the minimum mean coverage among the populations was 77x, sequencing read data of all samples was subsampled to a mean coverage of 77x. Plasmid variants detected in these samples are reported in Supplementary Table 20. The sample type is either of type 'total population' (TP) or 'pooled hosts' (PH). Wt: wild-type; Hm: hypermutator.

			Sequencing information							PCN statistics for populations at generation 800							
										37 °C				42°C			
Plasmid type	Host geno-type	Samp-le ID	Library preparation type	Sequencing platform	BioSample accession	SRA run accession	Mean coverage chromo-some	Mean coverage plasmid	PCN	*M*	*SD*	95% CI – Lower bound	95% CI – Upper bound	*M*	*SD*	95% CI – Lower bound	95% CI – Upper bound
pLC	Wt	S52	NexteraXT	NextSeq500	SAMN08956172	SRR7040497	185.86	371.73	2.00	20.86	4.86	15.76	25.96	4.79	3.21	1.43	8.16
pLC	Hm	S54	NexteraXT	NextSeq500	SAMN08956174	SRR7040483	208.26	2597.71	12.47	7.14	2.18	4.85	9.42	4.06	1.42	2.57	5.55
pHC	Wt	S51	NexteraXT	NextSeq500	SAMN08956171	SRR7040495	206.31	17765.17	86.11	605.01	501.28	78.94	1131.07	293.96	105.76	182.97	404.95
pHC	Hm	S53	NexteraXT	NextSeq500	SAMN08956173	SRR7040485	184.5	21314.50	115.53	154.50	63.44	87.91	221.08	252.59	106.33	141.01	364.18

Supplementary Table 23. Chromosomal variants. The table includes all chromosomal variants detected in the evolved populations using subsampled reads (average coverage104x). Allele frequencies are listed together with annotation of the mutation locus within the *E. coli* reference genome sequence (GenBank acc. no. NC_000913.3). NA indicates that the read coverage at the given position was insufficient to call variants (coverage <10). The table and a description of all table fields can be found on the appendix CD.

Supplementary Table 24. ANOVA table for the test of main effects and interaction effects of the factors used in the experiment on allele frequencies of mutations observed in more than one population (detailed list in Supplementary Table 23). Note, that the three-way factorial ANOVA was performed on aligned rank transformed allele frequencies (Wobbrock et al. 2011).

Factor/interaction term	*df*	*Residual df*	*Sum of Squares*	*Residual Sum of Squares*	*F*-value	*P*(>*F*)
plasmid type	1	6904	6.48E+08	1.41E+10	318.49	1.11E-69
temperature	1	6904	4.25E+08	1.42E+10	206.55	3.58E-46
host genotype	1	6904	2.61E+06	1.18E+10	1.53	2.16E-01
plasmid type:temperature	1	6904	5.51E+08	1.42E+10	267.95	4.08E-59
plasmid type:host genotype	1	6904	6.28E+08	1.41E+10	307.00	2.77E-67
temperature:host genotype	1	6904	4.04E+08	1.43E+10	195.75	7.00E-44
plasmid type:temperature: host genotype	1	6904	1.31E+09	1.42E+10	637.96	1.04E-134

Supplementary Table 25. ANOVA table for the test of main effects and interaction effects of plasmid type and temperature on allele frequency of parallel mutations (i.e., observed in more than one population). Mutations for which factors (i.e., plasmid type or temperature) or their interaction were found to have a significant effect on aligned rank transformed allele frequencies and ANOVA statistics are reported.

Variant ID	Factor/interaction term	*df*	*df*.res	Sum Sq.	Sum Sq.res	*F*	*P*
aas T22A	plasmid type	1	44	1728	4537.50	16.76	3.41E-03
ccmA 538 +C	plasmid type	1	44	1728	4554.50	16.69	3.41E-03
cheA G52G	plasmid type	1	44	1728	4539.50	16.75	3.41E-03
dps G93G	plasmid type	1	44	1728	4537.50	16.76	3.41E-03
fhuF N179S	plasmid type	1	44	1728	4537.50	16.76	3.41E-03
glnE S473S	plasmid type	1	44	1728	4537.50	16.76	3.41E-03
gltB P516P	plasmid type	1	44	1728	4917.83	15.46	3.50E-03
lacI V175I	plasmid type	1	44	1728	5194.50	14.64	4.16E-03
lptB F165L	plasmid type	1	44	1728	4545.00	16.73	3.41E-03
malQ G468G	plasmid type	1	44	1728	5280.00	14.40	4.16E-03
mdtL F235L	plasmid type	1	44	1728	4929.50	15.42	3.50E-03
melR F103L	plasmid type	1	44	1728	4537.50	16.76	3.41E-03
p G1636236A	plasmid type	1	44	1728	4545.00	16.73	3.41E-03
pepP E376E	plasmid type	1	44	1728	4537.50	16.76	3.41E-03
polB G401D	plasmid type	1	44	1728	4916.33	15.47	3.50E-03
prpE T320A	plasmid type	1	44	1728	4537.50	16.76	3.41E-03
pta P265P	plasmid type	1	44	1728	4906.83	15.50	3.50E-03
recF G128D	plasmid type	1	44	1728	4948.50	15.36	3.50E-03
rhsD T766A	plasmid type	1	44	1728	4545.00	16.73	3.41E-03
sfmH 332 +C	plasmid type	1	44	1728	4918.83	15.46	3.50E-03
stfR G1066S	plasmid type	1	44	1728	4718.83	16.11	3.50E-03
ybjD A415A	plasmid type	1	44	1728	4740.50	16.04	3.50E-03
ycaI E585E	plasmid type	1	44	1728	4537.50	16.76	3.41E-03
ycjN E39G	plasmid type	1	44	1728	4534.50	16.77	3.41E-03
yfgF A355V	plasmid type	1	44	1728	4537.50	16.76	3.41E-03
yfhR A74T	plasmid type	1	44	1728	4537.50	16.76	3.41E-03
yfjK S473I	plasmid type	1	44	1728	4545.00	16.73	3.41E-03
yhbJ S114S	plasmid type	1	44	1728	4537.50	16.76	3.41E-03
ymdB L166P	plasmid type	1	44	1728	4537.50	16.76	3.41E-03
yraK V325A	plasmid type	1	44	1728	4537.50	16.76	3.41E-03
i A2512766G	temperature	1	44	1680	5769.50	12.81	7.52E-03
insA S7S	plasmid type	1	44	1728	4637.00	16.40	3.41E-03
insA S7S	temperature	1	44	1728	4637.00	16.40	3.41E-03
insA S7S	plasmid type:temperature	1	44	1728	4637.00	16.40	3.41E-03
intA A21V	plasmid type	1	44	1728	4997.00	15.22	3.50E-03
intA A21V	temperature	1	44	1728	4997.00	15.22	3.50E-03
intA A21V	plasmid type:temperature	1	44	1728	4997.00	15.22	3.50E-03
miaB E113G	plasmid type	1	44	1728	5309.00	14.32	4.16E-03
miaB E113G	temperature	1	44	1728	5309.00	14.32	4.16E-03
miaB E113G	plasmid type:temperature	1	44	1728	5309.00	14.32	4.16E-03
polA N761S	plasmid type	1	44	2352	4957.00	20.88	3.41E-03
polA N761S	temperature	1	44	2352	4957.00	20.88	3.41E-03
polA N761S	plasmid type:temperature	1	44	2352	4957.00	20.88	3.41E-03
rpoS Q48*	plasmid type	1	44	1728	5309.50	14.32	4.16E-03
rpoS Q48*	temperature	1	44	1728	5309.50	14.32	4.16E-03
rpoS Q48*	plasmid type:temperature	1	44	1728	5309.50	14.32	4.16E-03
wcaA S44P	plasmid type	1	44	1728	4997.00	15.22	3.50E-03
wcaA S44P	temperature	1	44	1728	4997.00	15.22	3.50E-03
wcaA S44P	plasmid type:temperature	1	44	1728	4997.00	15.22	3.50E-03

6.4 CD

The Supplementary Table 23 is recorded as digital data (Microsoft Excel Table version 16.20) on a CD attached to the thesis.

7 References

Abeles AL, Friedman SA, Austin SJ. 1985. Partition of unit-copy miniplasmids to daughter cells. III. The DNA sequence and functional organization of the P1 partition region. J. Mol. Biol. 185:261–272.

Agnoli K, Schwager S, Uehlinger S, Vergunst A, Viteri DF, Nguyen DT, Sokol PA, Carlier A, Eberl L. 2011. Exposing the third chromosome of *Burkholderia cepacia* complex strains as a virulence plasmid. Mol. Microbiol. 83:362–378.

Agresti A, Coull BA. 1998. Approximate is better than “exact” for interval estimation of binomial proportions. Am. Stat. 52:119.

Altschul SF, Gish W, Miller W, Myers EW, Lipman DJ. 1990. Basic local alignment search tool. J. Mol. Biol. 215:403–410.

Andrews S. 2016. FASTQC. Available from: http://www.bioinformatics.babraham.ac.uk/projects/fastqc/

Anjem A, Varghese S, Imlay JA. 2009. Manganese import is a key element of the OxyR response to hydrogen peroxide in *Escherichia coli*. Mol. Microbiol. 72:844–858.

Antoine R, Locht C. 1992. Isolation and molecular characterization of a novel broad-host-range plasmid from *Bordetella bronchiseptica* with sequence similarities to plasmids from Gram-positive organisms. Mol. Microbiol. 6:1785–1799.

Arjan JA, Visser M, Zeyl CW, Gerrish PJ, Blanchard JL, Lenski RE. 1999. Diminishing returns from mutation supply rate in asexual populations. Science 283:404–406.

Bankevich A, Nurk S, Antipov D, Gurevich AA, Dvorkin M, Kulikov AS, Lesin VM, Nikolenko SI, Pham S, Prjibelski AD, et al. 2012. SPAdes: a new genome assembly algorithm and its applications to single-cell sequencing. J. Comput. Biol. 19:455–477.

Bansal V. 2017. A computational method for estimating the PCR duplication rate in DNA and RNA-seq experiments. BMC Bioinform. 18:43.

Barnett DW, Garrison EK, Quinlan AR, Stromberg MP, Marth GT. 2011. BamTools: a C++ API and toolkit for analyzing and managing BAM files. Bioinformatics 27:1691–1692.

Barrick JE, Lenski RE. 2013. Genome dynamics during experimental evolution. Nature 14:827–839.

Baxter JC, Funnell BE. 2014. Plasmid partition mechanisms. Microbiol. Spectr. 2(6).

Bazaral M, Helinski DR. 1968. Circular DNA forms of colicinogenic factors E1, E2 and E3 from *Escherichia coli.* J. Mol. Biol. 36:185–194.

Becker L, Steglich M, Fuchs S, Werner G, Nübel U. 2016. Comparison of six commercial kits to extract bacterial chromosome and plasmid DNA for MiSeq sequencing. Sci. Rep. 6:28063.

Bedhomme S, Perez Pantoja D, Bravo IG. 2017. Plasmid and clonal interference during post horizontal gene transfer evolution. Mol. Ecol. 26:1832–1847.

Bevan M. 1984. Binary *Agrobacterium* vectors for plant transformation. Nucleic Acids Res. 12:8711–8721.

Birky CW. 2001. The inheritance of genes in mitochondria and chloroplasts: laws, mechanisms, and models. Annu. Rev. Genet. 35:125–48.

Bodmer WF, Cavalli-Sforza LL. 1976. Genetics, evolution, and man. W H Freeman & Company.

Bolger AM, Lohse M, Usadel B. 2014. Trimmomatic: a flexible trimmer for Illumina sequence data. Bioinformatics 30:2114–2120.

Bouma JE, Lenski RE. 1988. Evolution of a bacteria/plasmid association. Nature 335:351–352.

Chen Z, Lin J, Ma C, Zhao S, She Q, Liang Y. 2014. Characterization of pMC11, a plasmid with dual origins of replication isolated from *Lactobacillus casei* MCJ and construction of shuttle vectors with each replicon. Appl. Microbiol. Biotechnol. 98:5977–5989.

Chiang CS, Bremer H. 1988. Stability of pBR322-derived plasmids. Plasmid 20:207–220.

Colegrave N. 2002. Sex releases the speed limit on evolution. Nature 420:664–666.

Czárán TL, Hoekstra RF, Pagie L. 2002. Chemical warfare between microbes promotes biodiversity. Proc. Natl. Acad. Sci. U.S.A. 99:786–90.

de Visser JAGM, Rozen DE. 2005. Limits to adaptation in asexual populations. J. Evol. Biol. 18:779–788.

Deatherage DE, Kepner JL, Bennett AF, Lenski RE, Barrick JE. 2017. Specificity of genome evolution in experimental populations of *Escherichia coli* evolved at different temperatures. Proc. Natl. Acad. Sci. U.S.A. 114:E1904–E1912.

Doron S, Melamed S, Ofir G, Leavitt A, Lopatina A, Keren M, Amitai G, Sorek R. 2018. Systematic discovery of antiphage defense systems in the microbial pangenome. Science 359:eaar4120.

Dower WJ, Miller JF, Ragsdale CW. 1988. High efficiency transformation of *E. coli* by high voltage electroporation. Nucleic Acids Res.16:6127–6145.

Dubey GP, Ben-Yehuda S. 2011. Intercellular nanotubes mediate bacterial communication. Cell 144:590–600.

Dykhuizen D, Hartl D. 1981. Evolution of competitive ability in *Escherichia coli*. Evolution 35:581–594.

Dykhuizen DE, Hartl DL. 1983. Selection in chemostats. Microbiol. Rev. 46:150–168.

Dziewit L, Pyzik A, Szuplewska M, Matlakowska R, Mielnicki S, Wibberg D, Schlüter A, Pühler A, Bartosik D. 2015. Diversity and role of plasmids in adaptation of bacteria inhabiting the Lubin copper mine in Poland, an environment rich in heavy metals. Front. Microbiol. 6:152.

Ekblom R, Smeds L, Ellegren H. 2014. Patterns of sequencing coverage bias revealed by ultra-deep sequencing of vertebrate mitochondria. BMC Genom. 15:467.

Fagerlund A, Granum PE, Håvarstein LS. 2014. *Staphylococcus aureus* competence genes: mapping of the SigH, ComK1 and ComK2 regulons by transcriptome sequencing. Mol. Microbiol. 94:557–579.

Fang H, Wu Y, Narzisi G, ORawe JA, Barrón LTJ, Rosenbaum J, Ronemus M, Iossifov I, Schatz MC, Lyon GJ. 2014. Reducing INDEL calling errors in whole genome and exome sequencing data. Genome Med. 6:1326.

Fernández-Tresguerres ME, Martín M, García de Viedma D, Giraldo R, Díaz-Orejas R. 1995. Host growth temperature and a conservative amino acid substitution in the replication protein of pPS10 influence plasmid host range. J. Bacteriol. 177:4377–4384.

Figurski DH, Helinski DR. 1979. Replication of an origin-containing derivative of plasmid RK2 dependent on a plasmid function provided in *trans*. Proc. Natl. Acad. Sci. U.S.A. 76:1648–1652.

Fulsundar S, Harms K, Flaten GE, Johnsen PJ, Chopade BA, Nielsen KM. 2014. Gene transfer potential of outer membrane vesicles of *Acinetobacter baylyi* and effects of stress on vesiculation. Appl. Environ. Microbiol. 80:3469–3483.

Garcia-Martin JA, Clote P. 2015. RNA thermodynamic structural entropy. PLoS ONE. 10:e0137859.

Georgopoulos CP, Eisen H. 1974. Bacterial mutants which block phage assembly. J. Supramol. Struct. 2:349–359.

Gillespie JH. 2010. Population genetics. Baltimore (MD). JHU Press.

Graur D. 2015. Molecular and genome evolution. Sunderland (MA). Sinauer Associates.

Gruber AR, Lorenz R, Bernhart SH, Neubock R, Hofacker IL. 2008. The Vienna RNA websuite. Nucleic Acids Res. 36:W70–W74.

Gullberg E, Albrecht LM, Karlsson C, Sandegren L, Andersson DI. 2014. Selection of a multidrug resistance plasmid by sublethal levels of antibiotics and heavy metals. mBio 5:e01918–14.

Guyot S, Pottier L, Hartmann A, Ragon M, Hauck Tiburski J, Molin P, Ferret E, Gervais P. 2014. Extremely rapid acclimation of *Escherichia coli* to high temperature over a few generations of a fed-batch culture during slow warming. Microbiologyopen 3:52–63.

Haemig HAH, Brooker RJ. 2004. Importance of conserved acidic residues in *mntH*, the Nramp homolog of *Escherichia coli*. J. Membr. Biol. 201:97–107.

Hall JPJ, Wood AJ, Harrison E, Brockhurst MA. 2016. Source-sink plasmid transfer dynamics maintain gene mobility in soil bacterial communities. Proc. Natl. Acad. Sci. U.S.A. 113:8260–8265.

Hanahan D. 1983. Studies on transformation of *Escherichia coli* with plasmids. J. Mol. Biol. 166:557–580.

Handa N, Morimatsu K, Lovett ST, Kowalczykowski SC. 2009. Reconstitution of initial steps of dsDNA break repair by the RecF pathway of *E. coli*. Genes Dev. 23:1234–1245.

Harrison E, Guymer D, Spiers AJ, Paterson S, Brockhurst MA. 2015. Parallel compensatory evolution stabilizes plasmids across the parasitism-mutualism continuum. Curr. Biol. 25:2034–2039.

He S, Hickman AB, Varani AM, Siguier P, Chandler M, Dekker JP, Dyda F. 2015. Insertion sequence IS 26 reorganizes plasmids in clinically isolated multidrug-resistant bacteria by replicative transposition. mBio 6:e00762–15.

He Y, Wu J, Dressman DC, Iacobuzio-Donahue C, Markowitz SD, Velculescu VE, Diaz LA Jr, Kinzler KW, Vogelstein B, Papadopoulos N. 2010. Heteroplasmic mitochondrial DNA mutations in normal and tumour cells. Nature 464:610–614.

Herendeen SL, VanBogelen RA, Neidhardt FC. 1979. Levels of major proteins of *Escherichia coli* during growth at different temperatures. J. Bacteriol. 139:185–194.

Hershfield V, Boyer HW, Yanofsky C, Lovett MA, Helinski DR. 1974. Plasmid ColE1 as a molecular vehicle for cloning and amplification of DNA. Proc. Natl. Acad. Sci. U.S.A. 71:3455–3459.

Hertwig S, Popp A, Freytag B, Lurz R, Appel B. 1999. Generalized transduction of small *Yersinia enterocolitica* plasmids. Appl. Environ. Microbiol. 65:3862–3866.

Hsu L, Jackowski S, Rock CO. 1991. Isolation and characterization of *Escherichia coli* K-12 mutants lacking both 2-acyl-glycerophosphoethanolamine acyltransferase and acyl-acyl carrier protein synthetase activity. J. Biol. Chem. 266:13783–13788.

Huynen M, Gutell R, Konings D. 1997. Assessing the reliability of RNA folding using statistical mechanics. J. Mol. Biol. 267:1104–1112.

Hyland EM, Wallace EWJ, Murray AW. 2014. A model for the evolution of biological specificity: a cross-reacting DNA-binding protein causes plasmid incompatibility. J. Bacteriol. 196:3002–3011.

Jahn M, Vorpahl C, Hübschmann T, Harms H, Müller S. 2016. Copy number variability of expression plasmids determined by cell sorting and Droplet Digital PCR. Microb. Cell Fact.15:211.

Jechalke S, Heuer H, Siemens J, Amelung W, Smalla K. 2014. Fate and effects of veterinary antibiotics in soil. Trends Microbiol. 22:536–545.

Klieve AV, Yokoyama MT, Forster RJ, Ouwerkerk D, Bain PA, Mawhinney EL. 2005. Naturally occurring DNA transfer system associated with membrane vesicles in cellulolytic *Ruminococcus* spp. of ruminal origin. Appl. Environ. Microbiol. 71:4248–4253.

Klümper U, Riber L, Dechesne A, Sannazzarro A, Hansen LH, Sørensen SJ, Smets BF. 2015. Broad host range plasmids can invade an unexpectedly diverse fraction of a soil bacterial community. ISME J. 9:934–945.

Koboldt DC, Chen K, Wylie T, Larson DE, McLellan MD, Mardis ER, Weinstock GM, Wilson RK, Ding L. 2009. VarScan: variant detection in massively parallel sequencing of individual and pooled samples. Bioinformatics 25:2283–2285.

Kopfmann S, Roesch SK, Hess WR. 2016. Type II toxin-antitoxin systems in the unicellular cyanobacterium *Synechocystis* sp. PCC 6803. Toxins (Basel) 8:E228.

Korea C-G, Badouraly R, Prevost M-C, Ghigo JM, Beloin C. 2010. *Escherichia coli* K-12 possesses multiple cryptic but functional chaperone-usher fimbriae with distinct surface specificities. Environ. Microbiol. 12:1957–1977.

Kunkel TA. 2010. Evolving views of DNA replication (in)fidelity. Cold Spring Harb. Symp. Quant. Biol. 74:91–101.

Lanfear R, Kokko H, Eyre-Walker A. 2013. Population size and the rate of evolution. Trends Ecol. Evol. 1:33-41.

Lederberg J, Tatum EL. 1946. Gene recombination in *Escherichia coli*. Nature 158(4016):558.

Lee HH, Popodi EE, Tang HH, Foster PLP. 2012. Rate and molecular spectrum of spontaneous mutations in the bacterium Escherichia coli as determined by whole-genome sequencing. Proc. Natl. Acad. Sci. U.S.A. 109:E2774–E2783.

Lenski RE, Rose MR, Simpson SC, Tadler SC. 1991. Long-term experimental evolution in *Escherichia coli*. I. Adaptation and divergence during 2,000 generations. Am. Nat. 138:1315–1341.

Li H, Durbin R. 2009. Fast and accurate short read alignment with Burrows-Wheeler transform. Bioinformatics 25:1754–1760.

Li H, Handsaker B, Wysoker A, Fennell T, Ruan J, Homer N, Marth G, Abecasis G, Durbin R. 2009. The Sequence Alignment/Map format and SAMtools. Bioinformatics 25:2078–2079.

Li H. 2014. Towards a better understanding of artefacts in variant calling from high-coverage samples. Bioinformatics 15:2843–51.

Lin-Chao S, Cohen SN. 1991. The rate of processing and degradation of antisense RNAI regulates the replication of ColE1-type plasmids *in vivo*. Cell 65:1233–1242.

Loftie-Eaton W, Bashford K, Quinn H, Dong K, Millstein J, Hunter S, Thomason MK, Merrikh H, Ponciano JM, Top EM. 2017. Compensatory mutations improve general permissiveness to antibiotic resistance plasmids. Nat. Ecol. Evol. 1:1354–1363.

Loftie-Eaton W, Yano H, Burleigh S, Simmons RS, Hughes JM, Rogers LM, Hunter SS, Settles ML, Forney LJ, Ponciano JM, Top EM. 2016. Evolutionary paths that expand plasmid host-range: implications for spread of antibiotic resistance. Mol. Biol. Evol. 33:885–897.

Lorenz MG, Gerjets D, Wackernagel W. 1991. Release of transforming plasmid and chromosomal DNA from two cultured soil bacteria. Arch. Microbiol. 156:319–326.

Lorenz R, Bernhart SH, Höner zu Siederdissen C, Tafer H, Flamm C, Stadler PF, Hofacker IL. 2011. ViennaRNA Package 2.0. Algorithms Mol. Biol. 6:26.

Maestro B, Sanz JM, Díaz-Orejas R, Fernandez-Tresguerres E. 2003. Modulation of pPS10 host range by plasmid-encoded RepA initiator protein. J. Bacteriol.185:1367–1375.

Majeed H, Gillor O, Kerr B, Riley MA. 2010. Competitive interactions in *Escherichia coli* populations: the role of bacteriocins. ISME J. 5:71–81.

Mansukhani S, Barber LJ, Kleftogiannis D, Moorcraft SY, Davidson M, Woolston A, Proszek PZ, Griffiths B, Fenwick K, Herman B, et al. 2018. Ultra-sensitive mutation detection and genome-wide DNA copy number reconstruction by error-corrected circulating tumor DNA sequencing. Clin. Chem. 64:1626–1635.

Marraffini LA, Sontheimer EJ. 2008. CRISPR interference limits horizontal gene transfer in staphylococci by targeting DNA. Science 322:1843–1845.

McKenna A, Hanna M, Banks E, Sivachenko A, Cibulskis K, Kernytsky A, Garimella K, Altshuler D, Gabriel S, Daly M, et al. 2010. The genome analysis toolkit: a MapReduce framework for analyzing next-generation DNA sequencing data. Genome Res. 20:1297–1303.

McKenzie GJ, Craig NL. 2006. Fast, easy and efficient: site-specific insertion of transgenes into enterobacterial chromosomes using Tn7 without need for selection of the insertion event. BMC Microbiol. 6:39.

Michael V, Frank O, Bartling P, Scheuner C, ker MGO, Brinkmann H, Petersen JOR. 2016. Biofilm plasmids with a rhamnose operon are widely distributed determinants of the “swim-or-stick” lifestyle in *Roseobacters*. ISME J. 10:2498–2513.

Millan AS, Toll-Riera M, Qi Q, Betts A, Hopkinson RJ, McCullagh J, MacLean RC. 2018. Integrative analysis of fitness and metabolic effects of plasmids in *Pseudomonas aeruginosa* PAO1. ISME J. 12:3014–3024.

Millan AS, Pena-Miller R, Toll-Riera M, Halbert ZV, McLean AR, Cooper BS, MacLean RC. 2014. Positive selection and compensatory adaptation interact to stabilize non-transmissible plasmids. Nat. Commun. 5:1–11.

Miller AW, Befort C, Kerr EO, Dunham MJ. 2013. Design and use of multiplexed chemostat arrays. JoVE:e50262.

Morikawa K, Takemura AJ, Inose Y, Tsai M, Nguyen Thi LT, Ohta T, Msadek T. 2012. Expression of a cryptic secondary sigma factor gene unveils natural competence for DNA transformation in *Staphylococcus aureus*. PLoS Pathog. 8:e1003003.

Muesing M, Tamm J, Shepard HM, Polisky B. 1981. A single base-pair alteration is responsible for the DNA overproduction phenotype of a plasmid copy-number mutant. Cell 24:235–242.

Münch KM, Müller J, Wienecke S, Bergmann S, Heyber S, Biedendieck R, Münch R, Jahn D. 2015. Polar fixation of plasmids during recombinant protein production in *Bacillus megaterium* results in population heterogeneity. Appl. Environ. Microbiol. 81:5976–5986.

Norberg P, m MBO, Jethava V, Dubhashi D, Hermansson M. 2011. The IncP-1 plasmid backbone adapts to different host bacterial species and evolves through homologous recombination. Nat. Commun. 2:272–11.

Nordström K. 2006. Plasmid R1--replication and its control. Plasmid 55:1–26.

Notley-McRobb L, Seeto S, Ferenci T. 2003. The influence of cellular physiology on the initiation of mutational pathways in *Escherichia coli* populations. Proc. Biol. Sci. 270:843–848.

Novick A, Szilard L. 1950. Description of the chemostat. Science 112:715–716.

Nurk S, Bankevich A, Antipov D, Gurevich AA, Korobeynikov A, Lapidus A, Prjibelski AD, Pyshkin A, Sirotkin A, Sirotkin Y, et al. 2013. Assembling single-cell genomes and mini-metagenomes from chimeric MDA products. J. Comput. Biol. 20:714–737.

O'Rawe J, Jiang T, Sun G, Wu Y, Wang W, Hu J, Bodily P, Tian L, Hakonarson H, Johnson WE, et al. 2013. Low concordance of multiple variant-calling pipelines: practical implications for exome and genome sequencing. Genome Med. 5:28.

Parekh S, Ziegenhain C, Vieth B, Enard W, Hellmann I. 2016. The impact of amplification on differential expression analyses by RNA-seq. Sci. Rep. 6:25533.

Patten CL, Kirchhof MG, Schertzberg MR, Morton RA, Schellhorn HE. 2004. Microarray analysis of RpoS-mediated gene expression in *Escherichia coli* K-12. Mol. Genet. Genomics 272:580–591.

Peng B, Kimmel M. 2005. simuPOP: a forward-time population genetics simulation environment. Bioinformatics 21:3686–3687.

PIRT SJ, CALLOW DS. 1960. Studies of the growth of *Penicillium Chrysogenumin* continuous flow culture with reference to penicillin production. J. Appl. Bacteriol. 23:87–98.

Porse A, Schønning K, Munck C, Sommer MOA. 2016. Survival and evolution of a large multidrug resistance plasmid in new clinical bacterial hosts. Mol. Biol. Evol. 33:2860–2873.

Projan SJ, Monod M, Narayanan CS, Dubnau D. 1987. Replication properties of pIM13, a naturally occurring plasmid found in *Bacillus subtilis*, and of its close relative pE5, a plasmid native to *Staphylococcus aureus*. J. Bacteriol. 169:5131–5139.

Quinlan AR, Hall IM. 2010. BEDTools: a flexible suite of utilities for comparing genomic features. Bioinformatics 26:841–842.

Ramirez MS, Don M, Merkier AK, Bistue AJS, Zorreguieta A, Centron D, Tolmasky ME. 2010. Naturally competent *Acinetobacter baumannii* clinical isolate as a convenient model for genetic studies. J. Clin. Microbiol. 48:1488–1490.

Robin ED, Wong R. 1988. Mitochondrial DNA molecules and virtual number of mitochondria per cell in mammalian cells. J. Cell. Physiol. 136:507–513.

Rodriguez-Beltran J, Hernandez-Beltran JCR, DelaFuente J, Escudero JA, Fuentes-Hernandez A, MacLean RC, a-Miller RPX, Millan AS. 2018. Multicopy plasmids allow bacteria to escape from fitness trade-offs during evolutionary innovation. Nat. Ecol. Evol. 2:873–881.

Roer L, Aarestrup FM, Hasman H. 2014. The EcoKI type I restriction-modification system in *Escherichia coli* affects but is not an absolute barrier for conjugation. J. Bacteriol. 197:337–342.

Rosano GL, Ceccarelli EA. 2014. Recombinant protein expression in *Escherichia coli:* advances and challenges. Front. Microbiol. 5:172.

Sakuma T, Tazumi S, Furuya N, Komano T. 2013. ExcA proteins of IncI1 plasmid R64 and Inclγ plasmid R621a recognize different segments of their cognate TraY proteins in entry exclusion. Plasmid 69:138–145.

Sambrook J, Russell DW. 2012. Molecular Cloning. CSHL Press.

Sandegren L, Linkevicius M, Lytsy B, Melhus Å, Andersson DI. 2011. Transfer of an *Escherichia coli* ST131 multiresistance cassette has created a *Klebsiella pneumoniae*-specific plasmid associated with a major nosocomial outbreak. J. Antimicrob. Chemother. 67:74–83.

San Millan A, Escudero JA, Gifford DR, Mazel D, MacLean RC. 2016. Multicopy plasmids potentiate the evolution of antibiotic resistance in bacteria. Nat. Ecol. Evol. 1:0010.

San Millan A, Heilbron K, MacLean RC. 2014. Positive epistasis between co-infecting plasmids promotes plasmid survival in bacterial populations. ISME J. 8:601–612.

Santos-Lopez A, Bernabe-Balas C, Ares-Arroyo M, Ortega-Huedo R, Hoefer A, San Millan A, Gonzalez-Zorn B. 2016. A naturally occurring SNP in plasmid pB1000 produces a reversible increase in antibiotic resistance. Antimicrob. Agents and Chemother. 61:e01735–16.

Satoh M, Kuroiwa T. 1991. Organization of multiple nucleoids and DNA molecules in mitochondria of a human cell. Exp. Cell Res. 196:137–140.

Schmidt R, Ahmetagic A, Philip DS, Pemberton JM. 2011. Catabolic Plasmids. In: eLS.

Scolnik PA, Haselkorn R. 1984. Activation of extra copies of genes coding for nitrogenase in *Rhodopseudomonas capsulata*. Nature 307:289–292.

Shetty RP, Endy D, Knight TF. 2008. Engineering BioBrick vectors from BioBrick parts. J. Biol. Eng. 2:5.

Shintani M, Sanchez ZK, Kimbara K. 2015. Genomics of microbial plasmids: classification and identification based on replication and transfer systems and host taxonomy. Front. Microbiol. 6:242.

Simon R, Priefer U, Pühler A. 1983. A broad host range mobilization system for in vivo genetic engineering: transposon mutagenesis in gram negative bacteria. 1:784–791.

Skulj M, Okrslar V, Jalen S, Jevsevar S, Slanc P, Strukelj B, Menart V. 2008. Improved determination of plasmid copy number using quantitative real-time PCR for monitoring fermentation processes. Microb. Cell Fact. 7:6.

Solovyev V, Salamov A. 2011. Automatic annotation of microbial genomes and metagenomic sequences. In: Metagenomics and its applications in agriculture, biomedicine and environmental studies (Ed. Li RW). Nova Science Publishers. p.61-78.

Sota M, Yano H, Hughes JM, Daughdrill GW, Abdo Z, Forney LJ, Top EM. 2010. Shifts in the host range of a promiscuous plasmid through parallel evolution of its replication initiation protein. ISME J. 4:1568–1580.

Spencer DH, Tyagi M, Vallania F, Bredemeyer AJ, Pfeifer JD, Mitra RD, Duncavage EJ. 2014. Performance of common analysis methods for detecting low-frequency single nucleotide variants in targeted next-generation sequence data. J. Mol. Diagn. 16:75–88.

Sperandeo P, Cescutti R, Villa R, Di Benedetto C, Candia D, Deho G, Polissi A. 2006. Characterization of lptA and lptB, two essential genes implicated in lipopolysaccharide transport to the outer membrane of *Escherichia coli*. J. Bacteriol. 189:244–253.

Sprouffske K, Wagner A. 2016. Growthcurver: an R package for obtaining interpretable metrics from microbial growthcurves. BMC Bioinformatics. 17:172

Stoesser N, Sheppard AE, Pankhurst L, De Maio N, Moore CE, Sebra R, Turner P, Anson LW, Kasarskis A, Batty EM, et al. 2016. Evolutionary history of the global emergence of the *Escherichia coli* epidemic clone ST131. mBio 7:e02162.

Summers DK, Sherratt DJ. 1988. Resolution of ColE1 dimers requires a DNA sequence implicated in the three-dimensional organization of the *cer* site. EMBO J. 7:851–858.

Suzuki H, Yano H, Brown CJ, Top EM. 2010. Predicting plasmid promiscuity based on genomic signature. J. Bacteriol. 192:6045–6055.

Szabó M, Nagy T, Wilk T, Farkas T, Hegyi A, Olasz F, Kiss J. 2016. Characterization of two multidrug-resistant IncA/C plasmids from the 1960s by using the MinION sequencer device. Antimicrob. Agents Chemother. 60:6780–6786.

Team RDC. R: A language and environment for statistical computing.

Textor S, Wendisch VF, De Graaf AA, Müller U, Linder MI, Linder D, Buckel W. 1997. Propionate oxidation in *Escherichia coli*: evidence for operation of a methylcitrate cycle in bacteria. Arch. Microbiol. 168:428–436.

Thomas CM, Nielsen KM. 2005. Mechanisms of, and barriers to, horizontal gene transfer between bacteria. Nat. Rev. Microbiol. 3:711–721.

Tomizawa J, Itoh T. 1981. Plasmid ColE1 incompatibility determined by interaction of RNA I with primer transcript. Proc. Natl. Acad. Sci. U.S.A. 78:6096–6100.

Troeschel SC, Thies S, Link O, Real CI, Knops K, Wilhelm S, Rosenau F, Jaeger K-E. 2012. Novel broad host range shuttle vectors for expression in *Escherichia coli*, *Bacillus subtilis* and *Pseudomonas putida*. J. Biotechnol. 161:71–79.

Ullrich A, Shine J, Chirgwin J, Pictet R, Tischer E, Rutter WJ, Goodman HM. 1977. Rat insulin genes: construction of plasmids containing the coding sequences. Science 196:1313–1319.

Vega NM, Gore J. 2014. Collective antibiotic resistance: mechanisms and implications. Curr. Opin. Microbiol. 21:28–34.

Vieira J, Messing J. 1982. The pUC plasmids, an M13mp7-derived system for insertion mutagenesis and sequencing with synthetic universal primers. Gene 19:259–268.

Villa L, García-Fernández A, Fortini D, Carattoli A. 2010. Replicon sequence typing of IncF plasmids carrying virulence and resistance determinants. J. Antimicrob. Chemother. 65:2518–2529.

Vogwill T, Phillips RL, Gifford DR, MacLean RC. 2016. Divergent evolution peaks under intermediate population bottlenecks during bacterial experimental evolution. Proc. Biol. Sci. 283:20160749.

Wada M, Itikawa H. 1984. Participation of *Escherichia coli* K-12 *groE* gene products in the synthesis of cellular DNA and RNA. J. Bacteriol. 157:694–696.

Wang Y. 2017. Spatial distribution of high copy number plasmids in bacteria. Plasmid 91:2–8.

Wiberg RAW, Gaggiotti OE, Morrissey MB, Ritchie MG. 2017. Identifying consistent allele frequency differences in studies of stratified populations. Methods Ecol. Evol. 8:1899–1909.

Wick LM, Weilenmann H, Egli T. 2002. The apparent clock-like evolution of *Escherichia coli* in glucose-limited chemostats is reproducible at large but not at small population sizes and can be explained with Monod kinetics. Microbiol. 148:2889–2902.

Wilharm G, Piesker J, Laue M, Skiebe E. 2013. DNA uptake by the nosocomial pathogen *Acinetobacter baumannii* occurs during movement along wet surfaces. J. Bacteriol. 195:4146–4153.

Williams HG, Day MJ, Fry JC, Stewart GJ. 1996. Natural transformation in river epilithon. Appl. Environ. Microbiol. 62:2994–2998.

Wilm A, Aw PPK, Bertrand D, Yeo GHT, Ong SH, Wong CH, Khor CC, Petric R, Hibberd ML, Nagarajan N. 2012. LoFreq: a sequence-quality aware, ultra-sensitive variant caller for uncovering cell-population heterogeneity from high-throughput sequencing datasets. Nucl. Acids Res. 40:11189–11201.

Wobbrock JO, Findlater L, Gergle D, Higgins JJ. 2011. The aligned rank transform for nonparametric factorial analyses using only ANOVA procedures. Proc. CHI'11. New York: ACM Press 143-146.

Xue H, Cordero OX, Camas FM, Trimble W, Meyer F, Guglielmini J, Rocha EPC, Polz MF. 2015. Eco-evolutionary dynamics of episomes among ecologically cohesive bacterial populations. mBio 6:e00552–15.

Yamamori T, Yura T. 1980. Temperature-induced synthesis of specific proteins in *Escherichia coli*: evidence for transcriptional control. J. Bacteriol. 142:843–851.

Yang YL, Polisky B. 1993. Suppression of ColE1 high-copy-number mutants by mutations in the *polA* gene of *Escherichia coli*. J. Bacteriol. 175:428–437.

Yano H, Rogers LM, Knox MG, Heuer H, Smalla K, Brown CJ, Top EM. 2013. Host range diversification within the IncP-1 plasmid group. Microbiol. 159:2303–2315.

Yano H, Wegrzyn K, Loftie-Eaton W, Johnson J, Deckert GE, Rogers LM, Konieczny I, Top EM. 2016. Evolved plasmid-host interactions reduce plasmid interference cost. Mol. Microbiol.101:743–756.

Ye K, Schulz MH, Long Q, Apweiler R, Ning Z. 2009. Pindel: a pattern growth approach to detect break points of large deletions and medium sized insertions from paired-end short reads. Bioinformatics 25:2865–2871.

Zaleski P, Wawrzyniak P, Sobolewska A, Łukasiewicz N, Baran P et al. 2015. pIGWZ12 – A cryptic plasmid with a modular structure. Plasmid 79:37–47.

Zheng J, Peng D, Ruan L, Sun M. 2013. Evolution and dynamics of megaplasmids with genome sizes larger than 100 kb in the *Bacillus cereus* group. BMC Evol. Biol. 13:1–11.

Zhong C, Peng D, Ye W, Chai L, Qi J, Yu Z, Ruan L, Sun M. 2011. Determination of plasmid copy number reveals the total plasmid DNA amount is greater than the chromosomal DNA amount in *Bacillus thuringiensis* YBT-1520. PLoS ONE. 6:e16025.

Zhou K, Zhou L, Lim Q', Zou R, Stephanopoulos G, Too H-P. 2011. Novel reference genes for quantifying transcriptional responses of *Escherichia coli* to protein overexpression by quantitative PCR. BMC Mol. Biol. 12:18.

8 Acknowledgements

Firstly, I would like to express my sincere gratitude to my advisor and mentor Tal for the continuous support of my Ph.D. study and related research, for her motivation, fruitful discussions, and for keeping her door always open. I could not have imagined having a better advisor and mentor for my Ph.D.

I would also like to acknowledge PD Charles Franz as the second reader of this thesis, and Prof. Ruth Schmitz-Streit and Prof. Stanislav Gorb for their interest in my work. I am gratefully indebted to them for their very valuable comments on this thesis.

I greatly appreciate the support received through the great collaborative work undertaken with Dr. Anne Kupczok, Dr. Nils Hülter, Tanita Wein, Dr. Christian Wöhle, Samer Kadib Alban and Dr. Giddy Landan and Prof. Itzhak Mizrahi – these outstanding collaborations resulted in our publications entitled ‘Segregational drift and the interplay between plasmid copy number and evolvability’ and ‘An evolutionary perspective on plasmid lifestyle modes.’

With a special thank I would also like to mention Anne for her interest in this work and the fast implementation of the simulations, Christian for your fantastic support during the initial phase of data analysis and to Tana who greatly supported me in and outside the lab!

With a special mention to all my collogues and Nils, Devani, Katrin, Samer, Fernando, Maxime and Sophie. It was fantastic to have the opportunity to work the majority of my research with you.

I am grateful to my daughter and my husband for their never ending patience and my siblings, who have provided me through moral and emotional support in my life.